

**Some pages of this thesis may have been removed for copyright restrictions.**

If you have discovered material in Aston Research Explorer which is unlawful e.g. breaches copyright, (either yours or that of a third party) or any other law, including but not limited to those relating to patent, trademark, confidentiality, data protection, obscenity, defamation, libel, then please read our [Takedown policy](#) and contact the service immediately (openaccess@aston.ac.uk)

THE INFLUENCE OF POSTERIOR CORNEAL SURFACE ASTIGMATISM ON  
RESIDUAL ASTIGMATISM

JONATHAN MAXWELL ROYSTON  
Doctor of Philosophy

THE UNIVERSITY OF ASTON IN BIRMINGHAM  
October 1990

This copy of the thesis has been supplied on condition that anyone who consults it is understood to recognise that its copyright rests with the author and that no quotation from the thesis and no information from it may be published without the author's prior, written consent.

The University of Aston in Birmingham  
THE INFLUENCE OF POSTERIOR CORNEAL SURFACE ASTIGMATISM  
ON RESIDUAL ASTIGMATISM

Jonathan Maxwell Royston  
Ph.D Thesis  
October 1990

## SUMMARY

It has often been found that corneal astigmatism exceeds the amount exhibited by the eye as a whole. This difference is usually referred to as residual astigmatism. Scrutiny of the studies of corneal astigmatism reveal that what has actually been measured is the astigmatic contribution of the anterior corneal surface alone. This anterior surface is easily measured whereas measurement of the posterior corneal surface is much more difficult.

A method was therefore developed to measure the radius and toricity of the posterior corneal surface. The method relies upon photography of the first and second Purkinje images in three fixed meridians. Keratometry, comparison of anterior and posterior corneal Purkinje images and pachometric data were applied to three meridional analysis equations, allowing the posterior corneal surface to be described in spherocylindrical form.

Measurements were taken from 80 healthy subjects from two distinct age groups. The first consisted of 60 young subjects, mean age 22.04 years and the second consisted of 20 old subjects, mean age 74.64 years. The young group consisted of 28 myopes, 24 emmetropes and 8 hyperopes. The old group consisted of 6 myopes and 14 hyperopes. There was an equal number of males and females in each group. These groupings allowed the study of the effects of age, ametropia and gender on the posterior corneal toricity.

The effect of the posterior corneal surface on residual astigmatism was assessed and was found to cause an overall reduction. This reduction was due primarily to the posterior corneal surface being consistently steeper relative to the anterior surface in the vertical meridian compared to the horizontal meridian.

Key Words: Astigmatism, Purkinje images, Three meridional analysis, Anterior corneal surface toricity, Posterior corneal surface toricity,

For MRB, TRF and, of course, BBK.

## ACKNOWLEDGEMENTS

I would like to thank Mr. D.A. Barnes for his help and supervision.

I would also like to thank Dr. M.C.M. Dunne for his assistance with a number of problems.

Mr. J. Doig and Mr. D. Deeley were most helpful as regards using computer facilities.

I am most grateful to all the subjects who sat for this study.

That's about it really. The rest is just ..... visual.

LIST OF CONTENTS	Page
CHAPTER ONE	
THE HUMAN CORNEA	
1.1 Introduction	18
1.2 Microstructure of the Cornea	18
1.2.1 Precorneal Tear Film	18
1.2.2 Anterior Epithelium	19
1.2.3 Bowman's Membrane	20
1.2.4 Substantia Propria or Stroma	20
1.2.5 Descemet's Membrane	21
1.2.6 Endothelium	21
1.3 Corneal Thickness	21
1.3.1 Central Corneal Thickness	21
1.3.2 Peripheral Corneal Thickness	22
1.3.3 Variations of Corneal Thickness with Age, Gender and Ametropia	22
1.4 Anterior Corneal Surface	23
1.4.1 Mean Corneal Dimensions and Radius	23
1.4.2 Surface Contour	23
1.4.3 Variations of Anterior Corneal Radius with Age, Gender and Ametropia	25
1.5 Posterior Corneal Surface	26
1.5.1 Mean Radius	26
1.5.2 Surface Contour	27
1.5.3 Variations of Posterior Corneal Surface Radius with Age, Gender and Ametropia	27
1.6 Schematic Modelling of the Cornea	27
1.7 Summary	29

## CHAPTER TWO

### ASTIGMATISM

2.1 Introduction	31
2.2 Description and Discovery of Astigmatism	31
2.3 Refractive Astigmatism	32
2.3.1 Incidence	32
A) Cylindrical Power	32
B) Cylinder Axis Orientation	33
2.3.2 Variations of Refractive Astigmatism with Age	33
A) Cylindrical Power	33
B) Cylinder Axis Orientation	35
2.3.3 Variations of Refractive Astigmatism with Spherical Ametropia	35
2.3.4 Variations of Refractive Astigmatism with Gender	36
2.4 Anterior Corneal Surface Astigmatism	37
2.4.1 Incidence	37
A) Cylindrical Power	37
B) Cylinder Axis Orientation	38
2.4.2 Variations of Anterior Corneal Surface Astigmatism with Age	39
A) Cylindrical Power	39
B) Cylinder Axis Orientation	40
2.4.3 Variations of Anterior Corneal Surface Astigmatism with Spherical Ametropia	41
2.4.4 Variations of Anterior Corneal Surface Astigmatism with Gender	41
2.5 Residual Astigmatism	42
2.5.1 Mean Values	42
2.5.2 Causes of Residual Astigmatism	44
A) Crystalline Lens	44
B) Posterior Corneal Surface	45

C) Asymmetry of the Optical System of the Eye	45
2.6 Summary	47
CHAPTER THREE	
MERIDIONAL ANALYSIS	
3.1 Introduction	50
3.2 Review of Meridional Analysis Techniques	50
3.2.1 Three Meridional Analysis	50
3.2.2 Multi-Meridional Analysis	52
3.3 Meridional Analysis Equations used in Present Study	53
3.3.1 Derivation of Equations of Fowler (1989)	53
3.4 Summary	56
CHAPTER FOUR	
ANTERIOR CORNEAL RADIUS	
4.1 Introduction	59
4.2 Anterior Corneal Radius	59
4.3 Measurement of Anterior Corneal Radius: Present Study	61
4.4 Subject Profile	62
4.4.1 Age Groups	61
4.4.2 Ametropia Groups	63
4.4.3 Gender Groups	63
4.5 Precision of Anterior Corneal Radii Measurements	63
4.6 Keratometric Results	64
4.6.1 Group Mean Anterior Corneal Radii in Three Meridians	65
4.6.2 Group Mean Data in Sphero-cylindrical Form after Three Meridional Analysis	65
4.7 Correlation Between the Measured Keratometric Data in Sphero-cylindrical Form and that Derived by Three Meridional Analysis	66
4.8 Error Analysis	70
4.9 Summary	72



CHAPTER FIVE  
MEASUREMENT OF REFRACTION

5.1 Introduction	75
5.2 Objective Optometers	75
5.3 Measurement of Refraction: Present Study	76
5.3.1 Measurement of Refraction - Procedure	77
5.4 Subject Profile	79
5.5 Precision of Refractive Measurements	79
5.6 Measurement of Refraction: Results	80
5.6.1 Group Mean Refraction in Three Meridians	80
5.6.2 Group Mean Refractive Power in Sphero-cylindrical Form after Three Meridional Analysis	81
5.7 Correlation Between the Measured Refractive Sphero- cylindrical Data and that Derived by Three Meridional Analysis	81
5.8 Summary	85

CHAPTER SIX  
MEASUREMENT OF CORNEAL THICKNESS

6.1 Introduction	88
6.2 Corneal Thickness and Pachometric Techniques	88
6.3 Measurement of Corneal Thickness: Present Study	90
6.3.1 Measurement Procedure	92
6.4 Subject Profile	92
6.5 Precision of Corneal Thickness Measurements	92
6.6 Measurement of Corneal Thickness: Results	93
6.7 Summary	93

## CHAPTER SEVEN

### POSTERIOR CORNEAL RADIUS

7.1 Introduction	93
7.2 Posterior Corneal Radius	93
7.3 Measurement of Posterior Corneal Radius: Present Study	94
7.3.1 Correlation of Data from One-source and Two-source Measurements	99
7.4 Subject Profile	101
7.5 Posterior Corneal Radius: Measurement Procedure	101
7.6 Computation of Results	102
7.7 Repeatability of Posterior Corneal Radius Measurements	103
7.8 Assessment of Magnification and Distortion from Grid Photographs	106
7.9 Validation of Purkinje Image Technique	108
7.9.1 Validation Procedure	108
7.9.2 Validation Results	111
7.10 Investigation of the relationship between Purkinje image height and keratometry readings	113
7.11 Measurements of Posterior Corneal Radius: Results	115
7.11.1 Group Mean Posterior Corneal Radii in Three Meridians	116
7.11.2 Group Mean Data in Sphero-cylindrical Form after Three Meridional Analysis	116
7.12 Summary	117

## CHAPTER EIGHT

### STATISTICAL ANALYSIS

8.1 Introduction	120
------------------	-----

8.2 Parameters to be Analysed	120
8.2.1 Spherical Component	120
A) Influence of Gender	120
B) Influence of Spherical Ametropia	121
C) Influence of Age	122
8.2.2 Cylindrical Component	123
A) Influence of Gender	123
B) Influence of Spherical Ametropia	124
C) Influence of Age	125
8.2.3 Cylinder Axis Orientation	126
A) Influence of Gender	127
B) Influence of Spherical Ametropia	127
C) Influence of Age	128
8.2.4 Corneal Thickness	130
A) Influence of Gender	130
B) Influence of Spherical Ametropia	130
C) Influence of Age	131
8.3 Summary	132

## CHAPTER NINE

### EFFECT OF POSTERIOR CORNEAL SURFACE ON RESIDUAL ASTIGMATISM

9.1 Introduction	134
9.2 Comparison of the Effects of a One-surface and a Two-surface Cornea	134
9.2.1 One-surface Cornea	136
9.2.2 Two-surface Cornea	136
9.2.3 Mean Values of $R_1$ , $R_2$ and $\Delta R$	137
9.3 The Effect on Residual Astigmatism of the Relationship between the Anterior and Posterior Corneal Surfaces	139
9.4 Summary	141

## CHAPTER TEN

### SUMMARY AND DISCUSSION

10.1 Review of Previous Chapters	143
10.2 Suggestions for Further Study	147

### APPENDICES

APPENDIX A	150
Appendix 4.1 : Keratometric Results from Three Meridians	150
Appendix 4.2 : Anterior Corneal Sphero-cylindrical Components	152
Appendix 4.3 : Anterior Corneal Sphero-cylindrical Components	154
Appendix 5.1 : Refractive Sphero-cylindrical Components	156
Appendix 5.2 : Refractive Error Measurements from Three Meridians	158
Appendix 5.3 : Refractive Sphero-cylindrical Components	160
Appendix 6.1 : Pachometric Measurements	162
Appendix 7.1 : Purkinje Image Heights in Three Meridians	164
Appendix 7.2 : Purkinje Image Ratios for the One-source and Two-source Methods	169
Appendix 7.3 : Posterior Corneal Radius in Three Meridians	171
Appendix 7.4 : Posterior Corneal Sphero-cylindrical Components	173
Appendix 7.5 : Posterior Corneal Radius in Three Meridians (Repeat Readings)	175
Appendix 7.6 : Posterior Corneal Sphero-cylindrical Components (Repeat Readings)	176
Appendix 7.7 : Assessment of Magnification and Distortion From Purkinje Image Photographs	177
Appendix 9.1 One-surface Cornea Sphero-cylindrical Components	178
Appendix 9.2 Equivalent Cornea Sphero-cylindrical Components	180
APPENDIX B Supporting Publications	186

LIST OF TABLES	Page
1.1 Variation in peripheral corneal thickness. Data taken from Hirji and Larke (1978).	22
3.1 Values for A predicted using equations 13 and 14 of meridional program.	56
4.1 Estimated precision of the keratometric measurements (mm) from readings taken in three meridians and along principal meridians.	64
4.2 Mean anterior corneal radii values (mm) in three meridians for the subject groups. Values in brackets refer to standard deviation.	65
4.3 Mean values of keratometric spherocylindrical component derived from application of meridional analysis. Values in brackets refer to standard deviation.	66
4.4 Population percentages for magnitudes of difference in sphere, cylinder and axis components between principal meridional measurements and analysis of three meridional measurements.	69
4.5 Comparison between mean measured keratometric data and that derived from meridional analysis.	70
4.6. Table to show the effect of induced "errors" in keratometry readings (mm) on the output values of meridional analysis. Percentage difference is between original output values and those derived when "error" values are applied. Values are given to two decimal places.	71
4.7. Table to show the effect of induced "errors" in keratometry readings (mm) on the output values of meridional analysis. Percentage difference is between original output values and those derived when "error" values are applied. Values are given to two decimal places.	72
5.1 Estimated precision of measurements taken with the Hartinger Optometer.	79
5.2 Mean refractive power (D) in three meridians for the subject groups. Values in brackets refer to standard deviation.	80

5.3 Mean values of the refractive sphero-cylindrical component for the subject groups. Values in brackets refer to standard deviation.	81
5.4 Population percentages for magnitudes of difference in sphere, cylinder and axis components between principal meridional measurements and analysis of three meridional measurements.	84
5.5 Comparison between mean measured refractive data and that derived from meridional analysis.	85
6.1 Estimated precision of pachometric measurements (mm).	90
6.2 Mean values of corneal thickness (mm). Values in brackets represent the standard deviation.	93
7.1 Magnitude of differences in Purkinje image ratios from one-source and two-source methods.	103
7.2 The range, mean and standard deviation of the total separation between grid lines in the horizontal and vertical planes of the photographed grid. Total number of observations per photograph is 40.	111
7.3 Variation of conversion factor, $u$ , for values of $d'$ .	113
7.4 Values for the posterior corneal radius in the vertical meridian obtained using slit lamp and Purkinje image methods.	115
7.5 Mean posterior corneal radii values (mm) in three meridians. Values in brackets refer to standard deviation.	119
7.6 Mean values of the posterior corneal sphero-cylindrical component derived from the application of meridional analysis. Values in brackets represent the standard deviation.	120
8.1 The influence of gender on the power (D) of the anterior and posterior corneal spherical component (mean $\pm$ SD) and on the power of the refractive spherical component (mean $\pm$ SD).	126
8.2 Influence of spherical ametropia on the power (D) of the anterior corneal and posterior corneal spherical component (mean $\pm$ SD).	126

8.3 Influence of age on the power of the anterior corneal and posterior corneal spherical component (mean $\pm$ SD).	127
8.4 Influence of gender on the power of the anterior corneal, posterior corneal and refractive cylindrical component (mean $\pm$ SD).	128
8.5 Influence of spherical ametropia on the power of the anterior corneal, posterior corneal and refractive cylindrical component (mean $\pm$ SD).	129
8.6 Influence of age on the anterior corneal, posterior corneal and refractive cylindrical component (mean $\pm$ SD).	131
8.7 Influence of gender on the variation of the cylinder axes orientation expressed as a percentage of the total number of subjects. (One subject in the female group, 2.5%, exhibited no refractive astigmatism).	132
8.8 Influence of spherical ametropia on the cylinder axis orientation of the anterior corneal cylinder, posterior corneal cylinder and the refractive cylinder. (One subject in the myopic group, 3%, exhibited no refractive astigmatism).	133
8.9 Influence of age on the orientation of the anterior corneal cylinder axis, posterior corneal cylinder axis and the refractive cylinder axis. (One subject in the young group, 2%, exhibited no refractive astigmatism).	134
8.10 Influence of gender on the central corneal thickness (mean $\pm$ SD) as measured by pachometry.	135
8.11 Influence of spherical ametropia on the central corneal thickness (mean $\pm$ SD).	136
8.12 Influence of age on the central corneal thickness (mean $\pm$ SD).	136
9.1 Values of $R_1$ , $R_2$ and $\Delta R$ for young and old subject groups.	142
9.2 Mean, standard deviation and range of ratios between the anterior and posterior corneal surfaces in the young and old subject groups.	144
9.3 Mean, standard deviation and range of values of $R_1$ , $R_{\text{theoretical}}$ and $\Delta R_{\text{theoretical}}$ .	145

LIST OF FIGURES	Page
1.1 Microscopic structure of the cornea in transverse section.	19
2.1 Distribution of corneal astigmatism in 2000 eyes. Taken from Tait, 1956.	39
2.2 Change in axis of corneal astigmatism with age, mean time 24 years. Taken from Lyle, 1971.	41
4.1 Scatter plot of spherical component (mm) measured by keratometry and that derived from meridional analysis.	67
4.2 Scatter plot of cylindrical component (mm) measured by keratometry and that derived from meridional analysis.	67
4.3 Scatter plot of cylinder axis component ( $^{\circ}$ ) measured by keratometry and and that derived from meridional analysis.	68
5.1 Diagram of target apparatus used with Hartinger Optometer and interchangeable between instruments.	78
5.2 Scatter plot of measured spherical component (D) and that derived from meridional analysis.	82
5.3 Scatter plot of measured cylindrical component (D) and that derived from meridional analysis.	82
5.4 Scatter plot of measured cylinder axis orientation ( $^{\circ}$ ) and that derived from meridional analysis.	83
7.1 Diagrammatic representation of the carriage with two light sources in the $90^{\circ}$ meridian.	98
7.2 Diagrammatic representation of the carriage with one source in each of the $90^{\circ}$ and $45^{\circ}$ meridians and two in the $180^{\circ}$ meridian.	98
7.3 Schematic side-view of perspex carriage mounted on the Canon R1 Optometer.	99
7.4 Photograph of the first and second Purkinje images as taken from the video monitor of the Canon R1 Optometer.	100
7.5 Diagrammatic representation of first and second Purkinje images as to be measured from the photographs.	101



7.6 Scatter plot of Purkinje image ratios (90° meridian) from one-source and two-source methods.	104
7.7 Scatter plot of original and repeat posterior corneal values (mm), 90° meridian.	106
7.8 Scatter plot of original and repeat posterior corneal values (mm), 180° meridian.	107
7.9 Scatter plot of original and repeat posterior corneal values (mm), 45° meridian.	107
7.10 Scatter plot of original and repeat posterior corneal spherical component (mm).	108
7.11 Scatter plot between original and repeat posterior corneal cylindrical component (mm).	108
7.12 Scatter plot between original and repeat posterior corneal cylinder axis orientation (°).	109
7.13 Scatter plot of posterior corneal radii values obtained from slit-lamp and Purkinje image methods.	116
7.14 Scatter plot between Purkinje image heights and corneal radius, 90° meridian.	117
7.15 Scatter plot between Purkinje image heights and corneal radius, 180° meridian.	118
7.16 Scatter plot between Purkinje image heights and corneal radius, 45° meridian.	118
9.1 Schematic representation of the one-surface cornea.	140
9.2 Schematic representation of the two-surface cornea.	140
9.3 Variation of $\Delta R$ in young subject group	143
9.4 Variation of $\Delta R$ in old subject group	143

CHAPTER ONE  
THE HUMAN CORNEA

# THE HUMAN CORNEA

## 1.1 INTRODUCTION

This chapter presents a brief review of the microstructure of the cornea along with variations of the anterior corneal surface, posterior corneal surface and corneal thickness which occur with age, gender and ametropia.

## 1.2 MICROSTRUCTURE OF THE CORNEA

Viewed microscopically, the cornea consists of five distinct layers and an outer tear film layer. These five layers are the anterior epithelium, Bowman's membrane, the stroma, Descemet's membrane and the posterior endothelium (Figure 1.1). Each of the layers is responsible for slight variations in the corneal refractive index.

### 1.2.1 Precorneal Tear Film

The anterior corneal surface is covered by a very thin tear film which consists of three distinct layers. These are a thin oily layer of about 0.9 to 0.2  $\mu\text{m}$ , a thick watery layer measuring about 6.5 to 7.5  $\mu\text{m}$ , and a thin mucin layer of about 0.5  $\mu\text{m}$  (Snell and Lemp, 1989). These thickness values are much too small to have any significant dioptric effect, though Ehlers (1965) stated that in the case of abnormal tear flow the effect would become significant if the total thickness of the tear layer exceeded 100 $\mu\text{m}$ . Calculation using the equations in section 1.6 shows that if the tear film did, in fact, reach a thickness of 100 $\mu\text{m}$  it would change the equivalent power of the cornea by about 0.02D.

### 1.2.2 Anterior Epithelium

The corneal epithelium measures about 50 $\mu$ m to 60 $\mu$ m in thickness and consists of five layers of cells.

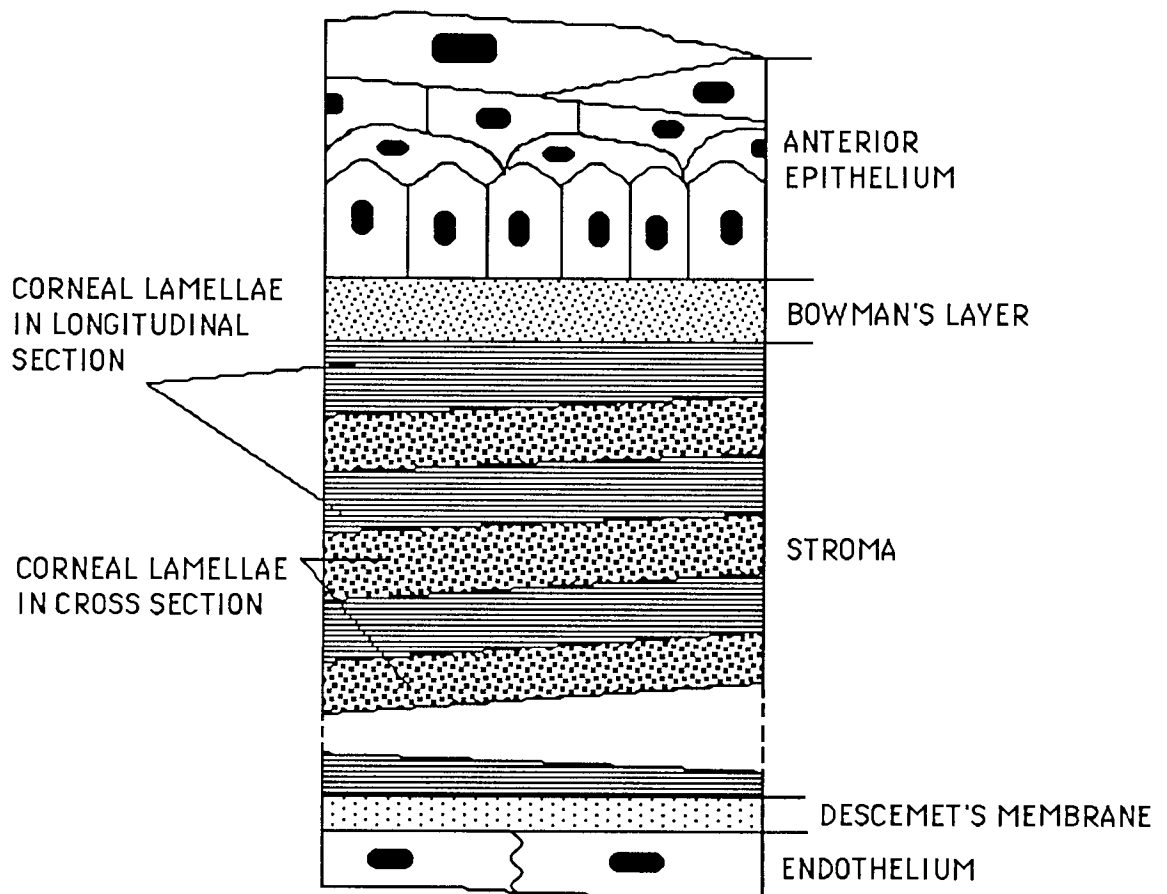


Figure 1.1 Microscopic structure of the cornea in transverse section.

The superficial cells are flattened and two to three cells thick. The middle zone of cells are polyhedral in shape, usually having a convex anterior surface and a concave posterior surface. The deepest basal cells are tall columnar cells and form a single layer resting on a basement membrane.

### 1.2.3 Bowman's Membrane

Immediately under the basement membrane of the corneal epithelium lies Bowman's Membrane. Its thickness can vary between  $8\mu\text{m}$  and  $14\mu\text{m}$  (Davson, 1984). It is acellular and consists of collagen fibrils randomly packed into layers, which is not markedly different from the stroma beneath it (Davson, 1984; Snell and Lemp, 1989).

### 1.2.4 Substantia Propria or Stroma

Almost 90% of the corneal thickness is taken up by the stroma, which is normally between  $400\mu\text{m}$  to  $500\mu\text{m}$  in thickness. Transparent, fibrous and compact it consists of collagen fibres arranged in 200-250 parallel lamellae (Maurice, 1957), each of which is about  $2\mu\text{m}$  in thickness. Fibres in adjacent lamellae are generally arranged at right angles to each other.

The apparent resemblance between the corneal and scleral stroma has stimulated research into why only the former is transparent. Maurice (1957) presented values for the refractive indices of the corneal collagen fibres and matrix of 1.47 and 1.345 respectively (at 500nm) which he thought would give the cornea an opaque appearance. He believed, however, that the cornea would still be transparent if the collagen fibres were of a constant size, orientation and spacing to form a regular lattice structure.

Smith (1969) found refractive index values for the fibres and matrix of 1.384 and 1.369 respectively, and concluded that the similarity of these values meant a lattice structure was not necessary. Nevertheless, subsequent studies (Cox et al, 1970; Feuk, 1970; Benedek, 1971; Farrell et al., 1973) have shown that transparency

depends on an ordered arrangement of collagen fibres.

### 1.2.5 Descemet's Membrane

This layer lies on the posterior surface of the stroma layer and forms the basement membrane of the endothelium. The layer is strong, homogeneous and usually varies in thickness between 5 $\mu$ m and 10 $\mu$ m. It is distinctly defined from the stroma layer and is thicker than the endothelium.

This layer is composed of fine collagen fibres arranged in a hexagonal manner and embedded in matrix.

### 1.2.6 Endothelium

The final layer of the cornea consists of a single layer of flattened cells which are 5 $\mu$ m high and 20 $\mu$ m wide. The cells cover the posterior surface of Descemet's membrane and are continuous with the endothelial cells that line the anterior surface of the iris. This layer of cells play a significant role in controlling the normal hydration of the cornea.

## 1.3 CORNEAL THICKNESS

### 1.3.1 Central Corneal Thickness

According to Von Bahr (1948), the first measurements of corneal thickness were taken from post-mortem material and so correspond to the thickness of maximally swollen corneae.

The first attempts to measure the thickness of the living cornea

were undertaken by Blix (1880). Numerous studies since that date suggest an average value for the central corneal thickness of 0.55mm (Von Bahr, 1948; Maurice and Giardini, 1951; Mishima, 1968; Mishima and Hedbys, 1968; Mandell and Polse, 1969; Lowe, 1969; Kruse-Hansen, 1971; Tomlinson, 1972; Olsen and Ehlers, 1984).

### 1.3.2 Peripheral Corneal Thickness

Peripheral thickness of the cornea is said to increase to 0.7mm (Steindorf, 1947; Maurice and Giardini, 1951; Mandell and Polse, 1969; Hirji and Larke, 1978). Hirji and Larke (1978) studied the variation of peripheral corneal thickness and their results are summarized in Table 1.1.

Quadrant	15° off-axis	30° off-axis	Order of thickness
Superior	0.61mm	0.69mm	Thickest
Nasal	0.60mm	0.69mm	
Inferior	0.58mm	0.65mm	
Temporal	0.57mm	0.63mm	Thinnest

Table 1.1 Variation in peripheral corneal thickness. Data taken from Hirji and Larke (1978).

### 1.3.3. Variations of Corneal Thickness with Age, Gender and Ametropia

The central corneal thickness generally shows no significant variation with gender (Maurice and Giardini, 1951; Kruse-Hansen, 1971; Olsen and Ehlers, 1984). Kruse-Hansen (1971) has also reported that there is no significant variation due to refractive error, though he emphasised the limited refractive range of the

subjects he used. Lowe (1969) and Kruse-Hansen (1971) have found no significant variation with age, though Olsen and Ehlers (1984) have reported a slight decrease in thickness with age which failed to reach statistical significance.

## 1.4 ANTERIOR CORNEAL SURFACE

### 1.4.1 Mean Corneal Dimensions and Radius

Many early measurements of the overall corneal dimensions (Duke-Elder and Wybar, 1961) suggest an average width of 11.6mm horizontally and 10.6mm vertically. The mean anterior corneal surface radius is about 7.80mm (Bennett and Rabbetts, 1984), with a range of values in normal eyes is between 7.00mm and 8.60mm (Stenstrom, 1946).

### 1.4.2 Surface Contour

The peripheral ellipsoidal flattening of the cornea was first revealed following the pioneering work of Senff and Helmholtz (Helmholtz, 1924). The work of Mattheissen (1902) based on the data of other workers supported this conclusion. More recently, there have been numerous studies to support this (Noto, 1961; Holden, 1970; Mandell and St.Helen, 1971; Kiely, et al 1982, 1984; Guillon et al 1986).

A number of other workers have attempted to describe the cornea in qualitative terms (Aubert, 1885; Sulzer, 1892; Eriksen, 1893; Gullstrand, 1924; Bier, 1956; Knoll, 1961a). Gullstrand (1924) came to the conclusion that the cornea possesses an approximately spherical central optical zone which extends horizontally about 4mm



and is decentred temporally and slightly inferiorly with respect to the line of sight. Peripheral flattening was said to occur more on the nasal and superior sides compared with the temporal and inferior sides.

Numerous studies also support the suggestion that there exists an optic zone of some 3 to 9mm in diameter (Bier, 1956; Obrig, 1957; Knoll, 1961a; Grosvenor, 1961; Jenkins, 1963; Girard, 1970; Fujii et al, 1972, Clark 1974a,b; Rubin,1975). The shape of the zone has been described as a horizontal ovoid by Grosvenor (1961) though Clark (1974a) found such an irregular outline that the true margins were difficult to identify. Bier (1956) was alone in suggesting the presence of a shallow depressed annulus surrounding the optic zone, which he referred to as the negative zone.

There is, however, general agreement that the corneal apex is decentred from the line of sight by about 0.50mm. The direction of this displacement, however, seems to be open to argument. Some workers suggest that the displacement is predominantly temporal (Grosvenor, 1961; Bonnet and Cochet, 1962; Jenkins, 1963; Tomlinson and Schwartz, 1979) whilst others find no directional trend (Mandell and St. Helen, 1969, 1971). Little evidence supports a displacement in the inferior or superior directions. The results of Bier (1956) are in almost complete opposition to the results of Gullstrand (1924), though it was suggested by Grosvenor (1961) that this could be partially resolved if Bier (1956) was understood to have used the geometric centre of the cornea as a reference point as opposed to the line of sight. The actual amounts of decentration determined by Bier (1956) were small, thus supporting the observations of Knoll (1980) who deduced that the corneal apex was very close to its geometrical centre.

Most workers are in agreement with Gullstrand (1924) in that the cornea tends to be flatter on the nasal side than the temporal side (Bier, 1956; Grosvenor, 1961; Jenkins, 1963; Clark, 1974b). There seems to be a conflict of views, however, on the change of curvature in the superior and inferior portions. Some workers have suggested that the superior portion is the flatter (Knoll, 1961a,b; Clark, 1974a,b) though others have stated the opposite to be true (Bier, 1956). Jenkins (1963) could find no difference at all between the two portions.

All this previous work would suggest that the cornea is quite asymmetrical. It was stated by Ludlam and Wittenberg (1966a,b), however, that measurement of the corneal contour with reference to the line of sight would lead to the conclusion that the corneal surface exhibits asymmetry. They also added that the corneal asymmetries described by Gullstrand (1924) could be produced by the presence of a tilted ellipsoidal surface. A number of other workers (Holden, 1970; Kiely et al., 1982) have since shown that tilted and decentred ellipses could be used to represent the corneal profile.

#### 1.4.3 Variations of Anterior Corneal Radius with Age, Gender and Ametropia

There is no strong correlation between the radius of the anterior corneal surface and refractive status (Steiger, 1913; Gardiner, 1962; Baldwin, 1964) though in low ametropia the corneal surface is steeper in myopes and flatter in hyperopes when compared to emmetropic eyes (Tron, 1934; Baldwin, 1964; Sorsby et al., 1957). As regards the variation with gender, female subjects have slightly steeper anterior corneal surfaces when compared to males (Sorsby

et al., 1961; Fledelius, 1976). Fledelius and Stubgaard (1986) have reported a slight, non-significant tendency for older subjects to exhibit a steeper anterior corneal surface. Lowe (1969) found no correlation between the radius of the anterior corneal surface and age beyond 30 years of age. Leighton and Tomlinson (1972) studied two distinct age groups, "young" (mean age 25.2 years) and "old" (mean age 61.8 years) and forwarded the concept that the whole corneo-scleral envelope gets smaller with age. They also found evidence of more steeply curved corneae with old age.

## 1.5 POSTERIOR CORNEAL SURFACE

### 1.5.1 Mean Radius

The radius of the posterior corneal surface has to date received little attention because it is less accessible to measurement compared to the anterior surface. In most schematic eye models a value of between 6.50mm and 6.80mm is usually adopted (Bennett and Rabbetts, 1984). Gullstrand (Southall, 1924) and Tscherning (1924) found that they could not measure the posterior corneal curvature centrally due to the interference by the first catoptric (Purkinje) image so they calculated the radius of the surface from more peripheral measurements. More recently, attempts have been made to measure the central posterior corneal radius but readings have been confined to the vertical meridian. (Lowe and Clark, 1973; Hockwin et al., 1983). Lowe and Clark (1973) used a slit-lamp photographic technique and found a mean value of 6.46mm for normal eyes. Hockwin et al (1983) used a method based on the principle of Scheimpflug (1906) and found a mean value of just over 7.00mm.

### 1.5.2 Surface Contour

The studies of Tomlinson (1972) involving the variation of the corneal thickness towards the periphery came to the conclusion that the posterior corneal surface is reasonably constant in shape, relative to the anterior corneal surface, in most eyes, though no numerical values were presented to support this. Kooijman (1983) assumed the posterior corneal surface had the same elliptical contour as the anterior surface in his schematic eye model.

### 1.5.3 Variations of Posterior Corneal Surface Radius with Age, Gender and Ametropia

As there have been very few studies on the radius of the posterior corneal surface, there is little data on the variations which occur with gender, age and refractive error. The only data available is on the variation of the posterior corneal surface radius with age (Lowe and Clark, 1973), where no significant variation was found to occur.

## 1.6 Schematic Modelling of the Cornea

A number of assumptions are made when developing mathematical models of the cornea. Firstly, both the anterior and posterior surfaces are regarded as being spherical and as being axially aligned. Secondly, the refractive index of the cornea is assumed to be constant and in this study is taken to be 1.3771 (Le Grand and El Hage, 1980). Similarly, the aqueous humour, which lies behind the posterior cornea, is taken as having a constant refractive index of 1.3374 (Le Grand and El Hage, 1980) in this study.

Calculation of the surface powers of the cornea depends on how the

cornea is modelled. That is, whether it possesses one or two surfaces. If the cornea is taken as having one surface, the power of this surface is determined from the expression:

$$F_1 = 1000 (n_2 - n_1) / r_1$$

where  $F_1$  = power of the cornea (D);  $n_2$  = refractive index of cornea (taken in this case as that of aqueous, 1.3374;  $n_1$  = refractive index of air;  $r_1$  = anterior corneal radius (mm).

In the case of a two-surface cornea, the anterior corneal surface power is determined from:

$$F_1 = 1000 (n_2 - n_1) / r_1$$

where  $F_1$  = power of the cornea (D);  $n_2$  = refractive index of cornea (1.3771);  $n_1$  = refractive index of air;  $r_1$  = anterior corneal radius (mm).

The power of the posterior corneal surface, in a two-surface cornea, is determined from the expression:

$$F_2 = 1000 (n_3 - n_2) / r_2$$

where  $F_2$  = power of the posterior corneal surface (D);  $n_3$  = refractive index of aqueous (1.3374);  $n_2$  = refractive index of cornea (1.3771);  $r_2$  = posterior corneal radius (mm).

The equivalent power of the two-surface cornea ( $F_e$ ) is determined from the expression:

$$F_e = F_1 + F_2 - d/n F_1 \cdot F_2$$

where  $F_e$  = equivalent power of the cornea;  $F_1$  = power of the anterior corneal surface (D);  $F_2$  = power of the posterior corneal surface (D);  $d$  = corneal thickness (m);  $n$  = refractive index of cornea.

## 1.7 Summary

In this chapter the anatomy of the human cornea has been briefly reviewed. There have been numerous studies on its' central and peripheral thickness and on the anterior corneal surface. Despite this vast amount of knowledge, however, there is relatively little information regarding the radius of the posterior corneal surface. Of particular interest in this study is the role this surface might play in explaining the differences between astigmatism arising from the anterior corneal surface and that exhibited by the eye as a whole. This aspect is discussed in the following chapter.

## CHAPTER TWO

### ASTIGMATISM

## CHAPTER 2. ASTIGMATISM

### 2.1 Introduction

This chapter presents an overview of the condition called astigmatism. Past studies of the astigmatism arising from the anterior corneal surface and the eye as a whole (refractive astigmatism) are summarized. Attention is paid to the incidence of astigmatism and its variation with age, gender and ametropia. Differences arising between the astigmatism exhibited by the anterior corneal surface and the eye as a whole are discussed along with possible causes for these differences.

### 2.2 Description and Discovery of Astigmatism

Astigmatism is that type of refractive condition in which no point focus is formed due to unequal refraction of the incident light in different meridians of the eye (Duke Elder and Abrams, 1970), the refractive power changing gradually from one meridian to the next. Astigmatism arises due to the presence of toroidal as opposed to spherical refractive surfaces. Donders (1864) gave such a condition the name regular astigmatism. By contrast the condition of irregular astigmatism is essentially pathological in nature.

Borish (1970) reported that a defect of vision resembling astigmatism was described by Pare in 1575. Emsley (1974) revealed that Newton studied the defect in the early 1700's and astigmatism as a descriptive term was actually introduced by Whewall in the mid 1800's. Correction of the condition was first achieved by Airy (Borish, 1970; Emsley, 1974) in the early 1800's and around the



same time a Colonel Gaulier is reported to have studied several patients and prescribed cylindrical corrections (Tscherning, 1904).

Other sources attribute the actual discovery of astigmatism to Thomas Young in 1801 (Tscherning, 1904).

## 2.3 Refractive Astigmatism

For the purposes of this study, refractive astigmatism refers to that arising from the eye as a whole. It is customary to express the components of astigmatism in a sphero-cylindrical form. Therefore, the present study will refer to the cylindrical power component, in plus cyl. form, and cylindrical axis orientation component of this sphero-cylindrical form.

### 2.3.1 Incidence

Most eyes are detectable as being astigmatic (Tscherning,1904; Borish,1970; Duke Elder and Abrams,1970; Bennett and Rabbetts, 1984). For the purposes of this study, astigmatic subjects are taken as those exhibiting 0.25D of refractive astigmatism and 0.05mm of keratometric astigmatism.

#### A) Cylindrical Power

In the study of Sorsby et al. (1960), based on over 1,000 subjects, almost 40% of the sample exhibited less than 0.25D of refractive astigmatism. 90% of the sample had astigmatism not exceeding 1.00D.

Bennett (1965) provides useful data on the incidence of astigmatism, which was based on the analysis of almost 13,000 spectacle prescriptions. About 50% of the lenses had cylinder powers of between 0.25D and 0.50D, 25% were between 0.75D and 1.00D. Cylinders over 4.00D accounted for less than 1% of the sample.

Duke-Elder (1970) summarizes the work of a number of workers. Assuming the level of significant astigmatism to be 0.50D, values for the incidence of astigmatism vary from 7.5% to 75% of subject populations studied.

#### B) Cylinder Axis Orientation

Bennett (1965) provides some interesting data on the distribution of cylinder axis orientation based on a study of almost 7500 correcting lenses in plus cylinder form. He regarded any axis within 15° of the horizontal to be "against the rule" and within 15° of vertical to be "with the rule" and all other axes as oblique. On this basis, almost 40% of the sample indicated "with the rule" astigmatism. The remaining 60% was almost evenly split between "against the rule" and oblique.

### 2.3.2 Variations of Refractive Astigmatism with Age

#### A) Cylinder Power

Variations in refractive astigmatism with age are open to debate. Borish (1970), for example, states that infants generally show low amounts of astigmatism and the amount increases with age. The

study of Woodruff (1971) also showed that there was an overall increase in astigmatism with increasing age. For example, astigmatism of 0.75D or more was found to be present in 3% of a sample of 2 year olds; by age 6 years this figure had increased to 10%. A number of other workers have also found that there was an increase in astigmatism from birth up to about five years of age (Mohindra et al.,1978; Howland et al.,1978; Fulton et al.,1980; Mohindra and Held, 1981; Gwiazda et al.,1984). The studies of Atkinson et al. (1980) have reported, however, that there is a decline in the incidence of astigmatism by the time infants had reached the age of 18 months.

Hirsch (1963) found that up to the age of six years 81% of a random sample of children had less than 0.25D of astigmatism. By age 14 years is reached this figure had decreased slightly to 72%. As regards the overall change of astigmatism with age, Hirsch concluded that during the first eight years of school life it was not significant.

Kratz and Walton (1949) studied a group of almost 300 subjects who had been examined over a period of 10 to 20 years. They reported that the refractive astigmatism did not change significantly in more than 60% of the subjects. Walton (1950) later studied a further 1249 eyes and drew the same conclusion as that from his earlier work.

Anstice (1970), however, found a reduction in refractive astigmatism with age. From a study of more than 600 eyes, with an age range from 5 years to 75 years he found this reduction to be significant.

Gordon and Donzis (1985) found no great difference in the amount of astigmatism between young and old subjects.

#### B) Cylinder Axis Orientation

Hess (1911) reported data from several studies that indicated a prevalence of "against the rule" refractive astigmatism in older subject groups. Payne (1919) studied groups of subjects in an age range from 10-15 years to 70 years and over and recognized the possibility of a change of astigmatism with age as early as 1892, but did not publish any relevant data until 1919. The data did show, however, a change towards "against the rule" astigmatism with age. In the 10-15 years group, 27% of the subjects exhibited "against the rule" astigmatism. 100% of the subjects in the 70 years and over exhibited "against the rule" astigmatism.

A number of other studies have shown that most of the astigmatism in younger subjects is generally "with the rule", that "against the rule" is very rarely seen and that there is a marked shift towards "against the rule" astigmatism with increasing age (Marin-Amat, 1956; Tait, 1956; Hirsch, 1959; Hirsch, 1963; Lyle, 1965; Grosvenor, 1977; Lyle, 1971; Saunders, 1981; Gordon and Donzis, 1985).

#### 2.3.3 Variations of Refractive Astigmatism with Spherical Ametropia

The relationship between refractive astigmatism and spherical ametropia has received considerable attention. Czellitzer (1927) reported that about half of his subjects showed an increase in astigmatism as spherical ametropia increased, though in an

appreciable number the astigmatism actually decreased. The work of Kronfeld and Devney (1930) showed that relatively low astigmatic errors, that is, between 0.00D and 1.00D, which make up the largest group, are quite equally spread through the medium to high refractive groups.

Slataper (1950) reported a higher incidence of astigmatism associated with hyperopia than with myopia. Borish (1970), however, questioned the validity of Slataper's findings in that his data was collected from a youthful patient pool where strabismus associated with high hyperopia was more common. Borish (1970) also quoted studies which found 60% of hyperopes to lack any significant astigmatism compared to only 3.5% of myopes.

Hirsch (1964) suggested a high association between myopia and astigmatism in children particularly, with fewer myopes than expected showing no astigmatism. He also found a greater than expected number of emmetropes with no astigmatism.

Borish (1970) quotes studies which suggest that the incidence and variability of astigmatism tended to show a similar distribution to refractive error. That is, the farther from emmetropia, the greater its prevalence, with the higher amounts showing an irregular distribution.

#### 2.3.5 Variations of Refractive Astigmatism with Gender

There is little data on the variation of astigmatism with gender. Donders (1864) reported that he had come across more cases of "abnormal" astigmatism in males than in females, but the author

could find no statement as to what "abnormal" astigmatism might actually be. The data of Hirsch (1959) showed that astigmatism above 2.00D was more common in the male subjects he studied when compared to the females.

Duke-Elder and Abrams (1970) quote a number of authors who have studied the variation of astigmatism with gender. Some state that astigmatism is "more frequent and marked" in females, while others state the opposite. Thus, Duke-Elder and Abrams (1970) were of the opinion that any differences due to gender would not be significant. Saunders (1981) reported that refractive astigmatism was approximately the same for gender groups.

Saunders (1981) found no statistically significant difference in the power of the refractive astigmatism except in a very young age group. He also found no significant difference in the mean values of the axes between gender groups, though a group of middle aged subjects did show some significant differences.

## 2.4 Anterior Corneal Surface Astigmatism

Since between 66% and 75% of the total refracting power of the eye is provided by the cornea (Lyle, 1971; El Hage, 1971; Woodruff, 1971) the effects of any corneal toricity are bound to be significant.

### 2.4.1 Incidence

#### A) Cylindrical Power

Estimates of the amount of corneal astigmatism that occur normally

vary from between 0.50D to 1.00D (Donders; 1864; Gullstrand, 1890; Steiger, 1913; Kronfeld and Devney, 1930; Sorensen, 1944; Duke-Elder and Abrams, 1970).

Values for the incidence of significant corneal astigmatism vary appreciably, though most eyes are astigmatic (Borish, 1970). Leibowicz (1928) noted that in some 85% of his subjects there was corneal astigmatism of up to 2.00D present.

Figure 2.1 is taken from the data of Tait (1956) and shows that corneal astigmatism of up to 1.50D was present in about 75% of his subjects.

#### B) Cylinder Axis Orientation

In the vast majority of eyes, perhaps as many as 90% (Duke-Elder and Abrams, 1970), the flattest (or weakest) meridian lies approximately horizontal. Thus, if the flattest meridian lies within 30° of the horizontal, the astigmatism present is said to be "with the rule". If, however, the horizontal meridian is steepest, the astigmatism present is said to be "against the rule" (Duke-Elder and Abrams, 1970; Emsley, 1974).

Leibowicz (1928) reported that in 80% of his subjects the axis of the astigmatism fell within 15° of the horizontal or vertical meridian. Bannon and Walsh (1945) stated that of the 2,000 subjects examined in their study, 33% had "with the rule astigmatism", and 20% had "against the rule".

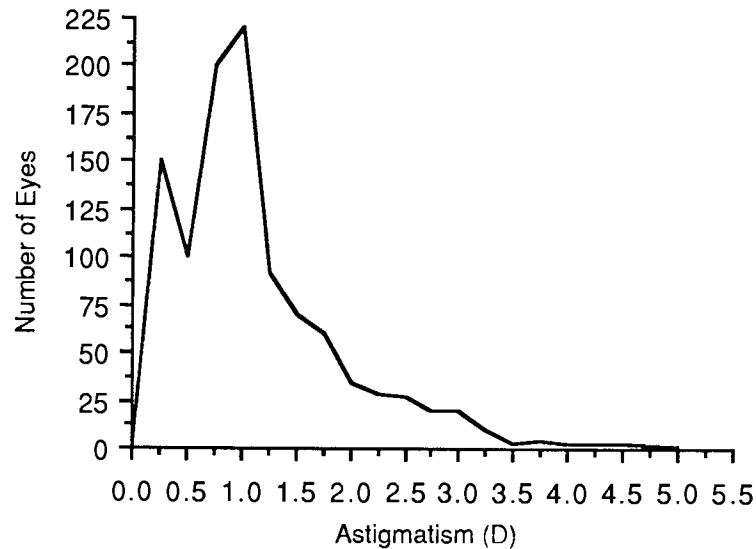


Figure 2.1 Distribution of corneal astigmatism in 2000 eyes. Taken from Tait, 1956.

#### 2.4.2 Variations of Anterior Corneal Surface with Age

##### A) Cylindrical Power

The variation of corneal astigmatism with age has received considerable attention, though the nature of the changes are open to debate. Donders was not aware of any change of astigmatism with age and stated corneal astigmatism maintained its original degree (Hirsch, 1963). Llandolt (1864) seemed to be in general agreement with this stating that corneal astigmatism stayed stationary throughout life.

Exford (1965) studied a group of subjects aged 40 years and over and made two main statements. Firstly, she stated that there was a modest but continuous increase in the power of the horizontal and vertical corneal meridians, the change generally being no more than 0.25D. Secondly, and more importantly, she stated that the corneal astigmatism showed no typical trend with age.



Lyle (1971) studied the variation of mean anterior corneal astigmatism in subjects ranging from 10 years of age to over 70 years and found a general trend for the astigmatism to decrease towards old age.

#### B) Cylinder Axis Orientation

A number of studies have shown that there is a tendency for corneal astigmatism to change from "with the rule" to "against the rule" with age.

Monod (1927) compared the prevalence of corneal astigmatism among 150 schoolchildren with that in 150 adults aged between 60 and 80 years. "With the rule" astigmatism was present in approximately 65% of the schoolchildren compared to 25% in the older group. Similarly, Kronfeld and Devney (1930) had suggested that a small amount of "with the rule" astigmatism at age 30 years is likely to be an astigmatism "against the rule" at the age of 60.

In a cross sectional study, Sorensen (1944) determined the mean corneal astigmatism in more than 100 eyes among each of three age groups - of mean ages 11, 31 and 60 years. He found a distinct trend towards "against the rule" astigmatism in the two older groups.

Phillips (1952) stated that in the age group 30 to 50 years the reduction in the incidence of corneal "with the rule" astigmatism is almost twice that in any other decade of life. At the same time, in the age group 24 to 55 years "against the rule" astigmatism shows an increase from 8% to 32%.

Of more recent studies, that of Baldwin and Mills (1981) state that there is an appreciable shift towards "against the rule" with increasing age.

Figure 2.2 is taken from the study of Lyle (1971) who studied the changes of the axis of astigmatism with age. The data suggests that the axis of astigmatism stays quite stationary with increasing age.

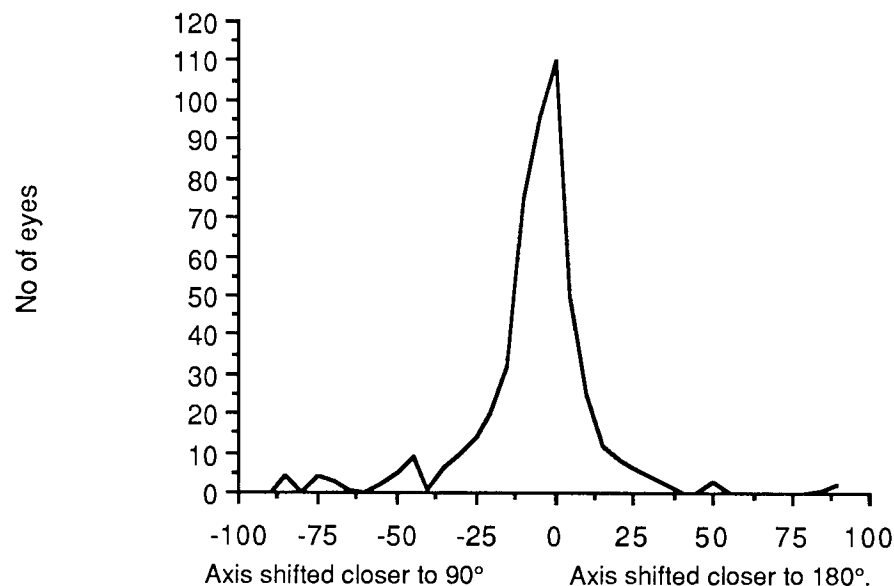


Figure 2.2 Change of axis of corneal astigmatism with age, mean time 24 years. Taken from Lyle, 1971.

#### 2.4.3 Variations of Anterior Corneal Astigmatism with Spherical Ametropia

Studies on the variation of astigmatism with spherical ametropia have been concerned with refractive rather than corneal astigmatism (see section 2.3.3).

#### 2.4.4 Variations of Anterior Corneal Astigmatism with Gender

Southall (1937) considered corneal astigmatism to be "more prevalent and severe in females", though Lyle (1971) emphasised there was some difficulty in assuming what subject group Southall was relating to.

Exford (1965) stated that corneal astigmatism showed no distinct trend in a group of male and female subjects in the middle to old age groups.

### 2.5 Residual Astigmatism

It is a common clinical finding that the refractive astigmatism differs from the astigmatism attributable to the toric anterior corneal surface as measured using keratometric techniques. If anterior corneal astigmatism is greater than the refractive astigmatism, then the residual astigmatism is "against the rule". It must be emphasised though that "against the rule" is the norm and therefore the terminology may be slightly misleading (Bennett, 1984).

#### 2.5.1 Mean Values

At the time when the keratometer was used to aid refraction, Javal (1890) formulated a relationship between corneal and ocular astigmatism. This expression can be represented as:

$$C = 1.25A - 0.50$$

The -0.50 value represents against the rule residual astigmatism. C

is the power of the correcting cylinder in the spectacle plane and A the corneal astigmatism from the keratometer. If the corneal astigmatism is "against the rule" then it must be given a minus sign. Javal (1890) emphasised that the coefficients in this expression were only approximations and improved methods of refraction would warrant possible amendments to his formula.

Carter (1963) used refractive error and keratometric measurements to calculate residual astigmatism in a group of 100 eyes and found the corneal astigmatism to exceed refractive astigmatism. A mean value of 0.60D "against the rule" was found, though the range of values was between 0.50D "with the rule" to 2.00D "against the rule".

Anstice (1971) carried out a similar study to that of Carter (1963). From a subject group of 600, he found a mean value of 0.36D "against the rule" residual astigmatism, with a range of from 0.75D "with the rule" to 2.00D "against the rule". He also found the amount of residual astigmatism to be reasonably stable with increasing age, though there was a slight increase overall in middle aged subjects.

Variations of residual astigmatism with gender and ametropia have not been studied to date.

The following sections examine the possible causes of residual astigmatism.

## 2.5.2 Causes of Residual Astigmatism

### A) Crystalline Lens

The crystalline lens may account for residual astigmatism as the many laminar zones it possesses may vary in optical density. The astigmatic effects so arising are thought to be small and "against the rule" (Duke-Elder and Abrams, 1970; Tscherning, 1904), though with sclerosis of the lens with age the effects may become more obvious. Jackson (1932) indicated that there was a change in lenticular astigmatism with age, and that there was a marked tendency towards "against the rule" astigmatism with age. The complex structure of the inner layers of the lens and its' astigmatic effect was emphasised by Sørensen (1944) who stated that variations in astigmatism of upto 2.00D can arise if the laminar zones of the lens were not concentric.

Astigmatism may also arise due to either or both of the surfaces of the crystalline lens being toroidal (Duke-Elder and Abrams, 1970; Anstice 1971). The measurements of Tscherning (1890) of the radii of the anterior lenticular surface were 10.2mm for the horizontal meridian and 10.1mm for the vertical meridian. For the posterior surface, values of 6.17mm and 6.13mm were derived for the horizontal and vertical meridians respectively. However, as the difference in the refractive index values of the lens and aqueous is small, a large difference in surface curves is required to get at least 0.50D. For the anterior surface, for example, the surface radii would need to be 10.00mm and 10.57mm to give rise to about 0.50D. For the posterior surface, radii of 6.00mm and 6.20mm would produce about the same value.

Whatever the causes of astigmatism arising from the crystalline lens, Czellitzer (1927) stated that lenticular astigmatism rarely exceeded 1.00D. A number of later studies stated that lenticular astigmatism rarely exceeded 2.00D, the normal range being between 0.50D and 1.25D (Sallman, 1934; Hruby, 1950).

Williams (1963) mentioned an interesting concept which he referred to as latent astigmatism. The theory behind this concept dated back to 1868 when Dobrowolosky (Williams, 1963) suggested that the ciliary body may undergo unequal contraction to compensate for corneal astigmatism. Lenticular astigmatism due to irregular contraction of the ciliary body is considered to be physiologically untenable, though Morgan et al. (1943) have shown that such a condition may be present in animals.

#### B) Posterior Corneal Surface

Residual astigmatism may also be attributed to the posterior corneal surface. This surface exhibits less astigmatic error than that associated with the anterior corneal surface (Duke-Elder and Abrams, 1970). From measurements taken from three subjects, Tscherning (1904) stated that the posterior corneal surface possessed between 0.25D and 0.50D of astigmatism, though it was suggested it may reach 1.00D. This astigmatism was found to be "against the rule" and so could, therefore, neutralize the effect of the anterior corneal surface astigmatism. In another study of the posterior corneal surface, Nicoletti (1927) obtained results similar to those of Tscherning (1904).

#### C) Asymmetry of the Optical System of the Eye

The astigmatism arising as a result of the asymmetry of the optical system of the eye may also explain residual astigmatism.

Duke-Elder and Abrams (1970) believed that none of the optical surfaces of the eye are geometrically centred or share a common axis of symmetry. This point is thought to apply particularly to the crystalline lens, which is not centred relative to the other refracting surfaces of the eye.

Bennett (1984) stated that if both the lens surfaces were spherical or had axial symmetry, astigmatism could still arise if the lens were tilted with respect to the optical axis of the cornea. Tilting of the lens was considered quite normal by Tscherning (1890) after he had made studies on the position of the crystalline lens in the human eye. The deviation of the crystalline lens from a symmetrical position was considered to be made up of two components (Tscherning, 1890). The first was a tilt or rotation of between  $3^\circ$  and  $7^\circ$  around the vertical axis such that the temporal edge of the lens lies in front of the nasal edge. This is combined with a horizontal tilt of between  $0^\circ$  and  $3^\circ$  such that the upper edge of the lens lies in front of the lower edge.

The presence of a tilted crystalline lens prompted Bennett (1984) to ask the question: could such a tilt be responsible for the 0.50D of against the rule astigmatism implicit in Javal's expression.

Bennett (1984) stated that a tilt of the crystalline lens may only account for a small amount of the 0.50D of residual astigmatism as a tilt of some  $14^\circ$  is required to produce this amount of astigmatism. He, therefore, suggested that a study of the posterior

corneal surface may help in the detection of the source of ocular astigmatism.

Sheard (1920) attempted to determine the corneal contribution that arises as a result of the angle between the optical and visual axes. For angles between these axes of  $5^\circ$ ,  $7^\circ$  and  $9^\circ$ , calculated values of "against the rule" astigmatism which arose were 0.35D, 0.66D and 1.11D respectively.

Loper (1959), however, found that no relationship existed between residual astigmatism and the magnitude of misalignment between the pupillary axis and the visual axis.

Ludlam and Wittenberg (1966a) believed that corneal astigmatism could arise due to the cornea being tilted or rotated relative to the line of sight, even if it possessed spherical surfaces. They considered residual astigmatism to be an artifact of measurement of the anterior corneal surface astigmatism along the visual axis.

## 2.6. Summary

Most eyes are astigmatic to some degree (Duke-Elder and Abrams, 1970). The astigmatism from the anterior corneal surface is usually greater than the refractive astigmatism. The difference between these two parameters is called residual astigmatism.

Residual astigmatism is thought to arise from a number of sources such as the crystalline lens, the asymmetry of the optical system and the posterior corneal surface. As all three components may have some effect, it is pertinent to study the possible effects of each in



isolation. This study is confined to the role of the posterior corneal surface and measurements relative to this role are discussed in the following chapters.

CHAPTER THREE  
MERIDIONAL ANALYSIS

## MERIDIONAL ANALYSIS

### 3.1 INTRODUCTION

Available instrumentation makes the measurement of the toricity of the anterior corneal surface and of the refraction of the eye, by the location of the principal power meridians, straightforward. For measurement of the posterior corneal surface, however, the task is more difficult. The research literature reveals a solution to this problem in the form of analysis of radius or power in three or more meridians to produce results in spherocylindrical form. Such an approach is called meridional analysis.

This section presents a brief review of past meridional analysis techniques along with an explanation of the equations used in the present study.

### 3.2 Review of Meridional Analysis Techniques

The vast majority of work involving meridional analysis techniques has been related to the refraction of the eye. The equations used for meridional analysis are based upon an approximation derived by Laurence (1920) and the possibility of determining ocular refraction in spherocylindrical form from readings taken in pre-selected meridians was first proposed by Bennett (1960).

#### 3.2.1 Three Meridional Analysis

As the name implies, three meridional analysis is the method used

to derive a spherocylindrical correction from measurements taken in three meridians only.

Brubaker et al, (1969) adapted Bennett's (1960) equations to determine a spherocylindrical correction by taking measurements in three preselected meridians,  $90^\circ$ ,  $135^\circ$  and  $180^\circ$ .

The first practical application of meridional refraction was described by Reinecke et al. (1972), whereby measurements were made in three pre-determined meridians using a stenopaic slit. Useful refractive data has been obtained using the three meridional approach in conjunction with semi-automated refractometry (Reinecke et al, 1972) and laser meridional refraction (Haine et al, 1973; Phillips et al, 1975).

Malacara (1974) presented a combined graphical and algebraic method using readings from  $60^\circ$ ,  $120^\circ$  and  $180^\circ$  meridians and mentioned the possible application of meridional techniques to optical surfaces, although his technique was applied to refractive readings taken with an optometer.

Fowler (1989) has derived a set of equations for the assessment of toroidal surfaces by taking measurements of surface curvature in three fixed meridians. The derivation of these equations is quite different from those of Brubaker et al. (1969), and the chosen fixed meridians were  $90^\circ$ ,  $180^\circ$  and  $45^\circ$ . Furthermore, the equations of Fowler (1989) were designed to be used with data in the form of curvature while those of previous workers made use of refractive data. Both sets of equations can, however, function equally well

regardless of how the data is expressed, whether it be in the form of curvature, power or radius.

Most recently, Burek (1990) has developed a set of equations which enables measurements from any set of three meridians to be used for three meridional analysis. This study was published too late, however, to influence the equations used in this study.

Long (1974) described in detail how small errors incurred in the initial measurements could result in significantly large differences in the final prescription, particularly as regards the cylinder power and axis orientation.

### 3.2.2 Multi-Meridional Analysis

In an attempt to overcome the limitations of three meridional analysis, Long (1974) introduced a mathematical method which involved the measurement of refraction in four or more pre-selected meridians. This predicted the final prescription and gave estimates of the errors in sphere power, cylinder power and cylinder axis, whilst providing the refractionist with an indication of which meridional measurements should be re-evaluated if the estimated accuracy was inadequate. Worthey (1977) presented a simplified analysis of multi-meridional data for the special case in which meridians were evenly spaced.

An experimental study using meridional refraction was carried out by Haine et al. (1976), who compared the results of laser meridional refraction in four and six meridians with conventional optometric

methods. Good agreement was found among the techniques employed, the six meridional refraction agreeing better than for the four meridional refraction. The six meridional method was distinctly superior in the determination of the axis of astigmatism. Whitefoot and Charman (1980) went on to show that multi-meridional laser refraction gave results with precision and accuracy comparable to conventional subjective techniques.

### 3.3 Meridional Analysis Equations Used In Present Study

The equations derived by Fowler (1989) were made readily available to the author and were, therefore, used in the present study. In view of the developmental nature of the method of measuring posterior corneal radius, it was considered that three meridional analysis would be suitable as a first approximation rather than using the more complex multi-meridional techniques. There will now be a short discussion on the derivation of the equations of Fowler (1989).

#### 3.3.1 Derivation Of The Equations Of Fowler (1989)

Laurence (1920) derived an approximation which relates the power,  $M(A)$ , of a cylindrical lens of power,  $C$ , at a given angle,  $A$ , away from the axis of the cylinder:

$$M(A) = C.\sin^2 A \dots\dots 1$$

For an astigmatic surface of a spherical power,  $S$ , the power,  $M(A)$ , can be represented by the following:

$$M(A) = S + C.\sin^2 A \dots\dots 2$$

This approximation is readily recognised in the initial equations of Fowler (1989), which specify the power in the 45°, 180° and 90° meridians:

$$C_{45} = S + C \cdot \sin^2(A - 45) \dots\dots 3$$

$$C_{180} = S + C \cdot \sin^2 A \dots\dots 4$$

$$C_{90} = S + C \cdot \cos^2 A \dots\dots 5$$

From these equations the following quadratic equation can be derived:

$$\begin{aligned} &S^2 + S \cdot (-C_{90} - C_{180}) \\ &+ (0.5C_{90} \cdot C_{180} - 0.25C_{90}^2 + C_{45} \cdot C_{90} - 0.25C_{180}^2 + C_{180} \cdot C_{45} - C_{45}^2) = \\ &0 \dots\dots 6 \end{aligned}$$

As this equation is of the quadratic form :

$$aS^2 + bS + C = 0 \dots\dots 7$$

it follows that:

$$a = 1 \dots\dots 8$$

$$b = (-C_{90} - C_{180}) \dots\dots 9$$

$$c =$$

$$(0.5C_{90} \cdot C_{180} - 0.25C_{90}^2 + C_{45} \cdot C_{90} - 0.25C_{180}^2 + C_{180} \cdot C_{45} - C_{45}^2) \dots\dots 10$$

The solution for the spherical component, S, can thus be found by rearranging equation 7:

$$S = \frac{-b \pm \sqrt{b^2 - 4ac}}{2a} \dots\dots 11$$

The cylindrical component, C, is then :

$$C = C_{90} + C_{180} - 2S \dots\dots 12$$

The cylinder axis, A, is determined using either :

$$\text{Cos}2A = (C90 - C180)/C \dots\dots 13$$

or

$$\text{Sin}2A = (S + 0.5C - C45)/0.5C \dots\dots 14$$

Which of the last two equations (13, 14) is actually used to determine the axis value depends on the use of an algorithm. Table 3.1 indicates how the algorithm functions. In this Table, the value of S (6.00DS) and C (3.00DC) is fixed, and the value of A is varied from 15° to 180° at 15° intervals.

For each value of A, the meridional powers C45, C180 and C90 are calculated using equations 3, 4 and 5.

From Table 3.1 it is evident that the output of equations 13 and 14 are only equal between 0° and 45°, and after that point the values depart from one another. It can be seen that equation 13 gives the correct value for the axis lying between 0° and 90°. For axes of between 90° and 180°, the output of equation 3 is only correct if subtracted from 180°.

However, the true axis values are unknown quantities in the experimental case. To solve this problem it will be noted that the values from equation 14 are positive when the axis lies between 0° and 90° and negative when between 90° and 180°. Thus, it is possible to obtain the correct value for A by tallying the outputs of both equations 13 and 14. If the output of equation 14 is positive, then A is taken to be the output of equation 13; if the output of



equation 14 is negative, then A is taken as the output of equation 13 subtracted from 180°. The addition of this simple algorithm to the basic program allows the true cylinder axis (A) to be determined automatically. The equations of Brubaker et al. (1969) included an algorithm similar to this.

TRUE AXIS(°)	INPUT MERIDIONAL POWER (D)			OUTPUT A (°)	
	C45	C180	C90	EQN.13	EQN.14
15	6.750	6.201	8.799	15	15
30	6.201	6.750	8.250	30	30
45	6.000	7.500	7.500	45	45
60	6.201	8.250	6.750	60	30
75	6.750	8.799	6.201	75	15
90	7.500	9.000	6.000	90	0
105	8.250	8.799	6.201	75	-15
120	8.799	8.250	6.750	60	-30
135	9.000	7.500	7.500	45	-45
150	8.799	6.750	8.250	30	-30
165	8.250	8.250	6.201	15	-15
180	7.500	6.000	9.000	0	0

Table 3.1 Values for A predicted using equations 13 and 14 of meridional program.

### 3.4 Summary

This chapter has presented a review of previously used meridional analysis techniques. Three meridional techniques show a tendency to over-estimate the power of the cylindrical component in results expressed in sphero-cylindrical form and can also lead to variability in the estimate of the cylinder axis orientation. These problems can be remedied using multi-meridional techniques, which make use of four or six meridians.

Keratometers and optometers make the measurement of the anterior corneal surface toricity and refractive astigmatism relatively easy. In the case of the posterior corneal surface toricity, however, the measurement is more difficult. The use of meridional analysis is thus the most convenient method of being able to obtain measurements from this surface in spherocylindrical form. Although the flaws of only using three meridians for such analysis, as described above, are acknowledged, the developmental nature of the method for measuring the posterior corneal radius described in chapter 7 precludes the need for multi-meridional analysis at this stage.

Before applying meridional analysis to readings taken from the posterior corneal surface, it is necessary to investigate the level of accuracy achieved when applying meridional analysis to refractive and keratometric data, which can be obtained using conventional instrumentation. This is described in chapters 4 and 5.

CHAPTER FOUR  
ANTERIOR CORNEAL RADIUS

## ANTERIOR CORNEAL RADIUS

### 4.1 Introduction

This chapter presents a review of the measurement of the anterior corneal radius using keratometric techniques. Three meridional analysis is applied to the keratometric results obtained from a group of 80 subjects.

### 4.2 Anterior Corneal Radius

Measurements of the radius of the anterior corneal surface are made using keratometric techniques. Clark (1973a,b) provides the most comprehensive review of keratometry, the findings of which will now be summarised.

Keratometry, or ophthalmometry, is the method used to measure the radius of curvature of the central portion of the anterior corneal surface. Although both terms are used synonymously, Clark (1973a) stated that whereas the latter technique can be applied to the measurement of a variety of ocular parameters, the former technique is specifically restricted to the measurement of the anterior corneal surface.

Scheiner (1619) undertook the first crude keratometric determinations. His basic technique was improved by Ramsden (Mandell, 1960) in the late 18th century when a doubling device was added. Helmholtz is also credited with the introduction of the doubling device, and it is he who is generally looked upon as being the original inventor of this method (Helmholtz, 1924). Various other workers are cited as introducing improvements to the overall

design of the keratometer such that it would become more suitable for clinical application to the anterior corneal surface - Coccius (1867), Llandolt (1878), Javal and Schiotz (1881), Sutcliffe (1907) and Hartinger (1935). All suggested different measuring devices, though Javal and Schiotz (Helmholtz, 1924) made the overall method more suitable.

Essentially, the value for the corneal radius is inferred from the separation of two corneally reflected target mire points which represent the ends of an object imaged by the convex surface of the cornea, that is, the first Purkinje image. The calibrated doubling device, that allows both mire points to be made coincident, facilitates the measurement of this separation, and hence the corneal radius which is directly proportional to it. The doubling method has the advantage that it makes the results independent of small eye movements and allows the easiest estimation of the principal meridians of corneal astigmatism.

When discussing the errors involved in keratometric measurements, a distinction between the accuracy and precision of the method must be made. The accuracy is an indication of how close the measured value is to the actual one. The precision relates to the reproducibility of the measurement. Littman (1951) suggested that the accuracy of keratometric readings were most seriously effected by imperfect focusing of the mires, incorrect focusing of the eyepiece and accommodation of the observers eye. Such errors could amount to 0.4mm in radius measurements (Stone, 1962). Stone (1962) also indicated that differences in the assumed corneal refractive index values, in keratometers which expressed results in terms of corneal power, could result in radius errors in the order of  $\pm 0.13\text{mm}$ .

Clark (1973a) was aware of a wide discrepancy between the values quoted by various authors as to the overall accuracy of keratometry. He estimated that a value of  $\pm 0.015\text{mm}$  was reasonable for conventional two-mire keratometry on human corneae. Charman (1972) stated that the precision of surface radii measurement by two-mire methods would be no better than  $\pm 0.04\text{mm}$  due to diffraction effects caused by the limited angular apertures used in keratometry and the finite wavelength of light.

If conventional keratometers were used to measure the peripheral cornea, the errors involved are proportional to the separation of the mires (Mandell, 1962, 1964, 1969). To overcome this problem attempts were made to modify keratometers by placing the mires closer together (Berg, 1929; Bonnet and Cochet, 1962; Mandell, 1965; Holden, 1970). Attempts to reduce the area of surface used when measuring the curvature, however, were shown by Charman (1972) to reduce the precision of the measurement. Thus, Mandell's (1965) small mire topographic keratometry was shown to have a lowest limit of precision of  $0.1\text{mm}$  (Charman, 1972).

#### 4.3 Measurement of Anterior Corneal Radius : Present Study

In the present study the anterior central corneal curvature was measured using a Zeiss (Jena) 110 Keratometer. Both target mires are collimated, thus reducing the errors induced by imperfect focusing of the mires, incorrect focusing or accommodation of the observer eye.

Checks were made on the calibration of the instrument at the beginning of each session. This was done in the absence of skew or astigmatic misalignment by placing a precision  $7.80\text{mm}$  surface in

the position normally occupied by the subject eye.

The subject's head was kept steady in a chin and forehead rest. The subject was then asked to fixate the target set between the mires of the keratometer. This ensured alignment of the instrument axis to the subjects line of sight. Three readings were taken of the anterior corneal radius along each of the 90°, 180° and 45° meridians, in keeping with requirements of the meridional analysis program. Mean and standard deviation values for the corneal radii were calculated from these measurements and are shown in appendix 4.1. These were converted to spherocylindrical form using the equations described in section 3.3 and the results are summarized in appendix 4.2. Three further readings each of the anterior corneal radius and axis of orientation were also taken along both principal meridians and are shown in appendix 4.3

#### 4.4 Subject Profile

The right eye only was used in all the subjects. All the subjects had good general and ocular health, possessed binocular vision and corrected to an acuity of at least 6/9. Contact lens wearers were excluded from the study so as to avoid the possible influence of contact lens wear on the corneal profile.

##### 4.4.1 Age Groups

Because of the anterior corneal surface variations with age outlined in chapters 1 and 2, two age ranges were considered. One group, consisting of 60 subjects, was taken from the undergraduate population attending the Ophthalmic Optics course at Aston University. The mean age in this group was 22.04 years ( $\pm 3.29$ ). The

second, smaller group consisted of 20 older subjects who normally attended the Vision Sciences Department in the undergraduate refraction clinic. The mean age in this group was 74.64 years ( $\pm 5.61$ ).

#### 4.4.2 Ametropia Groups

Because of the anterior corneal surface variations with ametropia outlined in chapters 1 and 2, measurements were taken from emmetropic, myopic and hyperopic subjects. For the purposes of this study emmetropic subjects were taken as having a mean refraction of within  $\pm 0.50\text{D}$ ; myopic subjects were taken as having a mean refraction of greater than  $-0.50\text{D}$ ; hyperopes were taken as having a mean refraction of greater than  $+0.50\text{D}$ .

The younger group consisted of 24 emmetropes (mean refraction,  $-0.09\text{D}$  spherical equivalent), 28 myopes (mean refraction,  $-4.03\text{D}$ , spherical equivalent) and 8 hyperopes (mean refraction,  $+1.21\text{D}$ , spherical equivalent). The older subject group consisted of 6 myopes (mean refraction,  $-1.47\text{D}$ , spherical equivalent) and 14 hyperopes (mean refraction,  $+2.57$ , spherical equivalent).

#### 4.4.3 Gender Groups

Each of the groups described above consisted of an equal number of male and female subjects. Any variation with gender of the anterior corneal surface would then be apparent.

### 4.5 Precision of Anterior Corneal Radii Measurements

Table 4.1 shows the estimated precision for the keratometric



measurements. The values used are from the readings taken in each of the 90°, 180° and 45° meridians (Appendix 4.1) and from the anterior corneal radius measured in spherocylindrical form (Appendix 4.3). The values for this table are determined on the same principle used by Clark (1973a). That is, the estimated precision was taken to be twice the value of the standard deviation based on the statistical assumption that the spread of 95% of the population is expected to fall within two standard deviations.

Keratometric Component	Mean	Range
Spherical Component (mm)	0.035	0.00 - 0.58
Cylindrical Component (mm)	0.020	0.00 - 0.24
Cylinder Axis Component(°)	1.50	0.00 - 9.0
90° Meridian	0.022	0.00 - 0.16
180° Meridian	0.020	0.00 - 0.14
45° Meridian	0.020	0.00 - 0.18

Table 4.1. Estimated precision of the keratometric measurements (mm) from readings taken in three meridians and along the principal meridians. N = 80. Mean precision is taken as twice the value of the standard deviation. Range is the range of standard deviations.

#### 4.6 Keratometric Results

For each subject group, the results were treated in terms of the average radius along the 90°, 180° and 45° meridians. This allows a direct comparison with the data relating to the posterior corneal radius (chapter 7). The mean spherocylindrical values, derived using the meridional analysis program described in section 3.3, are also shown. This again allows comparison with the data relating to the

mean posterior corneal sphero-cylindrical values (chapter 7).

#### 4.6.1 Group Mean Anterior Corneal Radii in Three Meridians

Table 4.2 shows the mean anterior corneal radii values (mm) arranged in terms of age, refractive group and gender (see appendix 4.3).

Statistical analysis of the results in each category is the subject of a later chapter (chapter 8).

Subject Group	MERIDIAN		
	90°	180°	45°
Young Male Myopes	7.78 (±0.23)	7.92 (±0.26)	7.85 (±0.23)
Young Female Myopes	7.78 (±0.31)	7.87 (±0.30)	7.85 (±0.31)
Old Male Myopes	7.81 (±0.12)	7.69 (±0.19)	7.72 (±0.16)
Old Female Myopes	7.45 (±0.11)	7.44 (±0.11)	7.42 (±0.13)
Young Male Emmetropes	7.86 (±0.20)	7.96 (±0.22)	7.91 (±0.23)
Young Female Emmetropes	7.74 (±0.28)	7.86 (±0.26)	7.79 (±0.26)
Young Male Hyperopes	8.05 (±0.24)	8.04 (±0.20)	7.98 (±0.15)
Young Female Hyperopes	7.83 (±0.30)	8.09 (±0.29)	8.00 (±0.27)
Old Male Hyperopes	7.87 (±0.26)	7.89 (±0.24)	7.86 (±0.22)
Old Female Hyperopes	7.53 (±0.25)	7.56 (±0.20)	7.51 (±0.17)

Table 4.2. Mean anterior corneal radii values (mm) in three meridians for the subject groups. Values in brackets refer to standard deviation. N = 80.

#### 4.6.2 Group Mean Radii Data in Sphero-cylindrical Form after Three-meridional Analysis

Table 4.3 shows the mean keratometric sphero-cylinder values arranged in terms of age, refractive group and gender (appendix 4.2).

Statistical analysis of the results in each category is the subject of a later chapter (chapter 8).

Subject Group	Sphere (mm)	Cylinder (mm)	Axis (°)
Young Male Myopes	7.74 (±0.23)	0.22 (±0.13)	81.6 (±31.2)
Young Female Myopes	7.73 (±0.29)	0.19 (±0.09)	85.8 (±36.7)
Old Male Myopes	7.67 (±0.18)	0.16 (±0.06)	135.2 (±66.6)
Old Female Myopes	7.39 (±0.12)	0.10 (±0.04)	54.5 (±35.3)
Young Male Emmetropes	7.85 (±0.21)	0.13 (±0.06)	83.0 (±26.3)
Young Female Emmetropes	7.73 (±0.27)	0.14 (±0.08)	79.5 (±20.8)
Young Male Hyperopes	7.91 (±0.16)	0.28 (±0.21)	69.5 (±30.7)
Young Female Hyperopes	7.82 (±0.30)	0.28 (±0.10)	99.3 (±56)
Old Male Hyperopes	7.81 (±0.26)	0.26 (±0.27)	58.3 (±47.7)
Old Female Hyperopes	7.44 (±0.22)	0.22 (±0.15)	79.8 (±36.1)

Table 4.3. Mean values of the keratometric sphero-cylindrical component derived from application of meridional analysis. Values in brackets represent the standard deviation. N = 80.

#### 4.7 Correlation Between the Measured Keratometric Data in Sphero-cylindrical Form and that Derived by Three Meridional Analysis

Figure 4.1 shows the scatter plot for the spherical component measured with the keratometer and that derived by the meridional analysis program described in chapter 3. A high correlation was found between the two sets of values ( $r = 0.99$ ;  $P < 0.001$ ).

Figure 4.2 shows the scatter plot for the measured and calculated cylindrical component values. A high correlation was again found between the two sets of values ( $r = 0.94$ ;  $P < 0.001$ ), though overall it is slightly lower than that for the spherical component.

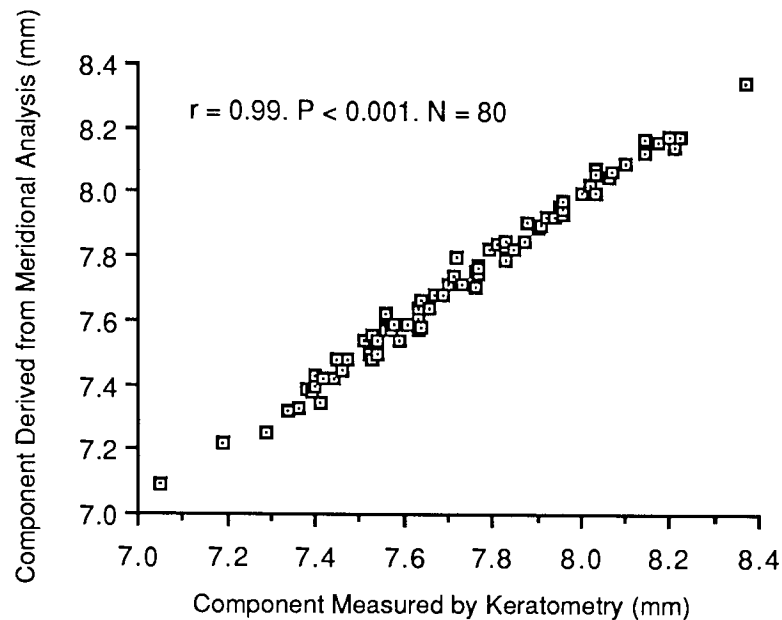


Figure 4.1 Scatter plot of spherical component (mm) measured by keratometry and that derived from meridional analysis.

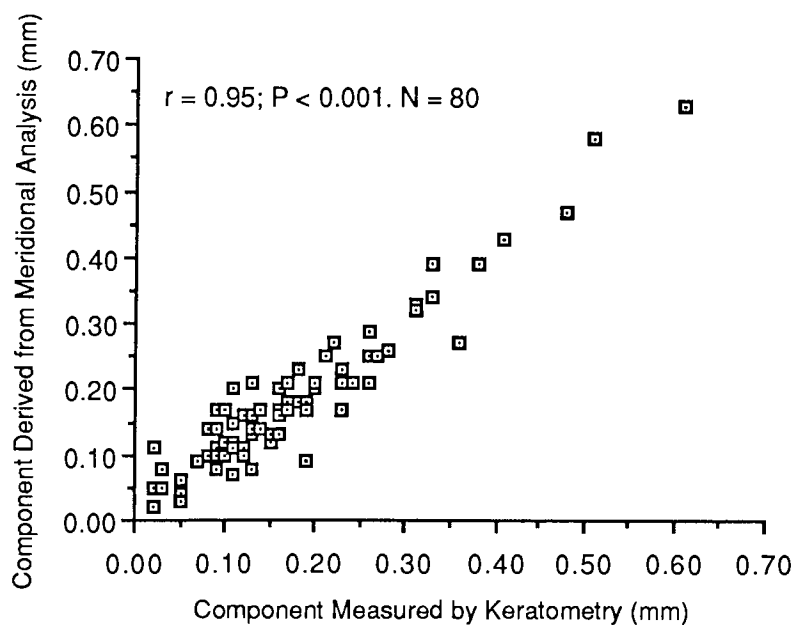


Figure 4.2 Scatter plot of cylindrical component (mm) measured by keratometry and that derived from meridional analysis.

Figure 4.3 shows the scatter plot for the cylindrical axis orientation obtained using the two methods. The values on the X and Y axis have been used to account for the cyclical nature of cylinder axis orientation. As with the spherical and cylindrical components a high correlation was found between the two sets of values ( $r = 0.93$ ;  $P < 0.001$ ) but slightly lower than that obtained for the spherical component.

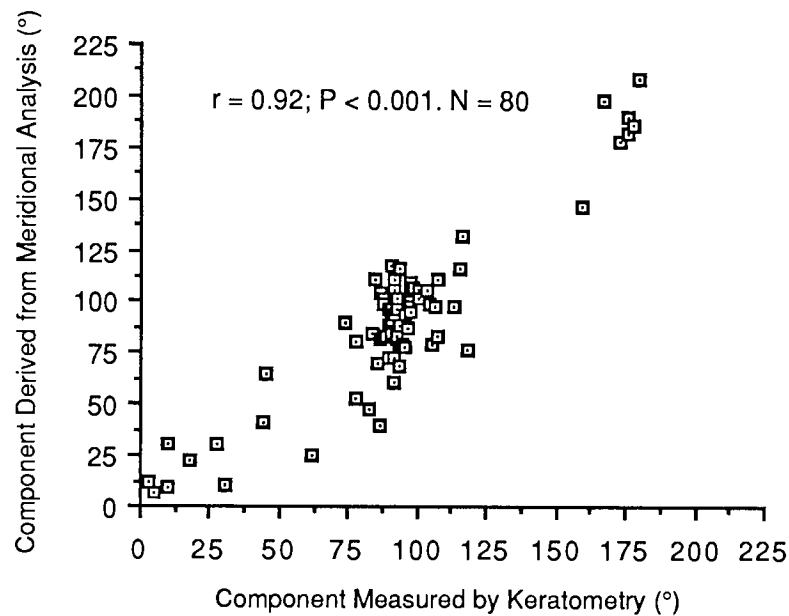


Figure 4.3 Scatter plot of cylinder axis orientation (°) measured by keratometry and that derived by meridional analysis.

In agreement with the findings of Long (1974), as mentioned in chapter 3, the highest correlation exists between the two sets of spherical values and the lowest between the cylinder axis orientation values. Overall, however, there is a very good correlation between the sphero-cylindrical values measured using a keratometer and those derived from meridional analysis.

Table 4.4 shows the magnitude of differences for percentages of the population measured. From the Table it can be seen that the

differences between the measured and computed spherical component data were all within  $\pm 0.08\text{mm}$ . The magnitude of differences for the cylindrical component data are slightly greater overall when compared to the spherical component. 95% of the population exhibited differences of within 0.08mm for the cylindrical component. As regards the cylinder axis component, 76.7% of the population exhibit differences of within  $20^\circ$ .

Keratometric Component		Percentage of Subjects (n = 80)
Sphere	$\pm 0.02\text{mm}$	55%
	$\pm 0.04\text{mm}$	85.9%
	$\pm 0.08\text{mm}$	100%
Cylinder	$\pm 0.02\text{mm}$	51.9%
	$\pm 0.04\text{mm}$	71.7%
	$\pm 0.08\text{mm}$	95%
	$\pm 0.10\text{mm}$	100%
Cylinder axis	$\pm 5^\circ$	33.4%
	$\pm 10^\circ$	55%
	$\pm 20^\circ$	76.7%
	$> 20^\circ$	23.3%

Table 4.4. Population percentages for magnitudes of differences in sphere, cylinder and axis components between principle meridional measurements and analysis of three meridional measurements.

Table 4.5 shows that despite the variability observed with respect to the cylindrical component and that of the cylinder axes of orientation, the group averaged measured and computed data indicate good overall agreement between the measured and computed spherocylindrical results.

The average computed cylindrical component was an overestimate of the measured value, as found by Long (1974), though the difference

which occurred fell within the range of the estimated precision for both instruments.

Keratometric Component		Mean±SD
Spherical Component (mm)	Measured	7.70±0.27
	Derived	7.69±0.27
Cylindrical Component (mm)	Measured	0.17±0.12
	Derived	0.18±0.12
Cylinder Axis Component (°)	Measured	94.1±40.1
	Derived	93.1±46.7

Table 4.5. Comparison between mean measured keratometric data and that derived from meridional analysis.

#### 4.8 Error Analysis

This section presents two numerical examples which would give an idea of the effect of errors in anterior corneal radius readings upon three-meridional analysis for keratometry.

Two corneal "models" are assumed. The first model exhibits astigmatism of approximately 3.00D and the second exhibits 0.3D.

A) The keratometry readings along the principal meridians are taken as:

$$7.80/+0.50 \times 90.$$

Application of meridional analysis to this reading yields values of:

$$45^\circ - 8.05\text{mm}, 180^\circ - 8.30\text{mm}, 90^\circ - 7.80\text{mm}.$$

An "error" of 0.01mm is introduced to each of the readings along these three meridians and the results are summarized in the Table

below.

"Error"	Meridional Analysis Output	Percentage Difference		
		Sph	Cyl	Axis
0.01mm in 45°	7.80/ 0.50 x 91.1	0.00%	0.08%	1.30%
0.01mm in 90°	7.81/ 0.49 x 89.4	0.13%	1.98%	0.65%
0.01mm in 180°	7.80/ 0.51 x 89.4	0.00%	2.02%	0.62%

Table 4.6. Table to show the effect of induced "errors" in keratometry readings (mm) on the output values of meridional analysis. Percentage difference is between original output values and those derived when "error" values are applied. Values are given to two decimal places.

The values presented in Table 4.6 indicate that in the case of a large cylindrical component, errors in the original keratometry readings induce only very small errors in the output data.

B) In the case of the second example, the keratometry readings along the principal meridians are taken as:

$$7.80 / +0.05 \times 90$$

Application of meridional analysis to this reading yields values of:

$$45^\circ - 7.825\text{mm}, 180^\circ - 8.850\text{mm}, 90^\circ - 7.800\text{mm}.$$

An "error" of 0.01mm is introduced to each of the readings along these three meridians and the results are summarized in the Table below.

The values presented in Table 4.7 indicate that in the case of a small cylindrical component, errors in the original keratometry readings induce only small errors in the spherical output data, larger errors in the cylindrical output data and moderate errors in cylindrical axis



output data.

Thus, as would be expected, the smaller the cylindrical component present the greater the possible errors particularly as regards the cylindrical axis output data.

"Error"	Meridional Analysis Output	Percentage Difference		
		Sph	Cyl	Axis
0.01mm in 45°	7.80/ 0.05 x 100.9	0.00%	7.70%	12.1%
0.01mm in 90°	7.81/ 0.04 x 82.9	0.12%	17.50%	7.80%
0.01mm in 180°	7.80/ 0.06 x 85.3	0.00%	21.70%	5.26%

Table 4.7. Table to show the effect of induced "errors" in keratometry readings (mm) on the output values of meridional analysis. Percentage difference is between original output values and those derived when "error" values are applied. Values are given to two decimal places.

#### 4.9 Summary

This chapter has presented a review of the measurement of the anterior corneal radius using keratometric techniques. Keratometric readings were obtained using a standard instrument and meridional analysis applied to these readings.

The degree of precision found for keratometric readings is reflected in the high correlation between the derived and measured values. Applying three meridional analysis to individual subject data can result in errors, particularly in the computed cylinder power and the axis of orientation. If the method is applied to large sample data, however, the mean becomes more reliable.

Three meridional analysis can, therefore, be applied reliably to keratometry readings. As keratometry involves the use of Purkinje images, this would imply that three meridional analysis can be applied to measurements of the posterior corneal surface also obtained using Purkinje images. This is the basis of the technique described in chapter 7 for the assessment of the radius and toricity of the posterior corneal surface.

The next chapter involves the measurement and application of meridional analysis to refractive readings.

CHAPTER FIVE  
MEASUREMENT OF REFRACTION

## MEASUREMENT OF REFRACTION

### 5.1 Introduction

An optometer was used in the present study to obtain objective measurements of the ocular refraction. This chapter presents a brief review of the basis on which these instruments function along with a description of the specific technique employed. The procedure followed to obtain refractive measurements and control possible accommodation and fixation variations is also explained. Results are presented and the application of meridional analysis to refractive data is evaluated.

### 5.2 Objective Optometers

Henson (1983) and Bennett and Rabbetts (1984) provide details of the vast range of techniques available for the determination of refractive error.

Objective optometers work on the basis that some of the light falling upon the retina will be reflected back by the retinal surface. A problem arises here in that the site of the reflecting layer may not necessarily coincide with the subjective focal plane. Several workers (Charman and Jennings, 1976; Millodot and O'Leary, 1978; O'Leary and Millodot, 1978) have suggested that several layers of the retina are jointly responsible for the reflection and that the dominant one can vary according to the wavelength of the light involved, whether it is polarised and the age of the subject. Thus, in an attempt to overcome this problem manufacturers calibrate their instruments against subjective measurements of refraction (Henson, 1983).

The studies of Ferree et al. (1931) and Millodot (1981,1984) both involved the use of coincidence optometers to measure peripheral refraction. Their studies indicated that the central refraction could be determined to a precision  $\pm 0.25D$ .

### 5.3 Measurement of Refraction: Present Study

In the present study, central refraction was measured using the Zeiss (Jena) Hartinger Coincidence Optometer. Henson (1983) and Bennett and Rabbetts (1984) provides a detailed description of this instrument, a summary of which will now be given.

The Hartinger Optometer makes use of a small target composed of three vertical lines divided in two and then passed through different parts of the subject's pupil. In the emmetropic eye the retinal images of both halves of the target are in alignment, whereas in the ametropic eye they are displaced relative to one another. The magnitude and direction of this displacement is related to the degree and type of ametropia (i.e. hyperopia or myopia). Adjustment of the vergence of the light entering the eye allows the two halves of the image to be aligned, so measuring the refractive error present. Readings of the refractive error are made from a scale incorporated into the instrument and calibrated in dioptres at intervals of  $\pm 0.25D$ .

The target also has two horizontal lines, which allow the axes of any astigmatism present to be determined. These again are divided and passed through different parts of the pupil such that if the instrument is not in alignment with one of the principal astigmatic axes, they do not align. The axis of any astigmatism can be found by rotating the whole instrument about its antero-posterior axis until

the lines are aligned. The amount of rotation required is read from a scale incorporated in to the instrument and calibrated in intervals of 1°.

With various other types of objective optometer there can be difficulty in judging when the target is exactly in focus. To assist in making this judgement, the Hartinger Optometer employs the more simple task of aligning target lines, thus giving rise to more accurate estimates of refractive error. Adjustment of the instrument eyepiece to the observers refraction is also important to eliminate accommodation and so ensure accurate readings.

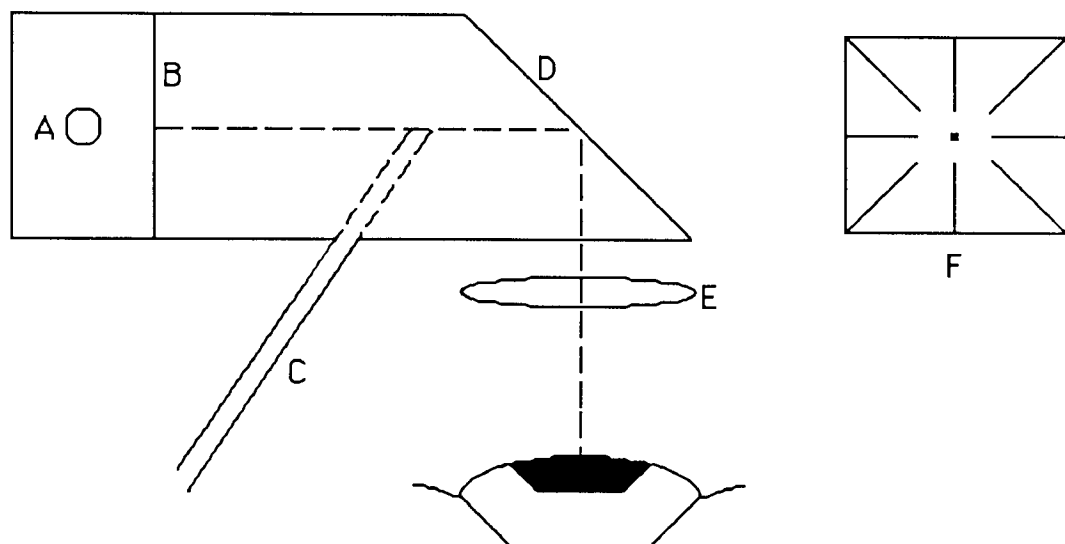
Two problems associated with the Hartinger Optometer are the brightness and the size of the target it uses (Henson, 1983; Bennett and Rabbetts, 1984). The brightness is a compromise between the illumination required to produce a visible retinal image and that which would have a minimal effect on the pupil size and accommodation. The target size of 2mm is also a compromise between the size required to allow sensitive readings and that which would allow measurements to be taken in subjects with small pupils. Furthermore, to reduce the effects of the change in the vergence of the light on accommodation as measurements are taken, it is necessary to approach the subject's refractive error from the positive side.

#### 5.3.1 Measurement of Refraction - Procedure

A chin and forehead rest acted to keep the subject's head steady. To keep fixation and accommodation steady, the non-test eye viewed a fixation target. This target was back illuminated to provide adequate contrast against the light arising from the Hartinger

optometer. The target box was also designed so that vertical and horizontal adjustments could be made in order to guide fixation to the required position. Fig. 5.1 shows a schematic diagram of the target apparatus.

The target apparatus was built in such a way that the target appeared to come from infinity. For ametropic subjects, a correcting lens could be used if needed. Subjects placed their head in the head rest. The instrument was placed in the straight ahead position and the subject asked to look directly into it. Appropriate adjustments were made to the height and position of the instrument until the instrument target could be seen by the observer, through the test eye. The fixation target apparatus was adjusted in front of the non-test eye such that it became coincident with the instrument target, as seen by the test eye.



- A - Light source
- B - Target
- C - Mount, allowing whole box to be adjusted
- D - Mirror
- E - Correcting lens (for ametropes)
- F - Subjects view of target

Figure 5.1 Diagram of target apparatus used with Hartinger Optometer and interchangeable between instruments.

This assured the instrument axis was correctly aligned with the subject's line of sight. Subjects were then asked to direct their attention to the fixation target. Three readings of the central refractive error and axis of orientation were then taken (Appendix 5.1) This was followed by taking three readings in each of the 90°, 180°, and 45° axes, in keeping with the requirements of the meridional analysis program (see section 3.3 and Appendix 5.2) Mean and standard deviation values were calculated from each set of readings. The meridional values were then incorporated into the three meridional analysis program (see section 3.3.1) to allow an evaluation of the application of three meridional analysis to refractive data.

#### 5.4 Subject Profile

The subject profile was as fully explained in section 4.4.

#### 5.5 Precision of Refractive Measurements

Table 5.1 shows the estimated precision of the refractive measurements. The values for this Table were determined in the same manner as described in section 4.5 using data shown in appendix 5.2.

Refractive Component	Mean	Range
Spherical Component	0.23D	0.00 - 1.04D
Cylindrical Component	0.23D	0.00 - 0.58D
Cylinder Axis Component	3.9°	0.00 - 13.3°

Table 5.1. Estimated precision of measurements taken with the Hartinger Optometer. N = 80. Mean precision is twice the value of the stanard deviation. Range is range of standard deviations



## 5.6 Measurement of Refraction: Results

For each subject group, the results are expressed in terms of the mean refraction taken in the 90°, 180° and 45° meridians and the mean refraction in sphero-cylindrical form following the application of three meridional analysis.

### 5.6.1 Group Mean Refraction in Three Meridians

Table 5.2 shows the mean meridional refractive values arranged in terms of age, refractive group and gender (see appendix 5.3 also). Statistical analysis of the results in each of category is the subject of a section of chapter 8.

Subject Group	MERIDIAN					
	90°		180°		45°	
Young Male Myopes	-3.21	(±1.63)	-3.09	(±1.48)	-3.09	(±1.56)
Young Female Myopes	-4.85	(±4.33)	-4.83	(±4.17)	-4.65	(±4.06)
Old Male Myopes	0.00	(±0.72)	-1.89	(±0.48)	-1.17	(±0.13)
Old Female Myopes	-1.30	(±1.28)	-1.97	(±1.12)	-1.50	(±0.95)
Young Male Emmetropes	-0.17	(±0.26)	-0.18	(±0.22)	-0.15	(±0.23)
Young Female Emmetropes	-0.04	(±0.29)	-0.05	(±0.33)	0.02	(±0.30)
Young Male Hyperopes	+1.35	(±0.99)	+0.48	(±1.18)	+0.58	(±0.73)
Young Female Hyperopes	+1.43	(±1.09)	+1.27	(±0.55)	+1.48	(±1.09)
Old Male Hyperopes	+2.36	(±1.04)	+2.44	(±1.34)	+2.48	(±1.11)
Old Female Hyperopes	+2.77	(±1.59)	+2.40	(±1.25)	+2.52	(±1.01)

Table 5.2. Mean refractive power (D) in three meridians for the subject groups. Values in brackets refer to standard deviation. N = 80.

## 5.6.2 Group Mean Refractive Power in Sphero-cylindrical Form after Meridional Analysis

Table 5.3 shows the mean refractive power in sphero-cylindrical form arranged in terms of age, refractive group and gender (see appendix 5.2). Statistical analysis of the results in each of category is the subject of a section of chapter 8.

Subject Group	Sphere (D)	Cylinder (D)	Axis (°)
Young Male Myopes	-3.61 (±1.51)	0.98 (±0.68)	110.9 9 (±41.1)
Young Female Myopes	-5.21 (±4.39)	0.95 (±0.73)	88.7 (±37.6)
Old Male Myopes	-1.94 (±0.50)	2.00 (±1.23)	7.3 (±5.9)
Old Female Myopes	-2.15 (±1.18)	1.01 (±0.41)	154.5 (±31)
Young Male Emmetropes	-0.36 (±0.22)	0.37 (±0.19)	81 (±51.3)
Young Female Emmetropes	-0.26 (±0.24)	0.44 (±0.28)	102.7 (±51.1)
Young Male Hyperopes	0.09 (±1.15)	1.65 (±1.57)	57.6 (±42.9)
Young Female Hyperopes	0.94 (±0.59)	0.81 (±0.52)	103.5 (±44.7)
Old Male Hyperopes	1.97 (±1.12)	0.86 (±0.64)	136.8 (±40)
Old Female Hyperopes	2.02 (±1.19)	1.13 (±0.62)	84.8 (±57.5)

Table 5.3. Mean values of the refractive sphero-cylindrical component for the subject groups. Values in brackets represent standard deviation. N = 80.

## 5.7 Correlation Between the Measured and Refractive Sphero-cylindrical Data and that Derived by Three Meridional Analysis

Figure 5.2 shows the scatter plot for the spherical refractive component values measured using the optometer and that derived by meridional analysis. A high correlation is found between the two sets of values ( $r = 0.99$ ;  $P < 0.001$ ).

Figure 5.3 shows the scatter plot for the measured and calculated cylindrical component values. A high correlation is again found between the two sets of values ( $r = 0.89$ ;  $P < 0.001$ ), though overall it is slightly lower than that for the spherical component.

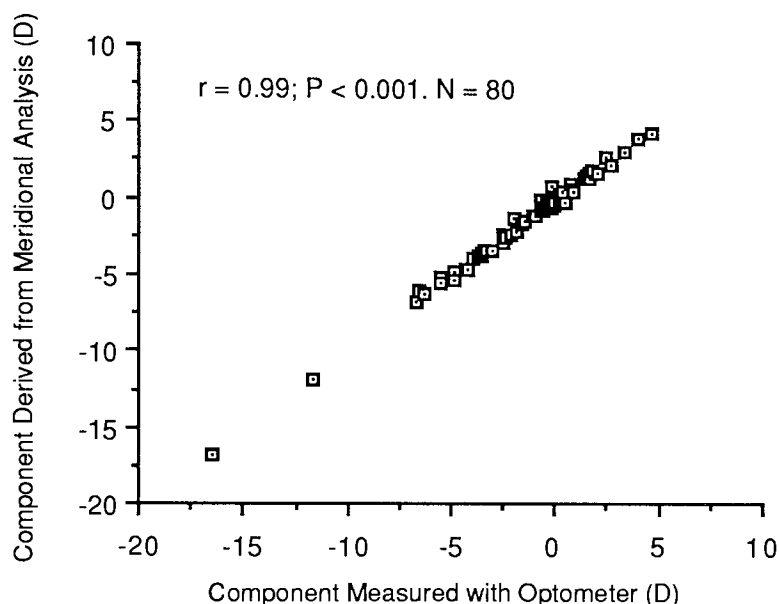


Figure 5.2 Scatter plot of measured spherical component (D) and that derived from meridional analysis.

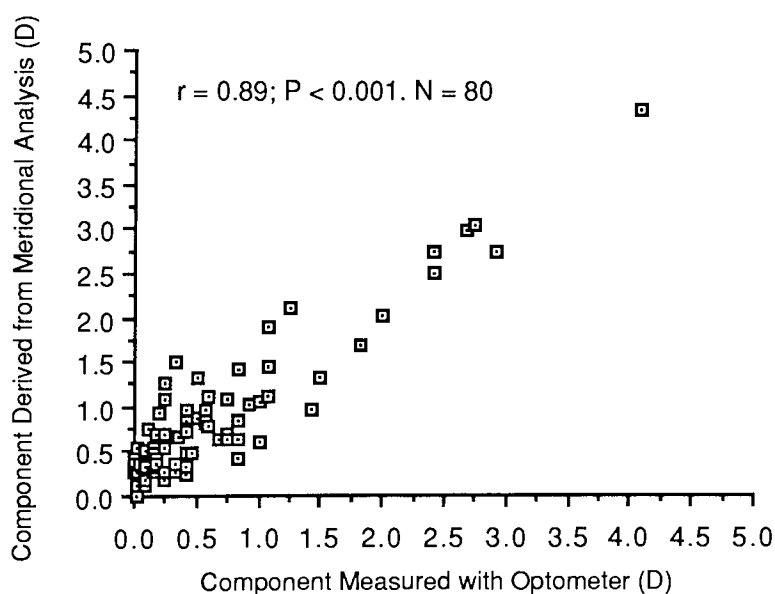


Figure 5.3 Scatter plot of measured cylindrical component (D) and that derived from meridional analysis.

Figure 5.4 shows the scatter plot for the measured and calculated cylinder axis orientation.

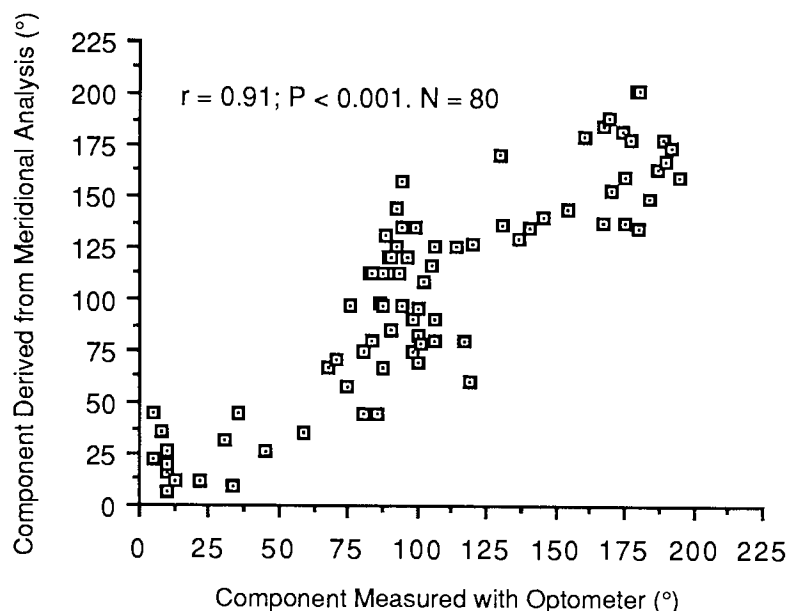


Figure 5.4 Scatter plot of measured cylinder axis orientation (°) and that derived from meridional analysis.

As for the spherical and cylindrical components, a high correlation for the cylinder axis orientation is found ( $r = 0.91$ ;  $P < 0.001$ ) but it is slightly lower than that for the spherical component.

Overall, high correlations were found for the measured and calculated refractive results. Correlations were, however, slightly lower than those found for the keratometric data (see chapter 4).

The relatively poor correlation for the measured and calculated cylindrical component results were in keeping with the comments made by Long (1974), in that errors in the original meridional refractive readings would lead to overestimation of the power of the cylindrical component and variability in the cylinder axis orientation.

Table 5.4 shows the magnitude of differences for percentages of the

population measured. From this Table it can be seen that the differences for the mean spherical component are quite small for a large percentage of the group. The magnitude of differences for the cylindrical component are slightly greater overall when compared to the spherical component. When considering the results for the cylinder axis orientation, the variability of cylinder axis orientation with three meridional analysis techniques described by Long (1974) seem to be evident, with approximately half of the readings being within  $\pm 20^\circ$ . This is in contrast to the value of 76.7% obtained for the keratometric readings (section 4.7).

Refractive Component		Percentage of Subjects N = 80
Sphere	$\pm 0.25D$	65.9%
	$\pm 0.50D$	93.4%
	$\pm 1.00D$	100%
Cylinder	$\pm 0.25D$	45.9%
	$\pm 0.50D$	84.2%
	$\pm 1.00D$	100%
Axis	$\pm 5^\circ$	18.4%
	$\pm 10^\circ$	32.5%
	$\pm 20^\circ$	49.2%
	$> 20^\circ$	50.8%

Table 5.4. Population percentages for the magnitude of differences in sphere, cylinder and axis components between principle meridional measurements and analysis of three meridional measurements.

Table 5.5 shows the group mean refractive data. It can be seen that there is reasonably good agreement between the measured readings and those derived from meridional analysis.

Refractive Component		Mean ( $\pm$ SD)
Spherical Component (D)	Measured	-0.53( $\pm$ 2.53)
	Derived	-0.68( $\pm$ 2.69)
Cylindrical Component (D)	Measured	0.69( $\pm$ 0.80)
	Derived	1.04( $\pm$ 0.90)
Cylinder Axis Component ( $^{\circ}$ )	Measured	118.2( $\pm$ 54.3)
	Derived	132.6( $\pm$ 47.3)

Table 5.5. Comparison between mean measured refractive data and that derived from meridional analysis.

The most obvious point that can be made from this Table is that the computed average cylinder is appreciably larger than the measured average cylinder. This finding is again in keeping with the comments of Long (1974).

## 5.8 Summary

This chapter has presented a brief review of how refraction can be measured using an optometer. A detailed description of the actual optometer used in this study and how it was used to obtain measurements in the principal meridians and three other meridians ( $45^{\circ}$ ,  $90^{\circ}$  and  $180^{\circ}$ ) was also presented.

A high correlation was found between the data obtained by direct measurement and that derived from meridional analysis. The results of the application of three meridional analysis to ocular refraction are susceptible to the errors described by Long (1974). Hence, errors arise for the cylindrical component and its axis of orientation when three meridional analysis is applied. Errors involved in the application of meridional analysis to refractive data were greater

than those found for keratometric data.

Having evaluated the use of meridional analysis on refractive and keratometric data, the following chapter discusses the measurement of corneal thickness.

CHAPTER SIX  
MEASUREMENT OF CORNEAL THICKNESS



## MEASUREMENT OF CORNEAL THICKNESS

### 6.1 Introduction

The accurate measurement of corneal thickness (pachometry) has attracted the attention of many workers in connection with contact lens fitting, corneal grafting and the study of such pathological conditions as glaucoma. This section presents an overview of pachometric techniques along with a description of the instrument used and the measurement procedure followed in the present study.

### 6.2 Corneal Thickness and Pachometric Techniques

The measurement of corneal thickness can be made using several different methods. One method is to successively focus the slit lamp microscope on the specular reflexes of the anterior corneal surface and the posterior corneal surface. The respective distances travelled then represent the apparent thickness of the cornea. To obtain the true values of thickness the conjugate foci relationship is applied (Bennett and Rabbetts, 1984). The first attempts to measure the corneal thickness (Blix, 1880; Ulbrich, 1914) used a similar approach to that described above. However, the problem with this method is that it is susceptible to involuntary movements of the subject's head as the measurements are being taken and, thus, measurements could only be made to an accuracy of  $\pm 0.1\text{mm}$  (Von Bahr, 1948).

Von Bahr (1948) developed a pachometer, to measure corneal thickness, in which two glass plates could be rotated about the vertical plane so that in the field of view of the slit lamp microscope, the reflection of the slit in the corneal endothelium

could be made to coincide with that of the corneal epithelium. The angular rotation of the glass plates required for the alignment of the two images could be read from a calibrated scale and related to the true corneal thickness by trigonometric calculations. Because this allowed the simultaneous observation of doubled specular reflexes, the problems caused by eye movement were overcome. The standard deviation obtained for the corneal thickness readings was found to be  $\pm 0.013\text{mm}$ . Various changes were made to Von Bahr's (1948) technique to improve the accuracy, subject alignment and measurements of thickness of the cornea in the periphery (Maurice and Giardini, 1951; Donaldson, 1966; Mandell and Polse, 1969; Hirji and Larke, 1978). A precision of  $\pm 0.03\text{-}0.04\text{mm}$  was reported by Hirji and Larke (1978) for measurements of the peripheral corneal thickness using topographic pachometry.

A technique for the measurement of the apparent thickness of the optical section as seen by diffuse reflection was described by Juillerat and Koby (1928). Later improvements to this technique allowed simultaneous observation of the anterior and posterior corneal surfaces by means of a split ocular (Lobeck, 1937). Jaeger (1952) then combined the rotating glass plate method of Von Bahr (1948) with a split ocular to produce an attachment for the Zeiss Opton slit lamp. The method of Jaeger (1952) was improved further and was made available for use with the Haag Streit 900 slit lamp (Lowe, 1966). This is now the standard and most widely used pachometer for the convenient and accurate measurement of central corneal thickness. Alsbirk (1974) found the random errors of this method, assessed by taking triple readings and successive examinations over several weeks, to be  $\pm 0.007\text{mm}$  and  $\pm 0.013\text{mm}$  respectively. Three components were identified by Edmund and La Cour (1986) as affecting the precision of pachometric

measurements: the day to day variation ( $\pm 0.006\text{mm}$ ), the variation due to slit lamp adjustment ( $\pm 0.005\text{mm}$ ) and that due to pachometer adjustment ( $\pm 0.013\text{mm}$ ). They suggested that at least three pachometric readings should be made on each occasion.

One of the drawbacks of the Haag Streit 900 slit lamp technique is that it makes depth measurements with respect to the line of sight. This may produce a systematically thicker corneal reading for the left eye than the right eye (Kruse-Hansen, 1971), as the line of sight does not pass through the geometric centre of the cornea. Alsbirk (1974), however, found no such difference. In an attempt to increase the accuracy of the Haag Streit 900 attachment, Mishima and Hedbys (1968) tried to ensure perpendicular alignment to the corneal surface. Subsequent workers used this improvement to measure the peripheral corneal thickness (Martola and Baum, 1968; Tomlinson, 1972).

Other more complex pachometric techniques have been developed, such as the electric pachometer of Binder et al (1977). An ingenious method involving the use of astigmatic light bundles has also been developed (Lindsted, 1916; Stenstrom, 1953; Tornquist, 1953). Generally, however, their complexities have led many workers to prefer conventional pachometers.

### 6.3. Measurement of Corneal Thickness: Present Study

Optical determinations of the corneal thickness were made with the Haag Streit 900 corneal thickness pachometer. Descriptions of this instrument are provided by Lowe (1966), and a summary of its use will now be given.

A vertical slit of light is used to illuminate a section of the eye to be measured. This section is viewed at an angle of 40° to the right, with respect to the observer. Two plane glass plates, one placed above the other, bisect the reflected light rays passing to the eyepiece for the observer's right eye. The lower glass plate is set at 90° to the reflected light so that rays passed directly through it. The upper glass plate can be pivoted, so deviating the light passing through it. A split ocular is used for the right eyepiece so that the images from the lower and upper glass plates may be seen in the lower and the upper halves of the field respectively.

When both plates are parallel a single image can be seen. After rotation of the upper plate, however, the upper set of images appear deviated. By this means the front surface of the cornea in the lower set of images may be aligned with the back surface of the cornea in the upper set. The rotation required to do this can be read directly from a millimetre scale calibrated in 0.01mm graduations. This scale is calibrated such that the readings obtained represented the corneal thickness for an assumed corneal radius of 8.00mm as well as an assumed value for the corneal refractive index of 1.376. However, for the purposes of this study, the corneal thickness readings from the scale were converted to apparent thickness using the equation:

$$d = 1000 + (((1.376 \times 1000) / d_1) - F_1)$$

Then true corneal thickness values were obtained using:

$$d_1 = (n \times 1000) / (F_1 + (1000/d))$$

where  $n = 1.3771$  (see section 1.6) and  $F_1 =$  value derived from keratometric readings as described in section 1.6

### 6.3.1 Measurement Procedure

A chin and forehead rest were used to keep the subject's head steady. The subject was asked to look into the slit beam with the test eye to ensure alignment with the line of sight. The non-test eye was occluded. Horizontal adjustments to the position of the pachometer were made such that the vertical slit was centred with respect to the pupil. Vertical adjustments were also made to ensure the split ocular was centred with respect to the pupil. The slit image was kept in focus at all times.

Three pachometric readings of the corneal thickness were taken from all the subjects from which mean and SD values were calculated. True corneal thickness readings were calculated using the method described above (Appendix 6.1)

### 6.4 Measurement of Corneal Thickness: Subject Profile

The subject profile was as described in section 4.4

### 6.5 Precision of Corneal Thickness Measurements

Table 6.1 shows the estimated precision for the pachometric measurements. These values are derived using the same principle as used to derive the values in section 4.5, from the results summarized in appendix 6.1.

	Mean	Range
Corneal Thickness (mm)	0.018	0.00 - 0.023

Table 6.1. Estimated precision of the pachometric measurements (mm) N = 80.

## 6.6 Measurement of Corneal Thickness: Results

The values for the corneal thickness are summarized in Table 6.2 in terms of age, refractive group and gender.

Statistical analysis of the results summarized below is the subject of a later chapter.

Subject Group	Corneal Thickness (mm)
Young Male Myopes	0.498 ( $\pm 0.018$ )
Young Female Myopes	0.484 ( $\pm 0.021$ )
Old Male Myopes	0.468 ( $\pm 0.010$ )
Old Female Myopes	0.48 ( $\pm 0.009$ )
Young Male Emmetropes	0.507 ( $\pm 0.047$ )
Young Female Emmetropes	0.492 ( $\pm 0.025$ )
Young Male Hyperopes	0.493 ( $\pm 0.009$ )
Young Female Hyperopes	0.518 ( $\pm 0.021$ )
Old Male Hyperopes	0.498 ( $\pm 0.031$ )
Old Female Hyperopes	0.481 ( $\pm 0.024$ )

Table 6.2. Mean values of corneal thickness (mm). Values in brackets represent the standard deviation. N = 80.

## 6.7 Summary

This chapter has presented a review pachometric technique. Despite the development of a number of complex methods for measuring corneal thickness, many workers prefer to use conventional pachometers. The actual instrument used in this study is a conventional instrument and the procedure followed to obtain measurements has been described. The results obtained and their precision are also summarized.

The following chapter describes a method that utilizes pachometric readings and keratometric readings to obtain values for the posterior corneal radius.

CHAPTER SEVEN  
POSTERIOR CORNEAL RADIUS



## POSTERIOR CORNEAL RADIUS

### 7.1 Introduction

Measurement of the radius of the posterior corneal surface has attracted relatively little attention when compared to the anterior corneal surface. A number of workers have made measurements of the radius of the surface in one meridian, but there have been few attempts to assess its toricity. A detailed description is presented of a technique developed to allow measurement of the posterior corneal radius in three meridians in keeping with the requirements of the meridional analysis program, thus allowing evaluation of the toricity of this surface.

### 7.2 Posterior Corneal Radius

Gullstrand (Southall, 1924) and Tscherning (1924) found that they could not measure the posterior corneal curvature centrally due to the interference by the first catoptric (Purkinje) image and so they calculated the radius of the surface from more peripheral measurements.

Attempts to measure the radius of the posterior corneal surface in large samples have been made by Lowe and Clark (1973) and Hockwin et al., (1983). However, these readings were confined to the vertical meridian because measurements were taken from corneal sections using either a photographic slit lamp (Lowe and Clark, 1973) or a Scheimpflug camera (Hockwin et al, 1983). Neither of these two methods readily lend themselves to the collection of data in meridians other than the vertical.

Alternatively, measurements of the catoptric (Purkinje) images arising from both corneal surfaces can be used to obtain values for the posterior corneal radius. As described in section 7.3, the apparatus required is relatively uncomplicated and allows the determination of radii in different meridians. Indeed, Tscherning (1904) used a similar technique to compare the posterior corneal surface radius in the horizontal and vertical meridians of three subjects. Only limited information can be gained from measurements taken in two meridians. A technique will be described in this chapter in which measurements may be taken in three meridians, thus fulfilling the requirements of the three meridional analysis program and so producing values for the spherocylindrical components of the posterior corneal surface.

### 7.3 Measurement of Posterior Corneal Radius : Present Study

The method described in this section allows the posterior corneal surface radii to be determined by measuring the catoptric (Purkinje) images in three fixed meridians. It is based on a modification to the Canon Auto-Ref R1 Optometer which is described below.

The Canon Auto-Ref R1 is an infra-red optometer, fully described elsewhere by Matsumura et al. (1983) and McBrien and Millodot (1985). The modifications that were made to allow Purkinje image photography involved the use of clear perspex carriages on which a number of fibre optic cables were mounted at various orientations. Two carriages were constructed (Figures 7.1 and 7.2). The first model used two fibre optic cables mounted in the vertical ( $90^\circ$ ) meridian. The second model was essentially a modification of the first one and used four fibre optic cables arranged in a slightly different manner. Two cables were placed in the horizontal

meridian, but only one was placed in each of the vertical ( $90^\circ$ ) and oblique ( $45^\circ$ ) meridians.

The fibre optic cables were linked to the illumination system of a Zeiss (Jena) 110 slit lamp, which was set at maximum intensity to provide sufficient light output to make the Purkinje images bright enough to be photographed.

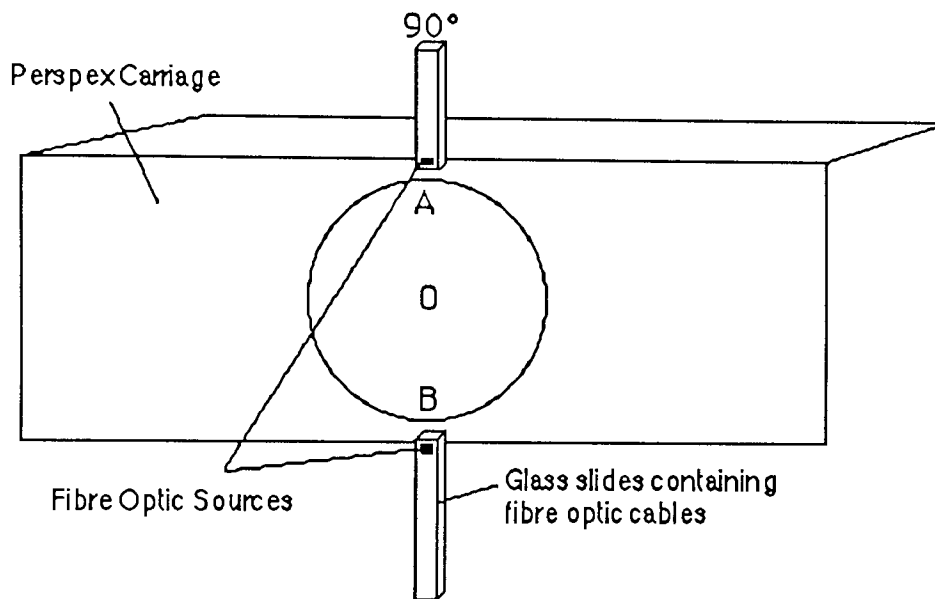


Figure 7.1 Diagrammatic representation of carriage with two light sources on the  $90^\circ$  meridian.

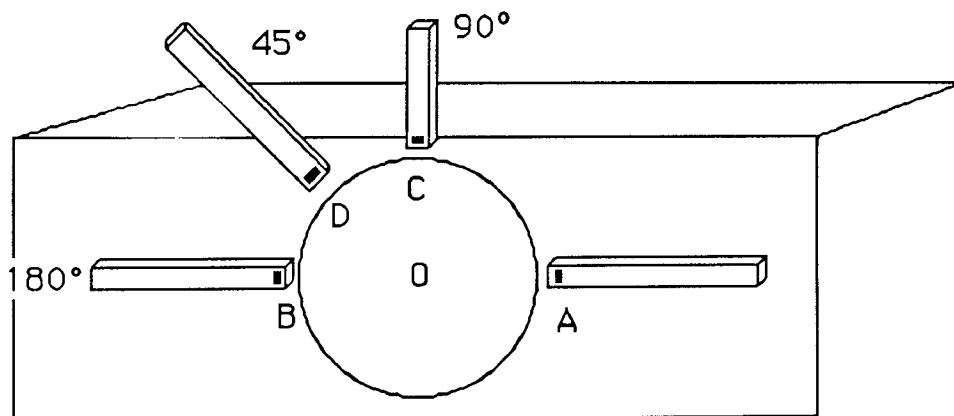


Figure 7.2 Diagrammatic representation of the carriage with one source in each of the  $90^\circ$  and  $45^\circ$  meridians

The fibre optic cables were sandwiched between glass microscopic slide plates at the correct orientation such that when the carriage was placed on the optometer the light they emitted would fall perpendicularly on the surface of the subject's cornea. Each source was set at a distance of about 50mm from the point O to ensure optimum separation of the first and second Purkinje images, whilst operating at a distance of about 50mm from the eye. The light sources were mounted on the Canon AutoRef R-1 (Figure 7.3) and the subjects visual axis was made to coincide with the instrument axis at point O. This point was, in fact, theoretical as the space between the light sources was left unobstructed to allow the subject a clear field of view.

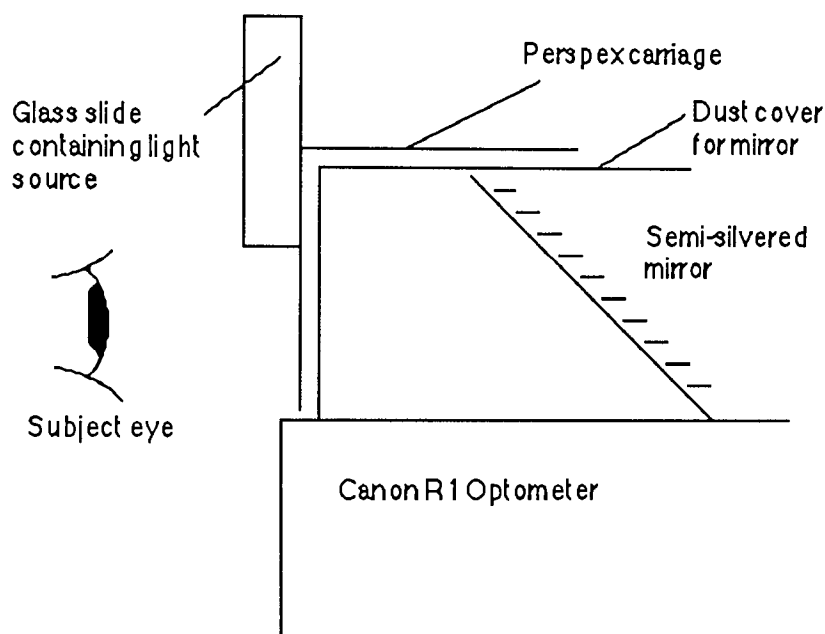


Figure 7.3 Schematic side-view of perspex carriage mounted on the Canon R1 Optometer

When using the optometer normally, use is made of a video monitor to ensure the instrument is correctly aligned before the subject eye. In addition, there are two infra-red light sources incorporated into the instrument which aid alignment. By extinguishing these and replacing them with the sources mentioned above, it was possible to obtain the Purkinje images from the anterior and posterior corneal

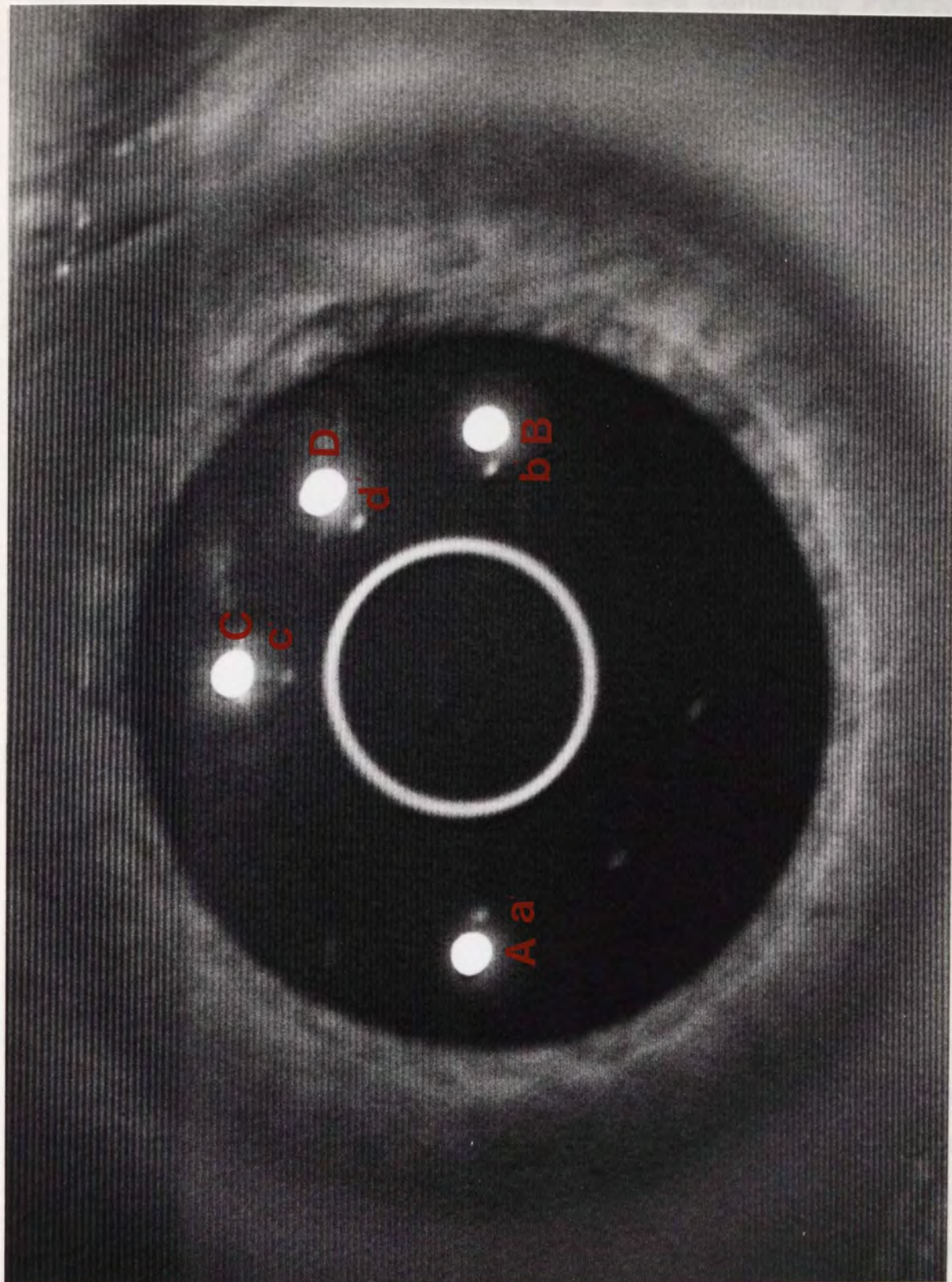


Figure 7.4 Photograph of the first and second Purkinje images as taken from the video monitor of the Canon R1 Optometer. See text also.

surfaces on the monitor screen. To photograph the images, a Tektronic C59 oscilloscope camera was used containing Polaroid Land Pack 3000 ASA black and white film. One photograph was taken per subject with the camera set at 1/25 second shutter speed and aperture number f/16. Figure 7.4 shows a sample photograph. One photograph was taken per film pack used of a 1mm square grid. This allowed the magnification and distortion arising from the whole system to be determined.

Purkinje image heights were measured as shown diagrammatically in Figure 7.5.

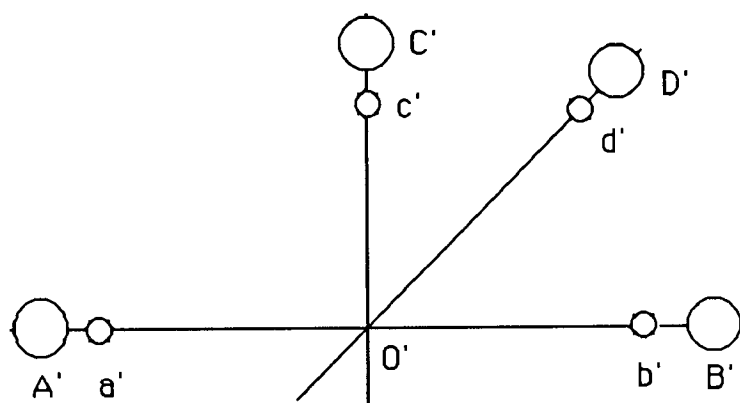


Figure 7.5 Diagrammatic representation of the first and second Purkinje images as to be measured from the photographs

The images arising from the anterior surface are represented by upper case letters and those from the posterior surface are represented by lower case letters. In the case of the two-meridional data, the separations were measured directly from the photograph, from between the two matching images in each meridian, i.e. A' to B', a' to b'. In the case of the three meridional data a slightly different approach was taken. With reference to Figure 7.5, a line was drawn on the photograph between the points A and a', and B and b'. Measurements along this line between the points gave values for the



Purkinje image heights in the horizontal meridian. To determine the heights in the other meridians, 90° and 45°, a line was drawn from C and D to bisect the horizontal line at point O. Anterior and posterior heights were then measured to the point O, and the true values obtained by multiplying this value by two. (i.e. 2 x CO, 2 x DO, 2 x c'O and 2 x d'O). Measurements were taken directly from the photographs, using engineering calipers, to the nearest  $\pm 0.1\text{mm}$ , representing  $\pm 0.016\text{mm}$  on the eye. This particular technique of measurement resembles that used by Van Veen and Goss (1988) in their analysis of Purkinje image size. Ten estimates of the Purkinje image height in each meridian were made and a Purkinje image ratio, P, was determined from:

$$P = P_2 / P_1$$

where  $P_1$  = height of first Purkinje image, and  $P_2$  = height of second Purkinje image (Appendix 7.1).

Ten measurements of the magnification in the horizontal and vertical planes were made per photograph taken of the grid to estimate distortion. Repeat photographs were taken on 23 of the subjects to assess the repeatability of the technique.

### 7.3.1 Correlation of Data from One-source and Two-source Measurements

The design of the carriages containing the fibre optic cables was governed by the construction of the optometer and the requirement for the rapid conversion of the instrument to and from its original form. It was these restrictions that resulted in the carriage used to take three meridional measurements (Figure 7.2) having only one light source in each of the 90° and 45° meridians. To investigate the possibility that such a situation would lead to inaccuracies, the

results obtained using the one source in the 90° meridian were correlated with those obtained using two sources in the 90° meridian.

Table 7.1 shows the magnitude of differences for the Purkinje image ratios from the one-source and two-source methods for percentages of the subjects studied. From this Table it can be seen that just over two-thirds of the measurements were within  $\pm 0.005$  units. All of the measurements were within 0.010 units. Such values indicate that the one-source method is a reasonably good substitute when it is not possible to use the two-source method, and that it can be applied with confidence to other meridians.

Difference between one and two source values of P	Percentage of Subjects (N = 80)
$\pm 0.005$ units	67.5%
$\pm 0.010$ units	32.5%
$\pm 0.015$ units	0%

Table 7.1. Magnitude of differences in Purkinje image ratios from one-source and two-source methods.

Figure 7.6 shows a scatter plot of the Purkinje image ratios derived from the one source and two source methods (Appendix 7.2). Overall there is a good correlation between the measurements taken using the two methods ( $r = 0.98$ ;  $P < 0.001$ ).



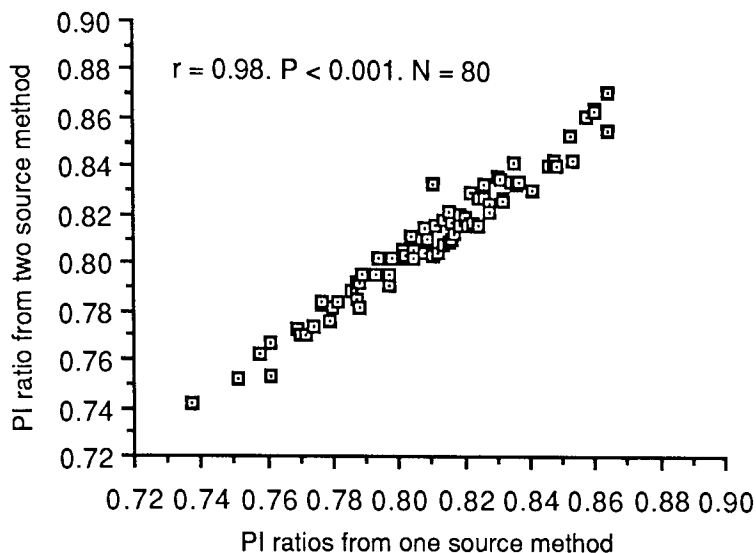


Figure 7.6. Scatter plot of Purkinje image ratios from one source and two source methods.

#### 7.4 Subject Profile

Subject profile was as described in section 4.4.

#### 7.5 Posterior Corneal Radius: Measurement Procedure

The subject's head was held steady in the chin and headrest incorporated into the instrument. Fixation was then guided towards the target apparatus mounted on the instrument (described in the section 5.3). The instrument was adjusted until the Purkinje images from the anterior and posterior corneal surfaces could be seen in focus on the monitor screen. Care was taken to ensure that the images were centred with respect to the cornea and pupil. Once the correct alignment had been obtained a single polaroid photograph was taken directly from the video monitor screen using the oscilloscope camera described earlier (section 7.3). Depending on the temperature in the research room, a period of between 40 and 60 seconds had to pass before the photograph was developed and could be examined.

The appropriate measurements, as described in section 7.3, were then taken from each photograph.

## 7.6 Computation of Results

The computer program allowing calculation of the posterior corneal radius requires information on the anterior corneal radius (section 4.3, appendix 4.1), the corneal thickness (section 6.2, appendix 6.1) and the Purkinje image ratios (section 7.3). With this data it is possible to calculate the posterior corneal radius along each of the selected meridians. The following equations, assuming a value for the refractive index of the cornea ( $n$ ) to be 1.3771 (Le Grand and El Hage, 1980) are those incorporated into the program.

Initially, the dioptric power of the anterior corneal surface ( $F_1$ ) is determined :

$$F_1 = ((n-1) \times 1000) / r_1$$

where  $n$  = refractive index of cornea, and  $r_1$  = corneal radius (mm).

The apparent position of the posterior corneal surface (the apparent corneal thickness,  $d'$ ) is then determined :

$$d' = 1000 / (((1000 \times n) / d) - F_1)$$

It is then possible to determine the apparent radius of the posterior corneal surface ( $r'_2$ ) :

$$r'_2 = P \times r_1$$

where  $P$  = Purkinje image ratio.

The posterior corneal radius,  $r_2$ , can be derived from :

$$r_2 = ((n \times 1000) / (F_1 + (1000 / (d' + r'_2)))) - d$$

Using these equations the radius of the posterior corneal surface was calculated in the 90°, 180° and 45° meridians (Appendix 7.3). The radii values obtained were incorporated into the meridional program described in section 3.3. This allowed the spherocylindrical components of the posterior corneal surface to be obtained (Appendix 7.4).

### 7.7 Repeatability of Posterior Corneal Radius Measurements

As mentioned in section 7.3, repeat readings were taken from 23 of the subjects in order to assess the repeatability of the method used. Repeat values for the posterior corneal radius in the 90°, 180° and 45° meridians and for the values expressed in spherocylindrical form were obtained as described in section 7.3 and 7.6. The repeat radii values are summarized in appendix 7.5 and the repeat values in spherocylindrical form are summarized in appendix 7.6.

Figure 7.7 shows the scatter plot for the correlation between the original and repeat radii values obtained in the 90° meridian. A high correlation was found ( $r = 0.96$ ;  $P < 0.001$ ).

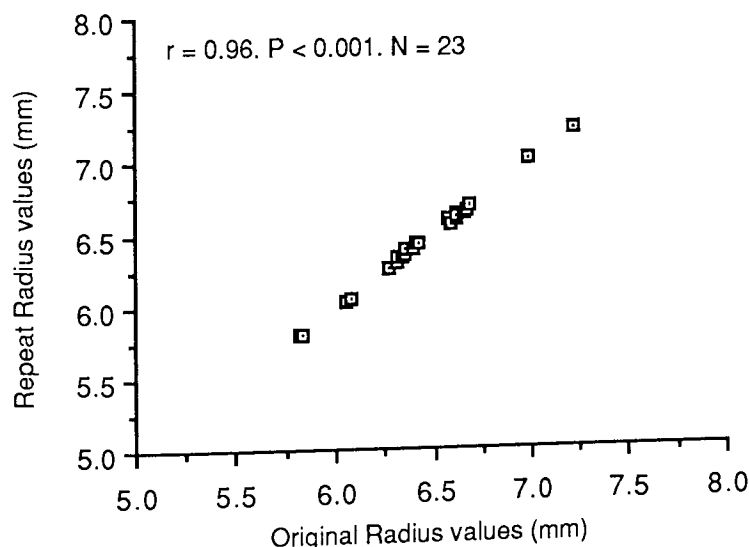


Figure 7.7 Scatter plot of original and repeat posterior corneal radius values (mm) 90° meridian.

Figure 7.8 shows the scatter plot for the correlation between the original and repeat radii values obtained in the 180° meridian. A high correlation was found ( $r = 0.98$ ;  $P < 0.001$ ).

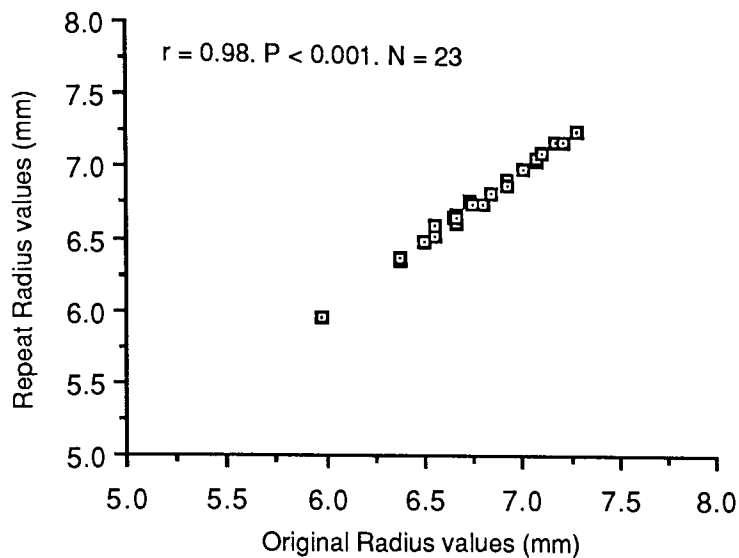


Figure 7.8 Scatter plot of original and repeat posterior corneal radius values (mm), 180° meridian.

Figure 7.9 shows the scatter plot for the correlation between the original and repeat radii values obtained in the 45° meridian. A high correlation was again found ( $r = 0.96$ ;  $P < 0.001$ ).

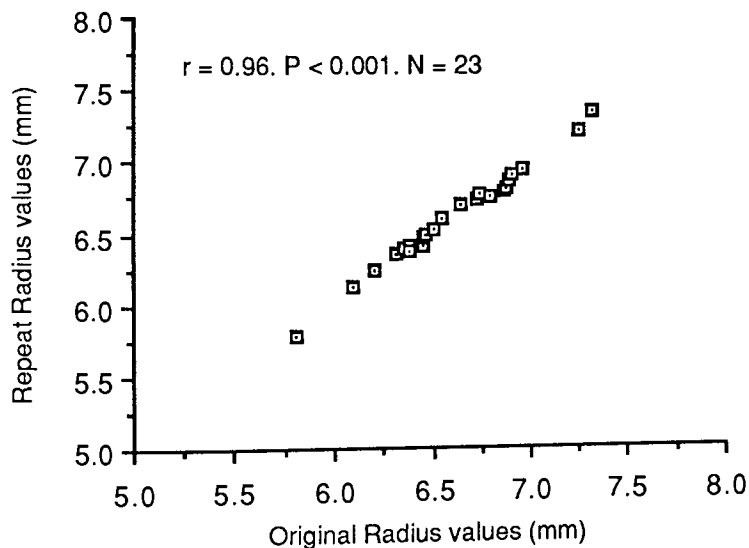


Figure 7.9 Scatter plot of original and repeat posterior corneal radius values (mm), 45° meridian.

Figures 7.10, 7.11 and 7.12 show scatter plots of the correlation for the spherocylindrical component data derived using the original and repeat radii values. There is a good correlation between the spherical components ( $r = 0.98$ ;  $P < 0.001$ ), the cylindrical components ( $r = 0.94$ ;  $P < 0.001$ ) and the cylinder axis orientation ( $r = 0.90$ ;  $P < 0.001$ ).

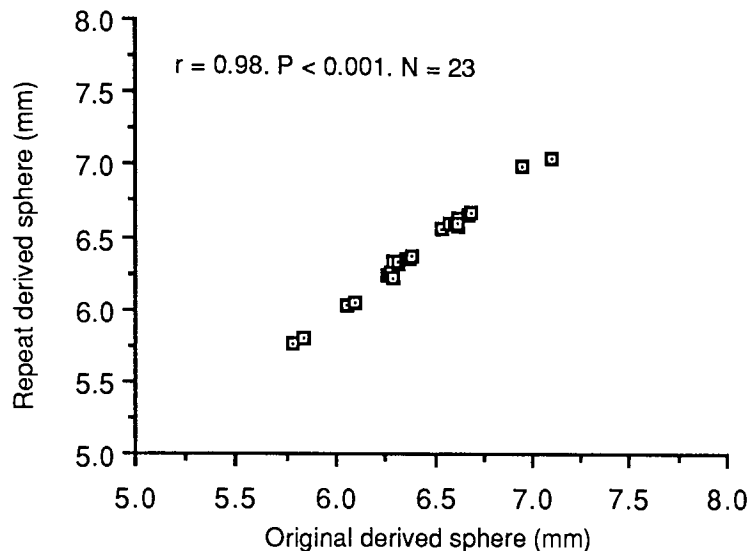


Figure 7.10 Scatter plot of original and repeat posterior corneal spherical component (mm).

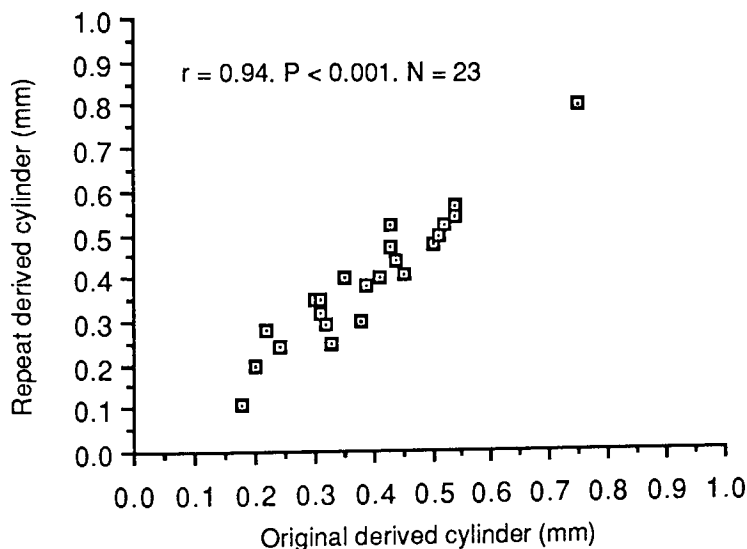


Figure 7.11 Scatter plot of original and repeat posterior corneal cylindrical component (mm).

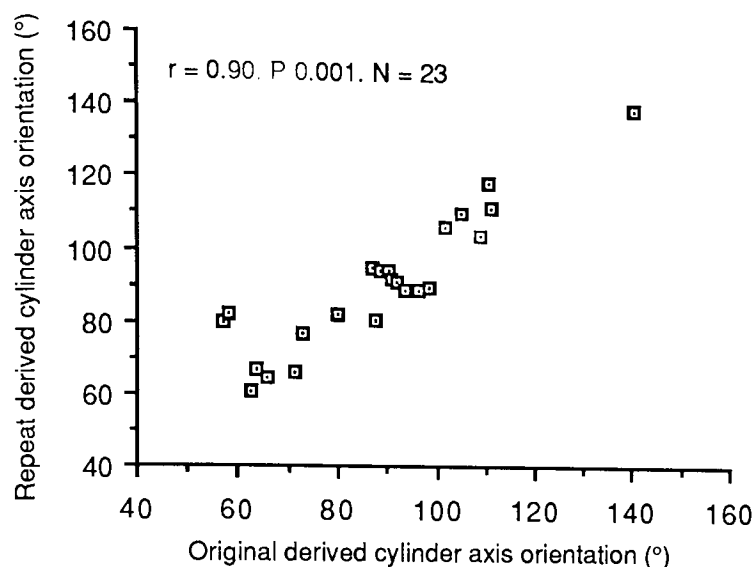


Figure 7.12 Scatter plot of original and repeat posterior corneal cylinder axis orientation (°).

The fall in correlation for the cylindrical component and the axis of orientation are in keeping with the findings of the application of meridional analysis to keratometric and refractive readings (chapters 4 and 5 respectively).

Overall, the data presented in these graphs would indicate that the technique developed in this study to measure posterior corneal radius produces results that are highly repeatable.

## 7.8 Assessment of Magnification and Distortion from Grid Photographs

As mentioned in the section 7.3, the magnification and distortion on the polaroid photographs of the corneal Purkinje images was assessed by taking one photograph, per pack used, of a grid placed in the position that would normally be occupied by the subject eye. The grid used consisted of fine drawn graph paper showing grid lines of 1mm separation. For measurement purposes a horizontal and vertical

line was drawn on the grid. These intersected each other in the centre of the grid which coincided with the centre of the photographic field. The photographs of the grid were then treated as those taken of the eye.

The interval between successive grid lines, which were positioned horizontally above and below as well as vertically to the right and left of the grid centre, were measured out to 4mm. The 8mm field thus used allowed the distortion to be assessed over an area larger than that covered by the Purkinje images. Measurements were made with engineering calipers to the nearest 0.10mm and the results are shown in appendix 7.7 Five measurements of the distance between each grid line were made. Therefore, the total number of observations (ie measurements) made per meridian per photograph equalled forty (ie  $5 \times 8$ ).

The real distance between the grid lines was 1mm. Therefore, the values measured from the photographs were a direct estimate of the magnification. For each meridian, the values between successive grid lines were added together. This value, when divided by the total number of grid lines, would correspond to the overall magnification. An overall magnification of 6.13x was determined in this way.

Table 7.2 shows the range, mean and standard deviation of the separations between the grid lines in the horizontal and vertical meridians of the grid.

The range of magnification values (distortion) found in both planes never exceeded 1mm which represented only 2% of the mean value and a scaled distance of 0.02mm. Therefore, any distortion which could have led to this spread in the results was considered to be

negligible.

Value	Total Separation Between Grid Lines	
	Horizontal Meridian	Vertical Meridian
Range	48.88-49.68mm	48.96-49.18mm
Mean	49.15mm	49.05mm
S.D.	±0.27mm	±0.09mm

Table 7.2. The range, mean and standard deviation of the total separation between grid lines in the horizontal and vertical meridians of the photographed grid. Total number of observations per meridian per photograph is 40.

## 7.9 Validation of Purkinje image Technique

A photographic slit-lamp technique was used to validate the values obtained from the Purkinje image method described in section 7.3.

### 7.9.1 Validation Procedure

The slit lamp photography method used was similar to that method used by Lowe and Clark (1973). A Zeiss photographic slit lamp model 211 was used. Slit lamp sections were obtained with the arms of the illumination and observation systems fixed at 60°. Photographs were taken with an aperture of f/4 and reproduction ratio of magnification x1.6 using Ilford HP5 400ASA black and white film. The slit beam was set at its maximum height (11mm) and minimum width (0.2mm) and the flash unit was set at the maximum energy setting (480Ws). An exposure of 100ms was made (three photographs were taken per subject). Measurements were made from photographic negatives after projection against a fixed screen.



To obtain values of the posterior corneal radius, the photographic sections were first projected against a fixed screen. The curves of the posterior corneal surface were then matched against arcs of set radius drawn on clear acetate sheets. These sheets were designed on the assumption that a line perpendicular to the cornea which passes through the centre of the pupil (pupillary axis) is an acceptable approximation for the optic axis (Gullstrand, 1924; Lancaster, 1943).

Once the sheet had been placed against the projected image of the slit lamp section, adjustments were made to the position of the sheet to ensure that the optic axis drawn on the sheet was passing through the centre of the pupil, that is, until the upper and lower edges of the iris were at equal distances from the optic axis. Three estimates of the apparent posterior corneal radius were made in this way for each of the subjects (that is, one per negative).

To compensate for the obliquity of the pathway through the cornea a correction factor was applied using the following expression (Bennett, pers. comm):

$$d = d' \sin (90 + b) / \sin (c-b)$$

where  $d$  = measurements corrected for camera angle;  $d'$  = value (mm) measured on the photograph;  $c$  = angle between the illumination and observation systems of the slit lamp ( $60^\circ$ );  $b$  = angle subtended at the camera by  $d'$  (angle  $b$  is the arctangent  $d'/q$ , where  $q$  is the distance between the first principle point of the objective lens system and the corneal vertex).

For a range of values of  $d'$  a conversion factor,  $u$  ( $d/d'$ ), can be derived for camera angle, as shown in Table 7.3.

d'	0.3	0.4	0.5	0.6	0.7
b	0.1719	0.2292	0.2865	0.3438	0.4011
d	0.3470	0.4629	0.5790	0.6952	0.8116
u (d/d')	1.1567	1.1573	1.1580	1.1587	1.1594

Table 7.3. Variation of conversion factor, u, for values of d'.

The value of u varies only slightly for all values of d'. Thus, it would be possible, without significant loss of accuracy, to select a constant value for u. A value for u of 1.158 was chosen (Bennett, pers. comm.)

On the basis that the arcs of fixed value r follow the equation,

$$r = (y^2 + s^2) / 2s$$

rearrangement of the formula gives,

$$s = r - \sqrt{(r^2 - y^2)}$$

This allows the derivation of values of s for corresponding values of r. The value of s will represent the oblique apparent distance (sag) for the fixed arc of radius r. The value of s is converted to the apparent distance ( $s_{app}$ ) by applying the conversion factor,

$$s_{app} = s \times 1.158$$

The apparent radius ( $r'_2$ ) can be derived using,

$$r'_2 = (y^2 + s_{app}^2) / 2s_{app}$$

The values of the apparent posterior corneal radius ( $r'_2$ ) were converted to the actual radius ( $r_2$ ) using the equation:

$$r_2 = ((n \times 1000) / (F_1 + (1000/(d' + r'_2)))) - d$$

where  $n = 1.3771$  (corneal refractive index);  $F_1$  = dioptric power of

the anterior corneal surface;  $d$  = corneal thickness.

The magnification and distortion arising from the slit lamp observation system, film processing and projection system were assessed simultaneously by photographing the 1mm scale divisions of a precision ruler placed horizontally and vertically in front of the slit lamp objective, and measuring its dimensions after projection. Three photographs were taken of the ruler in each position. After projection, the intervals between successive ruler divisions were measured out to 5mm from the centre of the objective field. This 10mm field was chosen to allow the magnification to be assessed over an area which was larger than that over which measurements were taken.

#### 7.9.2 Validation Results

Table 7.4 contains the posterior corneal radii values in the vertical meridian only for the two methods used in the study. For the data obtained from the 15 subjects the mean value for the radius of the posterior corneal surface was 6.35mm for the slit lamp method and 6.40mm for the Purkinje image method.

Figure 7.13 shows a scatter plot for the values of the posterior corneal radius (PCR) obtained in the vertical meridian using the slit lamp and Purkinje image methods. A high correlation coefficient was found,  $r = 0.92$ ,  $P < 0.001$ . There was a general tendency for the radii values obtained using the slit lamp method to be slightly steeper than those obtained using the Purkinje image method.

The magnification and distortion arising from the Purkinje image method is fully detailed in section 7.8. The range of magnifications

found over the horizontal and vertical plane for the slit lamp photography method was used in a manner similar to that detailed in section 7.8 to assess distortion.

SUBJ	Slit-lamp Method (mm)	Purkinje Image Method (mm)	Difference (mm)
1	6.31	6.29	-0.02
2	6.37	6.48	+0.11
3	6.37	6.40	+0.03
4	6.22	6.30	+0.08
5	6.30	6.49	+0.19
6	6.30	6.30	0.00
7	6.69	6.88	+0.19
8	6.31	6.51	+0.20
9	6.27	6.27	0.00
10	6.21	6.12	-0.09
11	6.30	6.21	-0.09
12	6.34	6.43	+0.09
13	5.79	5.83	+0.04
14	6.41	6.61	+0.20
15	7.00	6.87	-0.13
Mean	6.35	6.40	0.05

Table 7.4. Values for the posterior corneal radius (mm) in the vertical meridian obtained using slit lamp and Purkinje image methods.

Values of  $\times 43.3$  (range  $\times 42 - 44.5$ ) and  $\times 43.5$  (range  $\times 43 - 45$ ) were found for the horizontal and vertical meridians respectively. The difference between the two values (0.23%) was taken to be negligible and the overall magnification was taken to be  $\times 43.3$ . The range of magnifications (that is, distortion) represented 6.9% of the mean value. This value, in context, represents a scaled distance of 0.069mm and for the purpose of the study was assumed to be negligible.

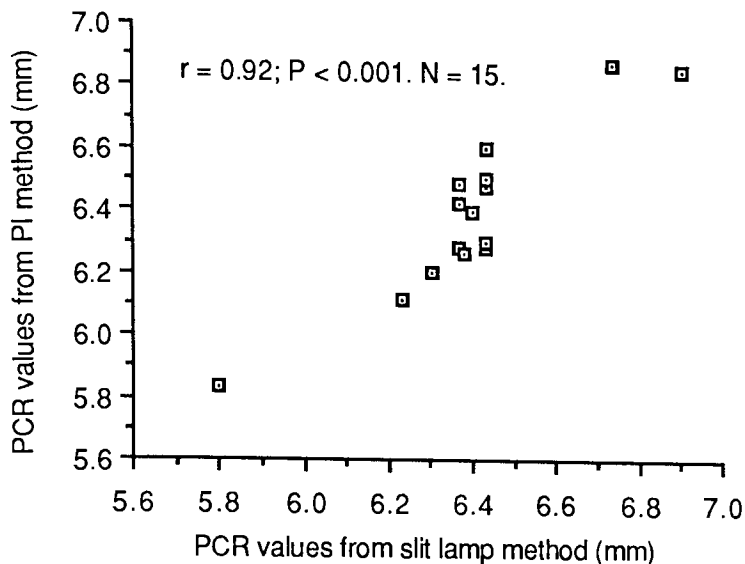


Figure 7.13 Scatter plot of posterior corneal radius values (mm) from slit-lamp and Purkinje image methods.

The data presented in this section would therefore imply that the method of measuring the posterior corneal radius using Purkinje images I and II produces values that compare well with those obtained by the slit lamp method. The values obtained using the two methods are slightly different in that those obtained with the slit lamp are generally flatter than those obtained using the Purkinje images.

#### 7.10 Investigation of the relationship between Purkinje image heights and keratometry readings.

In addition to the validation provided with slitlamp photography values in section 7.9, the collection of data from three meridians of the cornea allows the linearity of the results to be assessed. That is, by correlating the keratometry readings obtained in the  $90^\circ$ ,  $180^\circ$  and  $45^\circ$  meridians with the Purkinje image heights in these meridians, three scatter plots would be obtained that should share approximately the same form (Figures 7.14, 7.15 and 7.16). These plots give some indication of how well the the two parameters

correlate and thus how suitable the Purkinje image technique is for anterior corneal radius assessment. A good correlation would then suggest that the technique is adequate for the assessment of the posterior corneal surface radius as well.

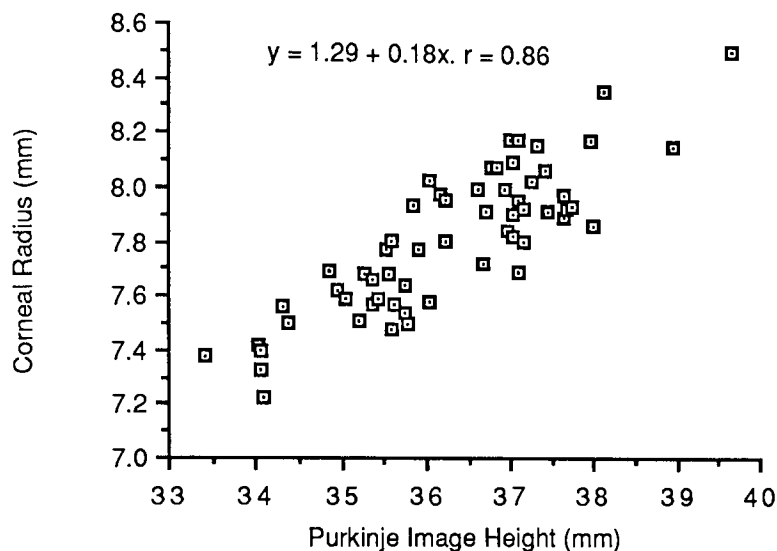


Figure 7.14 Scatter plot of Purkinje image height (mm) and anterior corneal radius (mm), 90° meridian.

The scatter plots between the Purkinje image heights and the anterior corneal radius in the 90°, 180° and 45° meridians all show a high correlation, with similar equations representing the lines through these plots.

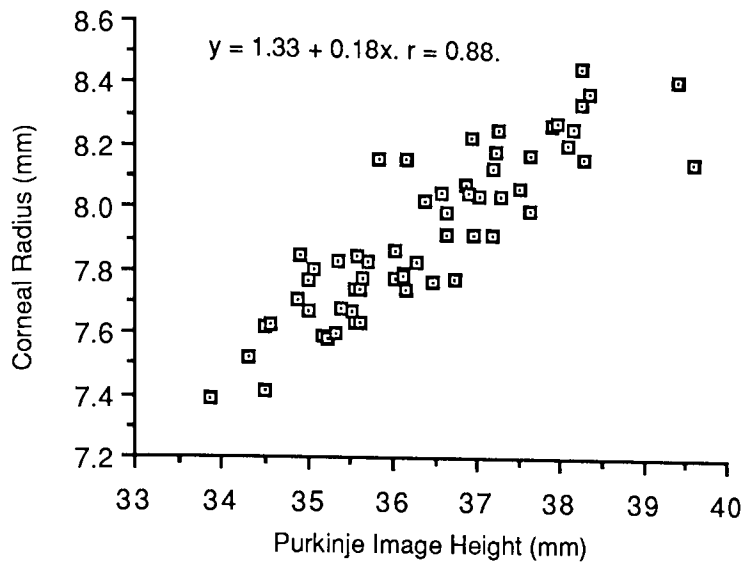


Figure 7.15 Scatter plot of Purkinje image height (mm) and anterior corneal radius (mm), 180° meridian.

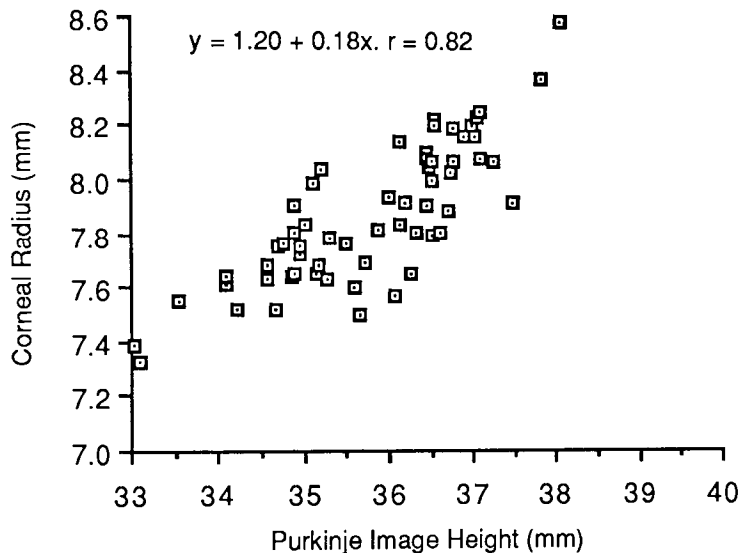


Figure 7.16 Scatter plot of Purkinje image height (mm) and anterior corneal radius (mm), 45° meridian.

### 7.11 Measurement of Posterior Corneal Radius: Results

For each subject group, the results obtained using the Purkinje image technique are presented in terms of the mean radius along the 90°, 180° and 45° meridians. This allows direct comparison with the data relating to the mean anterior corneal radius (chapter 4). Mean sphero-cylindrical values, derived using the meridional analysis

program described in section 3.3, is also shown for each group. This again allows direct comparison with the mean anterior corneal sphero-cylindrical components (chapter 4).

#### 7.11.1 Group Mean Posterior Corneal Radii in Three Meridians

Table 7.5 shows the mean posterior corneal radii (mm) arranged in terms of age, refractive group and gender (see appendix 7.2 also).

Subject Group	MERIDIAN		
	90°	180°	45°
Young Male Myopes	6.46 (±0.29)	6.79 (±0.30)	6.66 (±0.29)
Young Female Myopes	6.48 (±0.38)	6.75 (±0.29)	6.63 (±0.38)
Old Male Myopes	6.38 (±0.18)	6.60 (±0.08)	6.45 (±0.11)
Old Female Myopes	6.25 (±0.22)	6.32 (±0.16)	6.25 (±0.24)
Young Male Emmetropes	6.54 (±0.27)	6.83 (±0.22)	6.69 (±0.27)
Young Female Emmetropes	6.43 (±0.27)	6.65 (±0.30)	6.52 (±0.30)
Young Male Hyperopes	6.70 (±0.11)	6.96 (±0.12)	6.73 (±0.13)
Young Female Hyperopes	6.47 (±0.24)	6.84 (±0.27)	6.63 (±0.25)
Old Male Hyperopes	6.38 (±0.34)	6.78 (±0.20)	6.62 (±0.30)
Old Female Hyperopes	6.19 (±0.23)	6.51 (±0.24)	6.29 (±0.19)

Table 7.5. Mean posterior corneal radii values (mm) in three meridians. Values in brackets refer to standard deviation. N = 80.

#### 7.11.2 Group Mean Data in Sphero-cylindrical Form after Three Meridional Analysis

Table 7.6 shows the mean posterior corneal sphero-cylindrical values arranged in terms of age, refractive group and gender. (See appendix 7.3 also). Statistical analysis of the results in each of the categories of age, refraction and gender is the subject of chapter 8.



Subject Group	Sphere (mm)	Cylinder (mm)	Axis (°)
Young Male Myopes	6.40 ( $\pm 0.30$ )	0.45 ( $\pm 0.15$ )	95 ( $\pm 27.2$ )
Young Female Myopes	6.45 ( $\pm 0.37$ )	0.33 ( $\pm 0.15$ )	89.3 ( $\pm 31.9$ )
Old Male Myopes	6.35 ( $\pm 0.16$ )	0.29 ( $\pm 0.21$ )	63.8 ( $\pm 36.8$ )
Old Female Myopes	6.16 ( $\pm 0.19$ )	0.24 ( $\pm 0.03$ )	67.8 ( $\pm 35.2$ )
Young Male Emmetropes	6.51 ( $\pm 0.26$ )	0.35 ( $\pm 0.13$ )	91.2 ( $\pm 21$ )
Young Female Emmetropes	6.38 ( $\pm 0.26$ )	0.31 ( $\pm 0.11$ )	84.2 ( $\pm 20.4$ )
Young Male Hyperopes	6.60 ( $\pm 0.06$ )	0.46 ( $\pm 0.14$ )	71.6 ( $\pm 23.3$ )
Young Female Hyperopes	6.46 ( $\pm 0.24$ )	0.38 ( $\pm 0.09$ )	86.8 ( $\pm 4.9$ )
Old Male Hyperopes	6.36 ( $\pm 0.31$ )	0.45 ( $\pm 0.19$ )	83.3 ( $\pm 18.9$ )
Old Female Hyperopes	6.15 ( $\pm 0.19$ )	0.40 ( $\pm 0.07$ )	79.2 ( $\pm 15.7$ )

Table 7.6. Mean values of the posterior corneal sphero-cylindrical component derived from application of meridional analysis. Values in brackets represent the standard deviation. N = 80.

## 7.12 Error Analysis

In order to determine values for the radius of the posterior corneal surface ( $r_2$ ) it has been shown that values of the anterior corneal ( $r_1$ ), corneal thickness ( $d_1$ ) and Purkinje image height (P) are required. This section presents a number of examples to show the errors that may be induced in the posterior corneal radii values due to errors in the original input data.

### 7.12.1 Errors in Anterior Corneal Radius

Values assumed in this example are:  $r_1 = 7.80\text{mm}$ ,  $r_1 = 6.50\text{mm}$ ,  $d_1 = 0.55\text{mm}$ ,  $n = 1.3771$ . Using the equations described in section 7.6, a value for  $F_1$  is 48.35D,  $d'$  is 0.41mm and  $r'_2$  is 6.40. A value for P is

taken as 0.820 (Bennett & Rabbetts, 1984).

Assuming  $r_1$  is in error by 0.01mm,  $r_1$  then becomes 7.81mm.  $F_1$  is now 48.29D. Calculation of a value for  $r_2$  yields a value of 6.50mm, which is negligible in error compared to the original assumed value of  $r_2$ .

### 7.12.2 Errors in Pachometry

Using the values in Table 6.1, an error of 0.02mm is induced in the pachometry values. Values of  $r_1 = 7.80\text{mm}$ ,  $r_1 = 6.50\text{mm}$ ,  $n = 1.3771$ .  $d_1$  is taken as 0.57mm. Using the equations described in section 7.6, a value of  $d'$  is calculated as 0.42mm.

Calculation of  $r_2$  using this value gives 6.51mm, which is in error by 0.18% compared to the original value.

### 7.12.3 Errors In Purkinje image height

From the values presented in appendix 7.1, the average value of  $H_1$  (from the first Purkinje images) is 38.67mm. Using this value, and taking:

$$P = H_1 / H_2$$

$H_2$  is then taken as:

$$H_1 \times P$$

where  $P$  is taken to be 0.820 (Bennett & Rabbetts, 1984).

From the standard deviation values presented in appendix 7.1, the precision of the measurements of  $H_1$  and  $H_2$  (ie  $2 \times \text{SD}$ ) is 0.08mm.

Assuming the worse possible error would be an overestimate in one value of H and an underestimate in the other, the values would be taken as:

$$A) H_1 = (38.67 + 0.08) = 38.75\text{mm}$$

$$H_2 = (31.71 - 0.08) = 31.63\text{mm}$$

$$\text{Now } P = 0.816.$$

$$B) H_1 = (38.67 - 0.08) = 38.59\text{mm}$$

$$H_2 = (31.71 + 0.08) = 31.69\text{mm}$$

$$\text{Now } P = 0.824.$$

Now, assuming  $r_1 = 7.80\text{mm}$ ,  $d_1 = 0.55\text{mm}$ ,  $d' = 0.41$ ,  $P = 0.824$ ,  $r'_2 = P.r_1 = 6.43\text{mm}$ . Calculation of  $r_2$  gives a value of  $6.53\text{mm}$ , which is in error by approximately  $0.35\%$  compared to the original input value.

#### 7.12.4 Accumulation of Errors

From the above examples the accumulation of possible errors assumes:

$r_1 = 7.81\text{mm}$ ,  $d_1 = 0.57\text{mm}$ ,  $d' = 0.42$ ,  $P = 0.824$ ,  $F_1 = 48.28\text{D}$ ,  $r'_2 = 6.43\text{mm}$ . Calculation of  $r_2$  yields a value of  $6.52\text{mm}$ , which is in error by approximately  $0.36\%$ .

#### 7.13 Summary

This chapter has described in detail the method developed to allow photography of the Purkinje images arising from posterior corneal surface. Values for the radius of this surface were taken from three meridians, thus meeting the requirements of the meridional analysis program. The cylindrical values derived in this way are utilized in a

following chapter to assess the contribution of the posterior corneal surface to the astigmatism of the eye.

Validation studies were carried out on this newly-developed method. Firstly, the Purkinje image ratios derived when using one light source in the  $90^\circ$  meridian were correlated with those obtained using two light sources, the centre being defined by the two sources in the  $180^\circ$  meridian. A good correlation was found between the results suggesting a similar approach, using only one source, could be applied confidently to other meridians.

A second validation study correlated those posterior corneal radii measurements obtained with the Purkinje image technique with the values obtained using a more conventional slit-lamp method. Again a good correlation between the measurements was found, though the results of the latter method tended to be on average slightly steeper.

A study of the relationship between measured Purkinje image heights and measured anterior corneal radii showed a reasonably good correlation existed between the two parameters. Such a finding supports the use of the Purkinje image method developed in this study to measure posterior corneal radius.

The following chapter analyses a some of the data collected in the study.

CHAPTER EIGHT  
STATISTICAL ANALYSIS

## 8.1 Introduction

This chapter deals with the statistical analysis of the refractive, keratometric and posterior corneal data obtained in this study. The radii values for the anterior and posterior corneal surfaces have been converted to dioptric power values using the equations described in section 1.6.

## 8.2 Parameters to be Analysed

Variations in the spherical power, the cylindrical power (in plus cyl. form) and the cylindrical axis of the anterior and posterior corneal surface data and the refractive data are analysed. Variations in corneal thickness are also analysed. Each of these parameters is studied with reference to their variability with gender, ametropia and age.

### 8.2.1. Spherical Component

The values used in the statistical analysis of the refractive spherical component, anterior corneal spherical component and the posterior corneal spherical component is that taken from the relevant three meridional analysis output data (chapter 4, 5 and 7). The results obtained using an unpaired t-test (Bailey, 1983) will now be summarized.

#### A) Influence of Gender

From Table 8.1 it is apparent that the only significant difference is

in the anterior corneal spherical component, where the female subjects exhibit a significantly more powerful value ( $df = 78$ ;  $t = -2.237$ ;  $P = 0.029$ ). This is in agreement with the observations made by Sorsby et al. (1961) and Fledelius (1976).

Parameter	Male n = 40	Female n = 40
Anterior Corneal Sphere	47.31D $\pm 1.3$	48.11D $\pm 1.88$
Posterior Corneal Sphere	-6.18D $\pm 0.25$	-6.27D $\pm 0.30$
Refractive Sphere	-1.16D $\pm 2.37$	-1.66D $\pm 3.90$

Table 8.1. The influence of gender on the radius and power of the anterior and posterior corneal spherical component (mean $\pm$ SD) and on the power of the refractive spherical component (mean $\pm$ SD).

#### B) Influence of Spherical Ametropia

Parameter	Emmetropes n = 24	Myopes n = 34	Hyperopes n = 22
Anterior Corneal Sphere	47.61D $\pm 1.45$	47.82D $\pm 1.68$	47.61D $\pm 2.00$
Posterior Corneal Sphere	-6.18D $\pm 0.24$	-6.22D $\pm 0.30$	-6.27D $\pm 0.28$

Table 8.2. Influence of spherical ametropia on the power of the anterior corneal and posterior corneal component (mean  $\pm$ SD).

Table 8.2 summarizes the influence of spherical ametropia on the power of the anterior and posterior corneal spherical component.

Statistical analysis of this data indicates that there is no significant variation for these components. For the anterior corneal component, this in agreement with the findings of a number of authors who have studied anterior corneal powers (Steiger, 1913; Gardiner, 1962; Baldwin, 1964).

### C) Influence of Age.

Parameter	Young n = 60	Old n = 20
Anterior Corneal Sphere	47.40D ±1.58	48.60D ±1.74
Posterior Corneal Sphere	-6.17D ±0.27	-6.37D ±0.26
Refractive sph	-2.14D ±3.18	0.78D ±2.20

Table 8.3. Influence of age on the power of the anterior corneal and posterior corneal and the refractive spherical component (mean ±SD).

Table 8.3 summarizes the influence of age on the anterior corneal, posterior corneal and refractive spherical component. It appears that all three parameters vary significantly with age. The older subjects exhibit more powerful values for both the anterior (df = 78;  $t = -2.865$ ;  $P = 0.005$ ) and posterior (df = 78;  $t = 2.770$ ;  $P = 0.007$ ) corneal spherical component. In partial agreement with this, Fledelius and Stubgaard (1986) have reported a slight, non-significant tendency for older subjects to exhibit a more powerful anterior corneal surface. Due to the ametropia of the subject groups used, the difference in the refractive spherical value



is as would be expected ( $df = 78$ ;  $t = -3.787$ ;  $P < 0.001$ ). That is, the majority of the subjects in the young group exhibited myopia or a tendency towards it, while the majority in the old subject group exhibited hyperopia.

### 8.2.2. Cylindrical Component

This section deals with the statistical analysis of the refractive cylinder power, anterior corneal cylinder power, and posterior corneal cylinder power and their variation with gender, refractive error and age. In all three cases, the cylinder power actually used in the analysis is that taken from the relevant three meridional analysis output data (chapters 4, 5 and 7) and unpaired t-tests are applied throughout.

#### A) Influence of Gender

Parameter	Male n = 40	Female n = 40
Anterior Corneal Cylinder	1.13D $\pm 0.73$	1.18D $\pm 0.79$
Posterior Corneal Cylinder	0.37D $\pm 0.15$	0.32D $\pm 0.12$
Refractive Cyl	0.92D $\pm 0.94$	0.83D $\pm 0.68$

Table 8.4. Influence of gender on the power of the anterior corneal, posterior corneal and refractive cylindrical component (mean  $\pm$ SD).

Table 8.4 summarizes the influence of gender on the power of the anterior corneal, posterior corneal and refractive cylinder

component. No significant variation was found to exist in the cylinder powers studied due to the gender of the subjects. Although there is little data available regarding the variation of the power of astigmatism between males and females, Southall (1937) considered corneal astigmatism to be "more prevalent and severe in females", though Lyle (1971) emphasised that it was difficult to be sure exactly the subject group Southall was relating to. Saunders (1981) reported the power of refractive astigmatism between male and female groups to be approximately the same.

#### B) Influence of Spherical Ametropia

Table 8.5 summarizes the influence of spherical ametropia on the power of the anterior corneal, posterior corneal and refractive cylindrical component. A significant difference was found to exist in the anterior corneal cylinder power. Both groups of ametropic subjects exhibited significantly more anterior corneal cylinder than the emmetropic subjects (hyperopes,  $df = 44$ ;  $t = -2.570$ ;  $P = 0.013$ ; myopes,  $df = 56$ ;  $t = -2.230$ ;  $P = 0.03$ ).

Parameter	Emmetropes $n = 24$	Myopes $n = 34$	Hyperopes $n = 22$
Anterior Corneal Cylinder	0.84D $\pm 0.44$	1.23D $\pm 0.77$	1.37D $\pm 0.90$
Posterior Corneal Cylinder	0.30D $\pm 0.11$	0.34D $\pm 0.15$	0.39D $\pm 0.14$
Refractive Cyl	0.41D $\pm 0.24$	1.08D $\pm 0.87$	1.08D $\pm 0.94$

Table 8.5. Influence of spherical ametropia on the power of the anterior corneal, posterior corneal and refractive cylindrical component (mean $\pm$ SD).

The only significant difference as regards the posterior corneal cylinder power is between the emmetropic and hyperopic group ( $df = 44$ ;  $t = -2.590$ ;  $P = 0.013$ ).

The myopic subjects exhibit significantly more refractive cylinder than the emmetropic subjects ( $df = 56$ ;  $t = -3.651$ ;  $P = 0.001$ ) as do the hyperopic subjects ( $df = 44$ ;  $t = -3.40$ ;  $P = 0.001$ ). No significant difference was found to exist between the ametropic groups.

The overall finding that emmetropes lack significant astigmatism has been reported by Hirsch (1964), and Czellitzer (1927) reported that a significant number of subjects in his study showed an increase in refractive astigmatism as ametropia increased. It is also worth noting, however, that the latter study also recorded a reduction in astigmatism with increasing ametropia in some subjects. Borish (1970) has suggested that hyperopes lack significant astigmatism, which is in disagreement with findings of the above Table. Kronfeld and Devney (1930) stated that there seemed to be a tendency for the refractive astigmatism to increase as the spherical error increased, particularly with hyperopia, which would agree strongly with the above results.

### C) Influence of Age

The influence of age on the anterior corneal, posterior corneal and refractive cylinder powers is summarized in Table 8.6 below. Statistical analysis indicates that there is no significant variation in the anterior and posterior corneal cylinder powers due to the age of the subjects. Llandolt (1878) and Hirsch (1963) reported similar findings for the anterior corneal surface. Exford (1965) reported that there appeared to be no characteristic trends in corneal

astigmatism with age, which would support the values for the cornea presented above. Lyle (1971) has also studied the mean amount of corneal astigmatism and its variation with age and reported a small, non-significant change in the dioptric power of the astigmatism. This finding is supported by the present study. There is a significant difference in the power of the refractive cylinder between the two age groups ( $df = 78$ ;  $t = -2.320$ ;  $P = 0.023$ ).

It is perhaps worthy of mention that nearly all the subjects in the study exhibited astigmatism of some degree, which agrees with the findings of numerous other authors (Tscherning, 1904; Borish, 1970; Duke-Elder and Abrams, 1974; Saunders, 1981; Bennett and Rabbetts, 1984).

Parameter	Young n = 60	Old n = 20
Anterior Corneal Cylinder	1.17D $\pm 0.76$	1.11D $\pm 0.76$
Posterior Corneal Cylinder	0.33D $\pm 0.13$	0.36D $\pm 0.16$
Refractive Cyl	0.79D $\pm 0.79$	1.29D $\pm 1.00$

Table 8.6. Influence of age on the anterior corneal, posterior corneal and refractive cylindrical component (mean $\pm$ SD).

### 8.2.3. Cylinder axis orientation

The variation of the axis of the refractive cylinder, the anterior corneal cylinder and the posterior corneal cylinder is analysed with respect to the influence of gender, ametropia and age. The axis values are those taken from the output data of the three meridional analysis program (chapters 4, 5 and 7). The axis direction is

classified as being horizontal ( $180^\circ \pm 30^\circ$ ), vertical ( $90^\circ \pm 30^\circ$ ) or oblique ( $45^\circ/135^\circ \pm 15^\circ$ ) and a chi-squared test (Bailey, 1983) has been applied to the data.

#### A) Influence of Gender

The variation of the cylinder axes orientation with gender is summarized in Table 8.7 in terms of percentage of subjects exhibiting a certain axis orientation.

No significant variation in cylinder axes orientation was found to exist due to the influence of gender. This finding is partly backed up by the study of Lyle (1971), who reported that there was no substantial difference in the axis of corneal astigmatism between males and females.

	AXIS ORIENTATION					
	MALE (n = 40)			FEMALE (n = 40)		
	Horizontal	Vertical	Oblique	Horizontal	Vertical	Oblique
Ant.Corneal Cyl Axis	67.5%	22.5%	10%	72.5%	10%	17.5%
Post.Corneal Cyl Axis	5%	82.5%	12.5%	7.5%	77.5%	15%
Refractive Cyl Axis	37.5%	30%	32.5%	20%	30%	47.5%

Table 8.7. Influence of gender on the variation of the cylinder axes orientation expressed as a percentage of the total number of subjects. (One subject in the female group, 2.5%, exhibited no refractive astigmatism).

#### B) Influence of Spherical Ametropia

The variation of the cylinder axes with ametropia is summarized in Table 8.8 in terms of percentage of subjects exhibiting a certain

axis orientation.

	EMMETROPEES (n = 24)			AXIS ORIENTATION MYOPEES (n = 34)			HYPEROPEES (n = 22)		
	Horiz	Vert	Obl	Horiz	Vert	Obl	Horiz	Vert	Obl
Ant. Corneal Cyl Axis	83.4%	8.3%	8.3%	67.6%	20.6%	11.8%	59.1%	18.2%	22.7%
Post. Corneal Cyl Axis	0%	83.3%	16.7%	14.7%	73.5%	11.8%	0%	86.4%	13.6%
Refractive Cyl Axis	25%	20.8%	54.2%	29.4%	44.1%	23.5%	36.4%	22.7%	40.9%

Table 8.8. Influence of ametropia on the cylinder axis orientation of the anterior corneal cylinder, posterior corneal cylinder and the refractive cylinder. (One subject in the myopic group, 3%, exhibited no refractive astigmatism).

Statistical analysis of the results indicates that refractive error has no significant effect on the axis orientation of the above mentioned cylinders. Unfortunately, there seems to be little data available on axis variation with refractive error. As the natural refractive progression is towards hyperopia with increasing age, any variation could perhaps, theoretically, be related to a combination of a subjects age/ametropia.

### C) Influence of Age.

The influence of age on the orientation of the anterior corneal, posterior corneal and refractive cylinder axes is summarized in Table 8.9 in terms of percentage of subjects exhibiting a certain axis orientation.

The anterior corneal cylinder axis exhibits a significant tendency towards more horizontal than vertical orientation in the young subjects compared to the old ( $P < 0.001$ ,  $df = 1$ , chi-squared = 6.83). The older subjects also showed significantly more oblique axis

orientation when compared to the young ( $P < 0.05$ ;  $df = 1$ ; chi-squared = 7.47).

Parameter	YOUNG (n = 60)			OLD (n = 20)		
	Horiz	Vert	Obl	Horiz	Vert	Obl
Ant. Corneal Cyl Axis	81.7%	11.7%	6.6%	40%	30%	30%
Post. Corneal Cyl Axis	3.3%	83.3%	13.4%	10%	75%	15%
Refractive Cyl Axis	23.3%	33%	41.7%	55%	20%	25%

Table 8.9. Influence of age on the orientation of the anterior corneal cylinder axis, posterior corneal cylinder axis and the refractive cylinder axis.

Saunders (1981) has reported that with age his subjects showed an increased tendency towards both against the rule and oblique astigmatism.

No significant variation in the axis of the posterior corneal cylinder with age was found to exist. As there have been very few studies of the toricity of the posterior corneal there is no data to which these findings can be compared.

The refractive cylinder axis shows a significant tendency towards more vertical than horizontal orientations in the young subjects compared to the old ( $P < 0.05$ ,  $df = 1$ , chi-squared = 4.31). Many authors (see chapter 2) have reported on the tendency for young subjects to exhibit with the rule astigmatism and for older subjects to exhibit against the rule astigmatism.

#### 8.2.4. Corneal Thickness

This section deals with the variations in corneal thickness due to the influence of gender, refractive error and age. The thickness values are those obtained by pachometry and summarized in appendix 6.1. Unpaired t-tests (Bailey, 1983) were applied to the data and the results are summarized below.

##### A) Influence of Gender

Table 8.10 summarizes the influence of gender on the central corneal thickness.

Parameter	Male n = 40	Female n = 40
Corneal Thickness	0.498mm ±0.032	0.489mm ±0.024

Table 8.10. Influence of gender on the central corneal thickness (mean±SD) as measured by pachometry.

There is no significant variation in the corneal thickness due to the gender of the subjects. This is in agreement with work of Maurice and Giardini (1951); Kruse-Hansen (1971) and Olsen and Ehlers (1984).

##### B) Influence of Spherical Ametropia

Table 8.11 summarizes the influence of refractive error on the corneal thickness.

Statistical analysis of the data indicates that there is no significant variation in the corneal thickness due to the refractive



error of the subjects. Kruse-Hansen (1971) has reported similar findings, but emphasised the limited refraction range of the subjects he studied.

Parameter	Emmetropes n = 24	Myopes n = 34	Hyperopes n = 22
Corneal Thickness	0.50mm ±0.034	0.492mm ±0.020	0.495mm ±0.028

Table 8.11. Influence of refractive error on the corneal thickness (mean±SD).

### C) Influence of Age

Influence of age on the central corneal thickness is summarized in Table 8.12.

Parameter	Young n = 60	Old n = 20
Corneal Thickness	0.497mm ±0.028	0.485mm ±0.026

Table 8.12. Influence of age on the central corneal thickness (mean±SD).

There is no significant variation in the corneal thickness due to subject age, as reported by Lowe (1969) and Kruse-Hansen (1971). Olsen and Ehlers (1984) reported a non-significant decrease in the corneal thickness with age, which agrees completely with the values given above.

Thus, in the subject group studied, there is apparently no significant

variation in the corneal thickness with gender, refractive error or age.

### 8.3 Summary

This chapter has presented an analysis of the variation with age, refractive error and gender of the refractive, keratometric and posterior corneal data obtained in the study. The variation of the corneal thickness with age, refractive error and gender has also been analysed. Most of the findings in this chapter support the findings of a number of past studies.

Having considered the variation of the cylindrical component and the cylindrical axis component of the anterior and posterior corneal surface and of the refraction, the next chapter deals with the effect of the posterior corneal surface on residual astigmatism.

## CHAPTER NINE

### EFFECT OF POSTERIOR CORNEAL SURFACE ON RESIDUAL ASTIGMATISM

## 9.1. Introduction

This chapter investigates the astigmatic contribution of the posterior corneal surface to residual astigmatism.

As the astigmatic nature of the cornea is known to vary significantly with age, (ie there is a well-documented shift from with the rule astigmatism to against the rule astigmatism with increasing age, see section 2.3) data from the young and old subject groups will be assessed separately.

## 9.2 Comparison of the Effects of a One-surface and a Two-surface Cornea

The aim of this section is to determine whether the inclusion of a second corneal surface will reduce residual astigmatism. The aim of the following section (9.3) is to determine how the relationship between the anterior and posterior corneal surfaces influences this effect.

In attempting to describe the effects of a one-surface and a two-surface cornea, two simple models for the cornea are assumed. The first model (Figure 9.1) assumes the cornea to have a single surface which acts as the sole interface between air and aqueous. The radius of this single surface can be measured using keratometry (chapter four).

The second model (Figure 9.2) assumes the presence of an anterior and posterior corneal surface ( $r_1$  and  $r_2$  respectively) separated by a

corneal thickness ( $d$ ). The cornea and the aqueous possess different refractive indices. The anterior corneal surface radius is measured using keratometry (chapter four), the posterior corneal surface is measured using the method described in chapter seven and the corneal thickness is measured using pachometry (chapter six).

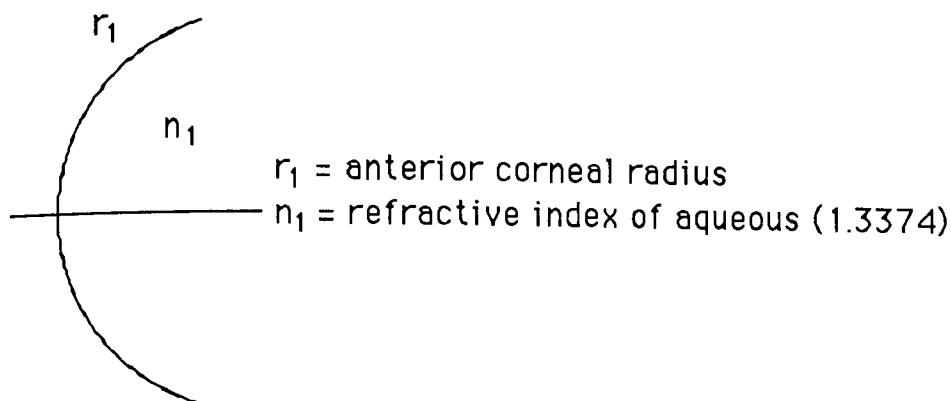


Figure 9.1 Schematic representation of the one-surface cornea

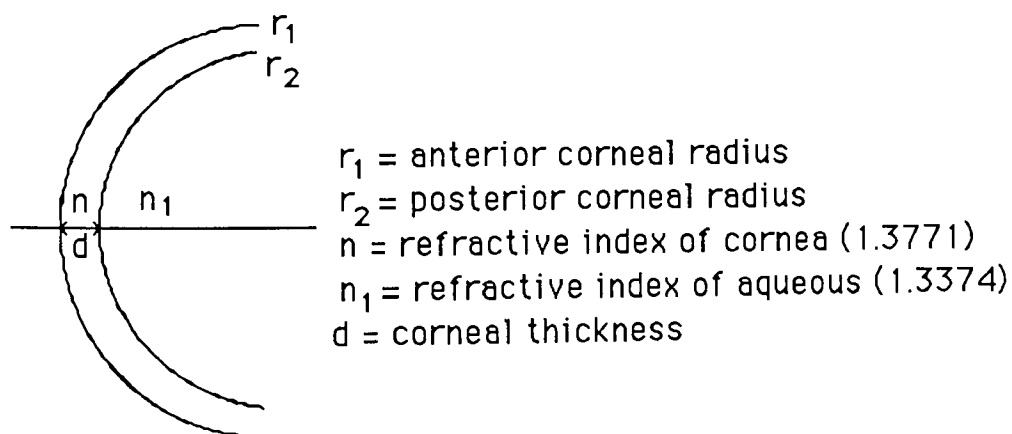


Figure 9.2 Schematic representation of the two-surface cornea

In the case of the one-surface model, the radii measurements are converted into dioptric power using the equation described in section 6.1. These dioptric powers are then incorporated into the meridional analysis program described in section 3.3 to derive values for the one-surface corneal spherocylindrical components (Appendix 9.1).

For the two-surface model, the anterior and posterior corneal radii values are converted into dioptric power as above. These dioptric values are then used to obtain an equivalent corneal power ( $F_e$ ) using the equations in section 6.1. The three meridional analysis equations are then applied to the equivalent corneal power values to derive the spherocylindrical components for the equivalent cornea (Appendix 9.2).

### 9.2.1 One-surface Cornea

The residual astigmatism present for a one-surface cornea is represented by the expression:

$$R_1 = \text{anterior corneal cylindrical component} - \text{refractive cylindrical component}$$

If the value of  $R_1$  is positive, the anterior corneal astigmatism is taken to be greater than the refractive astigmatism. If, however, the value of  $R_1$  is negative, then the anterior corneal astigmatism is less than the refractive astigmatism.

### 9.2.2 Two-surface Cornea

When a second corneal surface is present, the amount of residual astigmatism present is represented by the expression:

$$R_2 = \text{equivalent corneal cylindrical component} - \text{refractive cylindrical component}$$

If the value of  $R_2$  is positive, the equivalent corneal astigmatism is taken to be greater than the refractive astigmatism. If, however, the value of  $R_2$  is negative, the equivalent corneal astigmatism is taken to be less than the refractive astigmatism.

The effect of the introduction of a second corneal surface on the residual astigmatism is now represented by the expression:

$$\Delta R = R_1 - R_2$$

### 9.2.3 Mean Values of $R_1$ , $R_2$ and $\Delta R$

Values of  $R_1$ ,  $R_2$  and  $\Delta R$  were calculated for each subject and group mean data is summarized in Table 9.1. From this Table it can be seen that in the young subject group the mean value for  $\Delta R$  is +0.14D, which is equivalent to a reduction of about 54%. Therefore, in the young subject group, introduction of the posterior corneal surface has reduced the corneal astigmatism and hence the residual astigmatism. In the young group about 82% of the subjects exhibit a positive  $\Delta R$  value.

YOUNG	MEAN $\pm$ SD	RANGE (min to max)
$R_1$	+0.26D $\pm$ 0.62	-1.51 to +2.86D
$R_2$	+0.12D $\pm$ 0.62	-1.40 to +2.75
$\Delta R$	+0.14D $\pm$ 0.24	-0.63 to 0.86
-----		
OLD		
$R_1$	-0.13D $\pm$ 0.69	-1.91 to +0.78
$R_2$	-0.11D $\pm$ 0.67	-1.79 to +0.83
$\Delta R$	-0.02D $\pm$ 0.36	-0.92D to +0.82

Table 9.1. Values of  $R_1$ ,  $R_2$  and  $\Delta R$  for young and old subject groups.

In the old subject group, the  $\Delta R$  value is -0.02D. Thus, the introduction of a second corneal surface has increased the corneal astigmatism. For the one-surface cornea, however, the corneal astigmatism is less than the refractive, meaning the net effect in the old subject group has been to reduce the residual astigmatism by

0.02D, which is equivalent to a reduction of about 15%.

Figures 9.3 and 9.4 show the distribution of the  $\Delta R$  values in both subject groups. Application of an unpaired t-test to the data indicated that there was no significant difference in  $\Delta R$  between the two groups.

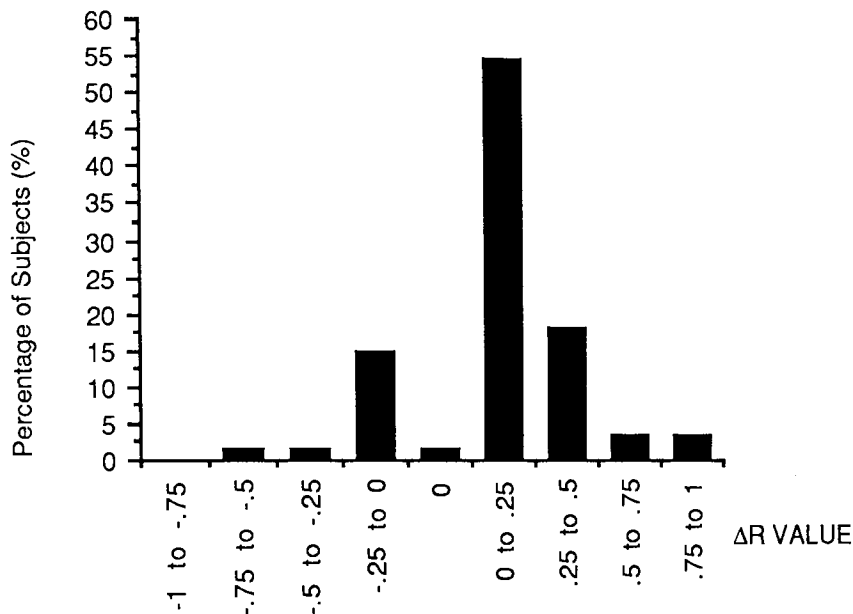


Figure 9.3 Variation of  $\Delta R$  in young subject group.

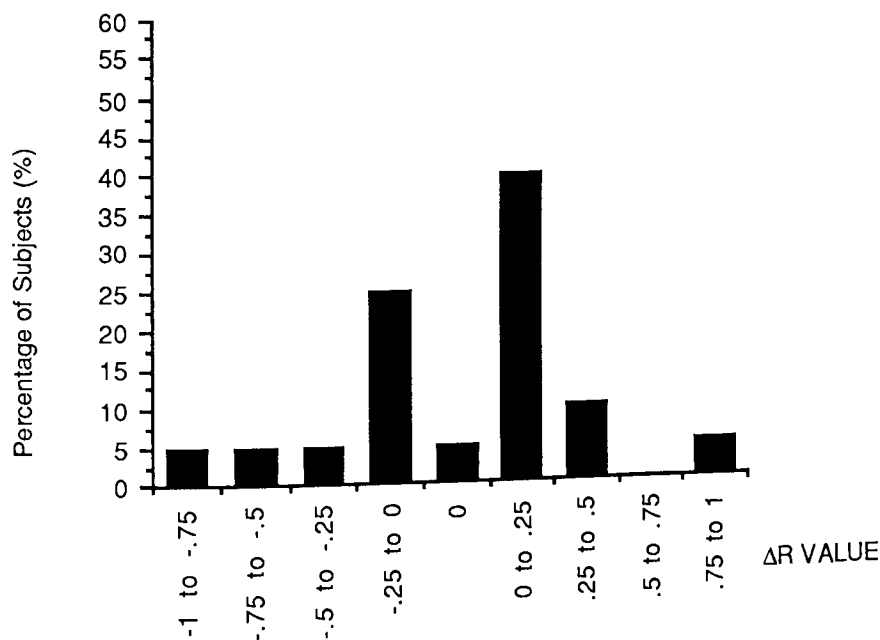


Figure 9.4 Variation of  $\Delta R$  in old subject group.



### 9.3 The Effect on Residual Astigmatism of the Relationship between the Anterior and Posterior Corneal Surfaces

Observation of the ratio between the anterior and posterior corneal surfaces in the vertical and horizontal meridians is summarized in Table 9.2. A consistent trend became apparent and showed the posterior corneal surface to be steeper relative to the anterior surface in the vertical meridian compared to the horizontal meridian. If such a trend did exist it would be expected that the cornea is thicker in the vertical meridian than in the horizontal meridian. Topographic pachometry, as summarized in section 1.3.2 confirms this finding. The question then arises as to whether this relationship contributes to the reduction of residual astigmatism established in section 9.2. In attempting to answer this, it is pertinent to consider whether the reduction would have been found if the ratio between the anterior and posterior corneal surfaces was constant in all meridians.

RATIO	YOUNG		OLD	
	Mean $\pm$ SD	Range	Mean $\pm$ SD	Range
Horizontal	1.169 $\pm 0.031$	1.097-1.229	1.165 $\pm 0.019$	1.142-1.202
Vertical	1.203 $\pm 0.031$	1.151-1.273	1.221 $\pm 0.042$	1.147-1.296

Table 9.2. Mean, standard deviation and range of ratios between the anterior and posterior corneal surfaces in the young and old subject groups.

To investigate this, a theoretical posterior corneal surface was derived in which the ratio between the anterior and posterior corneal surfaces was kept constant in all meridians. This was

achieved by taking a mean value of the Purkinje image ratios (Appendix 7.1) in each of the horizontal, vertical and oblique meridians and deriving new values for the posterior corneal radius for each subject with this mean ratio. Using this data a theoretical set of equivalent corneal values were derived .

The residual astigmatism,  $\Delta R_{\text{theoretical}}$ , can be calculated from the expression:

$$\Delta R_{\text{theoretical}} = \text{theoretical equivalent corneal cylindrical component} - \text{refractive cylindrical component}$$

It then follows that,

$$\Delta R_{\text{theoretical}} = R_1 - R_{\text{theoretical}}$$

where the value of  $R_1$  are the same as those shown in Table 9.1.

Table 9.3 summarizes the values for  $R_1$ ,  $R_{\text{theoretical}}$  and  $\Delta R_{\text{theoretical}}$  for young and old subject groups.

YOUNG	MEAN	SD	RANGE (Min-Max)
$R_1$	+0.26D	$\pm 0.62D$	-1.51D to +2.86D
$R_{\text{theoretical}}$	+0.27D	$\pm 0.65D$	-1.55D to +2.46D
$\Delta R_{\text{theoretical}}$	-0.01D	$\pm 0.39D$	-2.78D to 0.95D
-----			
OLD			
$R_1$	-0.13D	$\pm 0.69D$	-1.91D to +0.78D
$R_{\text{theoretical}}$	-0.18D	$\pm 0.75D$	-2.40D to +0.66D
$\Delta R_{\text{theoretical}}$	-0.05D	$\pm 0.11D$	+0.01D to +0.49D

Table 9.3. Mean, standard deviation and range of the values  $R_1$ ,  $R_{\text{theoretical}}$  and  $\Delta R_{\text{theoretical}}$

From this Table, a mean value for  $\Delta R_{\text{theoretical}}$  for the 60 young subjects can be taken to be  $-0.01D$ . The mean value for  $\Delta R_{\text{theoretical}}$  in the old subject group is  $-0.05D$ .

Therefore, the presence of the second corneal surface acts to reduce the residual astigmatism using the approach adopted here. This reduction is not solely due to the actual presence of the surface. The relationship between the surfaces has a significant effect - that is, the ratio between the surfaces would suggest that the posterior corneal surface is consistently steeper in the vertical meridian relative to the anterior surface. Removal of this consistent steepness by experimental manipulation has the effect of not reducing the residual astigmatism as much.

#### 9.4 Summary

The aim of this chapter was to investigate the effect of the posterior corneal surface on residual astigmatism. In both young and old subjects the effect of the introduction of a second surface was to reduce the amount of residual astigmatism.

Of particular interest was the relationship that was found to exist between the anterior and posterior corneal surface radii. The posterior corneal surface was found to be consistently steeper in the vertical meridian compared to the horizontal meridian. This finding is supported by data from topographical pachometry.

A theoretical corneal model was introduced which effectively removed any such relationship. It was found that when the relationship was removed an increase in residual astigmatism occurred. Thus it is concluded from this that the reduction in

residual astigmatism caused by the addition of the second corneal surface is due to the observed difference in the ratio between the anterior and posterior surfaces in the horizontal and vertical meridians.

CHAPTER TEN  
SUMMARY AND DISCUSSION

### 10.1 Review of Previous Chapters

Chapter one presented a review of the human cornea. Viewed microscopically it is seen to consist of five distinct layers and an outer tear layer. Theoretically, all of the layers could be responsible for slight variations in the overall corneal refractive index, though the tear layer rarely reaches a sufficient thickness to have any significant effect.

The development of specific instrumentation has made measurement of the thickness of the cornea, both centrally and peripherally, relatively straightforward. A number of studies to date have put forward values for the thickness of the central cornea and its variation with age, refractive error and gender.

Numerous studies have been made on the anterior corneal surface and mean values for its dimensions are well-established. It is accepted that the anterior cornea may be quite asymmetrical, though the direction of the asymmetry is open to debate. Most workers, for example, agree that the cornea tends to be flatter nasally than temporally, but there is a conflict of opinions as regards the superior and inferior portions.

The radius of posterior corneal surface has to date received very little attention. This may be so because it is much less accessible to measurement compared to the anterior surface and most schematic eye models that incorporate a posterior corneal surface use an assumed value only for its radius. Past attempts to measure the radius of the surface have mainly relied on photographic techniques.

Studies on the form of the posterior surface have suggested that it shares a similar form to that of the anterior surface.

Chapter two presented an overview of the condition of astigmatism. Studies on the astigmatism arising from the eye as a whole (refractive astigmatism) and from the anterior corneal surface were summarized. It is quite a common clinical finding that refractive astigmatism differs from the astigmatism attributable to the anterior corneal surface and this difference is usually called residual astigmatism. A number of possible causes for this residual astigmatism - the crystalline lens, the posterior corneal surface and the asymmetry of the optical system of the eye - were examined. As all three of these components may have some effect it would seem pertinent to study the effects of each in isolation, this study, of course, being confined to the role of the posterior corneal surface.

In chapter three the concept of meridional analysis was reviewed. This technique essentially allows a sphero-cylindrical equivalent for refraction, radius or curvature to be determined from measurements taken in a number of meridians. The number of meridians used can vary between three, giving rise to three meridional analysis, and four or six, giving rise to multi-meridional analysis. The meridians used are usually pre-determined, though a very recent study, published too late to influence the present work, has suggested that arbitrary meridians may also be used.

One of the main problems of taking measurements from only three meridians is that small errors in the initial measurements could result in significantly large differences in the cylinder power and axis orientation. To overcome this problem, mathematical methods

using four or more meridians have been proposed and when applied to refractive data have been shown to produce precise and accurate results.

In view of the developmental nature of the method used to measure the posterior corneal surface, however, a recently developed set of equations, using measurements from three meridians only, were used in the present study.

A review of the measurement of the radius of the anterior corneal surface using keratometric techniques was provided in chapter four. Readings of the radius and axis of orientation were taken along the principal meridians. Further readings were taken along three other meridians ( $90^\circ$ ,  $180^\circ$  and  $45^\circ$ ) to meet the requirements of the three meridional analysis program.

The radii values obtained by measurement were compared and correlated with those derived following the application of the meridional analysis program to data from the three specified meridians. Overall, a very good correlation was found to exist between the spherical, cylindrical and cylinder axis orientation components. As previous studies have shown, the highest correlation existed between the measured and derived spherical component and the lowest between the measured and derived cylinder axis orientation.

Chapter four also provided a detailed profile of the subjects used in the study. In total there were 60 young (mean age 22.04 years) and 20 old subjects (mean age 74.64 years), with an equal number of males and females in each group. The young group consisted of 28 myopes, 24 near-emmetropes and 8 hyperopes. The old group



consisted of 6 myopes and 14 hyperopes.

Measurement of refraction using an objective optometer was described in chapter five. Measurements were taken along the principal meridians of refraction and along three meridian ( $90^\circ$ ,  $180^\circ$  and  $45^\circ$ ) to meet the requirements of the three meridional analysis program.

The refractive values obtained by measurement were compared and correlated with those derived following the application of the meridional analysis program to data from the three specified meridians. Overall, a very good correlation was found to exist between the spherical, cylindrical and cylinder axis orientation components. As previous studies have shown, the highest correlation existed between the measured and derived spherical component and the lowest between the measured and derived cylinder axis orientation.

Chapter six was involved with the measurement of the corneal thickness. Several different methods are available for the actual measurement, but the present study used a conventional instrument. Values for corneal thickness were presented for the different subject groups and statistical analysis of these values was considered in a later chapter (chapter eight).

Chapter seven was mainly concerned with a method developed to allow photography of the Purkinje images arising from the posterior corneal surface. Radii values for this surface were obtained in three meridians to meet the requirements of the meridional analysis program. A number of validation checks were made on the photographic method and good results were obtained. The method

was also found to show good repeatability.

Statistical analysis of a number of parameters was covered in chapter eight. The main parameters were the anterior and posterior corneal surface spherical power, cylindrical power and cylindrical axis, the refractive cylindrical power and cylindrical axis, and the corneal thickness. The influence of gender, ametropia and age on these parameters was analysed.

Chapter nine investigated the effect of the posterior corneal surface on residual astigmatism. The effect of the introduction of a second surface was found to reduce the amount of residual astigmatism. The posterior corneal surface was found to be consistently steeper in the vertical meridian compared to the horizontal meridian. The effect of the removal of this relationship was to increase the residual astigmatism slightly.

## 10.2 Suggestions For Further Study

The most obvious improvement that could be made to the study is that of collecting data from additional meridians. That is, three meridional analysis has its flaws. The main flaw, which has been acknowledged, is that of cylinder power over-estimation and cylinder axis prediction. Small errors in the original measurements can lead to significant errors in the output data. If measurements could be taken along four or more meridians the output data may be more accurate.

The obvious problem here, however, is that the construction of the Canon AutoRef R-1 restricts the space available to mount light sources. Enhancement of the mounts that carry the light sources or

the construction of a modified system around a different instrument may make this proposed improvement possible.

There are a number of possible clinical applications of the method in its present or modified form which may form the basis of further studies. Effects of corneal or refractive surgery on the posterior corneal surface could be studied by taking pre- and post-operative measurements. The posterior corneal surface may, for example, be effected by cataract surgery in terms of the astigmatism that may be present prior to suture removal or adjustment. The radius of this surface in pathological cases could be studied as Lowe and Clark (1973) found a significant difference in the posterior corneal radius in normal subjects and those diagnosed as having closed-angle glaucoma.

The use of the Scheimpflug camera may, of course, improve the availability of data on the posterior corneal radius. With such an instrument as this, however, measurements are usually restricted to the single horizontal meridian thus making it impossible to use the data in a meridional analysis method. Acquisition of a Scheimpflug camera that would allow the collection of data from the vertical and oblique meridians would obviously be a most useful improvement. Collection of radius values from the central and peripheral posterior corneal surface would also allow the asphericity of the surface to be evaluated.

## APPENDICES

# APPENDIX 4.1: KERATOMETRIC RESULTS FROM THREE MERIDIANS.

\* † denotes female subject

\* Refractive groups: M = myope; E = near-emmetropes; H = hyperopes

\* Mean and standard deviation (SD) values are based on three repeat readings taken on one occasion only

\* Dimensions in mm

SUBJ	Refractive Group	MERIDIAN (°)					
		90		180		45	
		Mean	SD	Mean	SD	Mean	SD
DL	M	7.64	0.01	7.81	0.015	7.80	0.00
NS	M	7.91	0.025	7.83	0.003	7.84	0.01
AW	M	7.92	0.003	8.03	0.006	7.94	0.00
CS	M	7.96	0.01	8.16	0.008	8.04	0.01
CSd	M	7.94	0.01	8.08	0.008	8.05	0.018
PG	M	8.16	0.006	8.47	0.00	8.38	0.008
OC	M	7.42	0.008	7.60	0.00	7.50	0.006
SS	M	7.77	0.006	7.85	0.00	7.84	0.01
GL	M	7.59	0.006	7.67	0.006	7.64	0.01
SP	M	7.93	0.018	7.52	0.006	7.68	0.008
DW	M	7.72	0.015	7.83	0.01	7.76	0.00
PP	M	7.58	0.006	8.05	0.00	7.80	0.008
BW	M	8.00	0.012	8.18	0.01	8.07	0.009
JR	M	7.40	0.015	7.74	0.00	7.61	0.006
SP†	M	8.08	0.013	8.29	0.006	8.20	0.00
LMcP†	M	7.80	0.00	8.00	0.00	7.91	0.003
JB†	M	7.51	0.015	7.78	0.02	7.91	0.006
MDH†	M	7.93	0.003	8.17	0.003	8.07	0.003
CN†	M	7.56	0.015	7.68	0.006	7.64	0.01
CP†	M	7.98	0.006	8.07	0.005	8.10	0.00
SD†	M	7.48	0.015	7.58	0.015	7.52	0.012
AJ†	M	7.80	0.015	7.92	0.006	7.81	0.014
DT†	M	7.94	0.00	7.59	0.006	7.69	0.006
EH†	M	7.22	0.015	7.39	0.007	7.33	0.003
RP†	M	7.54	0.01	7.71	0.003	7.65	0.018
NB†	M	7.83	0.012	7.92	0.00	7.89	0.006
GH†	M	7.68	0.006	7.64	0.012	7.65	0.003
KR†	M	8.52	0.006	8.43	0.003	8.59	0.00
SJ	E	7.69	0.012	7.77	0.006	7.75	0.018
RS	E	8.03	0.006	8.16	0.003	8.08	0.006
CN	E	7.50	0.015	7.67	0.015	7.52	0.00
IM	E	8.18	0.01	8.35	0.015	8.25	0.00
RSt	E	7.77	0.008	7.78	0.003	7.75	0.00
SMc	E	7.96	0.01	7.99	0.012	7.99	0.006
FE	E	8.03	0.015	8.16	0.01	8.14	0.00
DD	E	7.54	0.015	7.62	0.006	7.57	0.008
KM	E	7.85	0.006	8.05	0.008	7.92	0.006
TE	E	7.98	0.006	8.14	0.01	8.08	0.00
PI	E	7.90	0.014	8.06	0.01	8.00	0.00
FD	E	7.92	0.01	7.80	0.00	7.82	0.00
MB†	E	7.50	0.005	7.77	0.008	7.60	0.00
RK†	E	7.57	0.021	7.74	0.005	7.63	0.006
DL†	E	8.18	0.01	8.23	0.008	8.16	0.013
DC†	E	7.68	0.006	7.83	0.008	7.79	0.003
KM†	E	7.80	0.023	7.87	0.025	7.78	0.00

SP†	E	7.38	0.01	7.41	0.006	7.39	0.017
HJ†	E	7.59	0.017	7.85	0.01	7.72	0.005
HO†	E	7.62	0.01	7.79	0.00	7.68	0.00
LK†	E	8.16	0.00	8.26	0.008	8.19	0.017
GB†	E	7.66	0.012	7.64	0.01	7.65	0.01
CT†	E	8.18	0.012	8.22	0.006	8.22	0.006
AW†	E	7.57	0.012	7.74	0.01	7.63	0.00
FE	H	8.07	0.00	8.28	0.006	8.16	0.008
KD	H	7.69	0.015	7.78	0.015	7.76	0.008
DC	H	8.37	0.008	7.92	0.01	7.92	0.01
MD	H	8.08	0.012	8.19	0.03	8.07	0.008
KD†	H	7.87	0.008	8.06	0.008	8.03	0.00
AMc†	H	8.10	0.006	8.27	0.006	8.20	0.012
AS†	H	8.00	0.012	8.39	0.03	8.23	0.00
LE†	H	7.33	0.008	7.63	0.006	7.55	0.015

# SENIOR CITIZEN GROUP

MrM	M	7.96	0.015	7.85	0.008	7.91	0.00
MrN	M	7.81	0.009	7.80	0.008	7.74	0.009
MrMk	M	7.67	0.013	7.42	0.00	7.52	0.00
MrH	H	7.78	0.005	7.60	0.006	7.66	0.008
MrS	H	7.60	0.008	7.71	0.005	7.72	0.00
MrHd	H	7.81	0.01	8.06	0.00	7.80	0.005
MrB	H	8.24	0.009	8.22	0.005	8.19	0.00
MrSs	H	7.99	0.003	7.89	0.003	7.92	0.00
MrMs	H	7.49	0.006	7.61	0.006	7.59	0.007
MrMy	H	8.20	0.015	8.15	0.005	8.14	0.008
MrsC†	M	7.52	0.01	7.40	0.00	7.43	0.00
MrsMk†	M	7.29	0.015	7.32	0.012	7.25	0.009
MrsS†	M	7.54	0.003	7.59	0.006	7.57	0.013
MrsN†	H	7.33	0.00	7.48	0.01	7.39	0.006
MrsM†	H	7.88	0.00	7.60	0.003	7.49	0.006
MrsL†	H	7.82	0.015	7.75	0.012	7.72	0.00
MrsMl†	H	7.72	0.009	7.88	0.012	7.80	0.00
MrsH†	H	7.44	0.003	7.49	0.008	7.49	0.006
MrsHd†	H	7.19	0.013	7.20	0.008	7.30	0.00
MissH†	H	7.36	0.006	7.54	0.013	7.41	0.01

# APPENDIX 4.2 : ANTERIOR CORNEAL SPHERO-CYLINDRICAL COMPONENTS

- \* † denotes female subject
- \* Refractive Groups : M = myope; E = near-emmetrope; H = hyperope
- \* Values derived using the equations of Fowler(1989)

SUBJ	Refractive Group	SPHERE (mm)	CYLINDER (mm)	AXIS (°)
DL	M	7.61	0.23	109.5
NS	M	7.82	0.10	18.5
AW	M	7.91	0.13	73
CS	M	7.96	0.20	83.5
CSd	M	7.93	0.16	106.1
PG	M	8.15	0.33	102.1
OC	M	7.42	0.18	87.7
SS	M	7.76	0.10	106.3
GL	M	7.59	0.08	98.8
SP	M	7.51	0.43	6.6
DW	M	7.72	0.11	82.9
PP	M	7.58	0.47	88.6
BW	M	8.00	0.18	83
JR	M	7.40	0.34	96.2
SP†	M	8.08	0.21	95.3
LMcP†	M	7.80	0.21	90.8
JB†	M	7.50	0.29	77.8
MDH†	M	7.93	0.25	94.1
CN†	M	7.56	0.12	98.2
CP†	M	7.94	0.17	118.2
SD†	M	7.48	0.10	82.2
AJ†	M	7.78	0.16	68.8
DT†	M	7.57	0.39	12
EH†	M	7.22	0.17	111
RP†	M	7.54	0.17	98.5
NB†	M	7.83	0.09	97.4
GH†	M	7.64	0.04	10.6
KP†	M	8.35	0.25	146.5
SJ	E	7.68	0.10	104.1
RS	E	8.03	0.13	83.9
CN	E	7.48	0.21	72.4
IM	E	8.18	0.18	82.4
RSt	E	7.75	0.05	47.9
SMc	E	7.95	0.05	110.9
FE	E	8.06	0.12	101.9
DD	E	7.54	0.08	83
KM	E	7.84	0.21	96.9
TE	E	7.98	0.16	96.8
PI	E	7.90	0.16	97
FD	E	7.79	0.14	18.9
MB†	E	7.50	0.27	82.8
RK†	E	7.58	0.17	78.9
DL†	E	8.15	0.11	60.4
DC†	E	7.67	0.17	100.5
KM†	E	7.77	0.13	29
SP†	E	7.38	0.03	70.2
HJ†	E	7.59	0.26	91.1

HD†	E	7.62	0.17	80.7
LK†	E	8.16	0.11	78.6
GB†	E	7.64	0.02	90
CT†	E	8.17	0.06	111.8
AW†	E	7.57	0.18	80
FE	H	8.07	0.21	85.3
KD	H	7.68	0.11	105.5
DC	H	7.83	0.63	22.6
MD	H	8.05	0.17	64.4
KD†	H	7.85	0.23	107.2
AMct	H	8.10	0.17	93.5
AS†	H	8.00	0.39	94.5
LE†	H	7.32	0.32	102.1

#### SENIOR CITIZEN GROUP

MrM	M	7.85	0.11	178.4
MrN	M	7.74	0.13	41.2
MrMk	M	7.42	0.25	6.1
MrH	H	7.59	0.20	9.8
MrS	H	7.57	0.17	116.5
MrHd	H	7.80	0.27	99.6
MrB	H	8.18	0.86	40
MrSs	H	7.89	0.10	10.2
MrMs	H	7.48	0.14	107.5
MrMy	H	8.13	0.09	24.8
MrsC†	M	7.39	0.14	12.3
MrsMk†	M	7.25	0.12	52.4
MrsSt	M	7.54	0.05	98.8
MrsN†	H	7.33	0.15	84.4
MrsM†	H	7.45	0.58	30
MrsL†	H	7.71	0.14	30.5
MrsMl†	H	7.72	0.17	88.6
MrsH†	H	7.43	0.07	115.9
MrsHd†	H	7.09	0.21	132.6
MissH†	H	7.35	0.20	76.9



# APPENDIX 4.3 : ANTERIOR CORNEAL SPHERO-CYLINDRICAL COMPONENTS

\* † denotes female subject

\* Refractive Groups : M = myope; E = near-emmetrope; H = hyperope

\* Values measured using keratometry

SUBJ	Refractive Group	SPHERE (mm)	CYLINDER (mm)	AXIS (°)
DL	M	7.63	0.18	97.5
NS	M	7.83	0.09	166.5
AW	M	7.88	0.15	89.8
CS	M	7.95	0.20	92.2
CSd	M	7.94	0.12	103.5
PG	M	8.14	0.31	92
CC	M	7.44	0.18	96.5
SS	M	7.76	0.10	100
GL	M	7.57	0.09	104.5
SP	M	7.52	0.41	4.7
DW	M	7.70	0.12	92.2
PP	M	7.56	0.48	89
BW	M	8.00	0.17	90.3
JR	M	7.40	0.33	92.3
SP†	M	8.03	0.23	97.2
LMcP†	M	7.83	0.17	90.3
JB†	M	7.54	0.26	95
MDH†	M	7.92	0.27	95
CN†	M	7.53	0.15	97
CP†	M	7.96	0.09	90.5
SD†	M	7.47	0.12	92
AJ†	M	7.77	0.13	93.2
DT†	M	7.57	0.38	3.2
EH†	M	7.19	0.19	106.7
RP†	M	7.54	0.16	105.9
NB†	M	7.79	0.19	113.3
GH†	M	7.66	0.05	30.3
KR†	M	8.37	0.21	159.3
SJ	E	7.69	0.08	86
RS	E	8.02	0.15	107.3
CN	E	7.53	0.13	91.2
IM	E	8.20	0.17	86.3
RSt	E	7.77	0.02	82.8
SMc	E	7.96	0.03	91.8
FE	E	8.03	0.11	87.3
DD	E	7.51	0.13	87.1
KM	E	7.81	0.24	90.2
TE	E	7.96	0.16	89.2
PI	E	7.91	0.13	89.2
FD	E	7.83	0.08	167.3
MB†	E	7.52	0.22	88.7
PK†	E	7.64	0.10	94.2
DL†	E	8.21	0.02	91.7
DC†	E	7.64	0.17	96.9
KM†	E	7.77	0.13	180
SP†	E	7.39	0.05	85.8
HJ†	E	7.58	0.28	90.1
HO†	E	7.56	0.23	77.3

LK†	E	8.17	0.09	93.5
GB†	E	7.63	0.02	74
CT†	E	8.14	0.05	84.5
AW†	E	7.56	0.17	104.7
FE	H	8.07	0.20	90.7
KD	H	7.67	0.11	91.8
DC	H	7.85	0.61	18
MD	H	8.06	0.1	45
KD†	H	7.83	0.23	98.5
AMc†	H	8.10	0.19	91.8
AS†	H	8.03	0.33	90.7
LE†	H	7.34	0.31	100.6

#### SENIOR CITIZEN GROUP

MrM	M	7.87	0.11	172.5
MrN	M	7.71	0.16	44.3
MrMk	M	7.42	0.26	177.8
MrH	H	7.61	0.16	10.2
MrS	H	7.63	0.1	93.3
MrHd	H	7.72	0.36	87.8
MrB	H	8.22	0.03	86.5
MrSs	H	7.90	0.09	176.3
MrMs	H	7.45	0.14	97.5
MrMy	H	8.14	0.07	62
MrsC†	M	7.38	0.13	175.7
MrsMk†	M	7.29	0.10	77.2
MrsS†	M	7.59	0.02	96.5
MrsN†	H	7.36	0.11	84
MrsM†	H	7.46	0.51	27.3
MrsL†	H	7.76	0.09	9.5
MrsMI†	H	7.73	0.14	93.3
MrsH†	H	7.40	0.11	115.3
MrsHd†	H	7.05	0.26	116
MissH†	H	7.41	0.1	117.7

# APPENDIX 5.1: REFRACTIVE SPHERO-CYLINDRICAL COMPONENTS

\*† denotes female subject

\* Refractive groups : M = myope; H = hyperope; E = emmetrope

\* Sphero-cylindrical values measured by optometer

\* Power in dioptres (D)

SUBJ	Refractive Group	SPH (D)	CYL (D)	AXIS (°)
DL	M	-4.83	0.42	84
NS	M	-3.42	0.92	175.3
AW	M	-1.08	0.41	112.5
CS	M	-1.92	0.25	130.3
CSd	M	-1.00	0.01	145.3
PG	M	-4.33	1.00	117.3
CC	M	-4.92	0.42	118.7
SS	M	-2.17	0.02	7.7
GL	M	-3.92	0.42	100
SP	M	-5.50	2.92	8.7
DW	M	-3.58	0.58	94.5
PP	M	-6.33	1.50	84
BW	M	-3.7	0.59	86.3
JR	M	-3.50	2.00	90
SP†	M	-2.50	0.25	76
LMcP†	M	-3.25	0.17	94
JB†	M	-5.50	0.58	100.3
MDH†	M	-6.75	0.75	74.3
CN†	M	-3.25	0.18	98.3
CP†	M	-1.50	0.42	67.5
SD†	M	-5.04	0.04	67.5
AJ†	M	-0.75	0.75	9.7
DT†	M	-4.25	2.75	10.3
EH†	M	-6.58	1.08	120.3
RP†	M	-2.50	0.02	106.3
NB†	M	-11.63	0.6	90
GH†	M	-2.42	0.34	99.7
KR†	M	-16.50	0.50	88.3
SJ	E	-0.25	0.33	169
RS	E	0.00	0.17	154.3
CN	E	-0.08	0.16	59.3
IM	E	-0.50	0.42	96.3
RSt	E	-0.58	0.08	180
SMc	E	-0.25	0.02	92.7
FE	E	-0.58	0.16	105.7
DD	E	-0.59	0.02	82.7
KM	E	-0.75	0.08	5.3
TE	E	-0.25	0.25	106
PI	E	0.00	0.08	5.3
RD	E	0.33	0.33	178.7
MB†	E	0.25	0.50	80.3
RK†	E	-0.50	0.25	85.7
SL†	E	0.50	0.08	101.7
DC†	E	0.25	0.17	14.3
KM†	E	-0.24	0.47	180
SP†	E	-0.17	0.02	87.3
HJ†	E	-0.17	0.42	170.3
HO†	E	-0.42	0.42	91.3

LK†	E	0.25	0.08	94.7
GB†	E	-0.17	0.09	159.7
CT†	E	-0.08	0.08	35
AW†	E	-0.75	0.25	113.7
FE	H	0.12	0.25	70.7
KD	H	0.73	0.01	89.3
DC	H	-1.67	4.08	12.7
MD	H	1.42	0.83	45
KD†	H	0.39	0.83	101
AMct†	H	0.33	0.17	80.7
AS†	H	1.64	1.83	175.3
LE†	H	1.41	1.00	136.3

#### SENIOR CITIZEN GROUP

MrM	M	-1.92	2.67	173.3
MrN	M	-2.00	0.25	33.3
MrMk	M	-2.17	2.42	176.7
MrH	H	2.67	1.25	100.3
MrS	H	0.83	0.10	174.7
MrHd	H	2.08	0.33	140.3
MrB	H	2.00	0.01	130
MrSs	H	4.00	0.42	98.7
MrMs	H	2.50	0.67	9.7
MrMy	H	0.92	0.83	167.3
MrsC†	M	-3.00	1.08	7
MrsMk†	M	-0.75	1.08	9.7
MrsS†	M	-2.58	0.16	93
MrsN†	H	1.75	1.42	87.3
MrsM†	H	3.33	2.42	30.7
MrsL†	H	4.67	0.83	10.3
MrsMl†	H	1.67	0.75	22
MrsH†	H	1.67	0.20	166.6
MrsHd†	H	0.92	0.58	3.7
MissH†	H	1.58	0.25	92.7

# APPENDIX 5.2 : REFRACTIVE ERROR MEASUREMENTS FROM THREE MERIDIANS.

\* † denotes female subject

\* Refractive groups : M = myope; H = hyperopes; E = emmetropes

\* Mean and standard deviation (SD) values are based on three repeat readings taken on one occasion only

\* Power in dioptres (D)

SUBJ	Refractive Group	MERIDIAN					
		90°		180°		45°	
		Mean	SD	Mean	SD	Mean	SD
DL	M	-5.17	0.14	-4.58	0.14	-4.58	0.14
NS	M	-2.42	0.14	-3.42	0.14	-2.83	0.14
AW	M	-1.00	0.00	-0.83	0.14	-0.83	0.14
CS	M	-1.25	0.00	-1.33	0.14	-0.67	0.14
CSd	M	-0.92	0.14	-1.00	0.00	-0.75	0.00
PG	M	-4.58	0.14	-3.58	0.14	-4.25	0.00
OC	M	-4.75	0.25	-4.50	0.00	-4.83	0.14
SS	M	-2.17	0.14	-2.25	0.00	-2.33	0.14
GL	M	-4.00	0.00	-3.58	0.14	-3.75	0.00
SP	M	-2.24	0.14	-5.17	0.29	-3.75	0.00
DW	M	-3.00	0.00	-3.58	0.14	-3.00	0.00
PP	M	-6.17	0.29	-4.92	0.14	-5.75	0.00
BW	M	-3.75	0.25	-3.00	0.00	-3.25	0.00
JR	M	-3.50	0.00	-1.50	0.00	-2.67	0.14
SPT†	M	-2.83	0.14	-2.17	0.14	-2.42	0.14
LMcP†	M	-3.42	0.14	-2.75	0.00	-3.00	0.25
JB†	M	-5.33	0.29	-4.83	0.29	-4.75	0.00
MDH†	M	-6.67	0.58	-6.00	0.00	-6.42	0.14
CN†	M	-3.25	0.00	-3.08	0.14	-3.33	0.29
CP†	M	-1.42	0.14	-1.00	0.00	-1.33	0.14
SD†	M	-5.08	0.14	-4.83	0.14	-5.08	0.14
AJ†	M	-0.08	0.14	-0.75	0.00	0.00	0.00
DT†	M	-1.92	0.38	-5.50	0.00	-4.00	0.00
EH†	M	-5.33	0.58	-4.83	0.29	-4.17	0.14
RP†	M	-2.50	0.00	-2.50	0.00	-2.50	0.00
NB†	M	-11.58	0.14	-11.08	0.14	-10.83	0.29
GH†	M	-2.17	0.29	-2.17	0.14	-1.83	0.14
KR†	M	-16.25	0.00	-16.08	0.14	-15.50	0.14
SJ	E	0.00	0.00	-0.25	0.00	-0.17	0.14
RS	E	0.17	0.14	0.08	0.14	0.25	0.00
CN	E	0.00	0.25	-0.17	0.14	-0.35	0.00
IM	E	-0.33	0.14	0.00	0.00	0.17	0.00
RSt	E	-0.58	0.14	-0.58	0.14	-0.42	0.14
SMc	E	-0.25	0.00	-0.08	0.14	0.08	0.14
FE	E	-0.42	0.14	-0.33	0.14	-0.25	0.00
DD	E	-0.08	0.00	-0.17	0.14	-0.07	0.14
KM	E	-0.50	0.00	-0.58	0.14	-0.58	0.00
TE	E	-0.33	0.14	-0.08	0.14	-0.17	0.14
PI	E	0.00	0.00	0.00	0.00	-0.25	0.00
FD	E	0.25	0.00	0.00	0.00	0.00	0.00
MB†	E	0.00	0.00	0.75	0.00	0.17	0.14
RK†	E	-0.25	0.00	-0.25	0.00	-0.33	0.14
DL†	E	-0.17	0.14	-0.18	0.00	0.17	0.14
DC†	E	0.50	0.00	0.42	0.14	0.67	0.14
KM†	E	0.17	0.14	-0.17	0.14	-0.17	0.14

SP†	E	-0.25	0.00	-0.17	0.14	-0.25	0.00
HJ†	E	0.42	0.14	-0.17	0.14	0.50	0.00
HO†	E	-0.50	0.00	0.00	0.00	0.00	0.00
LK†	E	0.00	0.25	0.00	0.00	0.10	0.29
GB†	E	0.00	0.00	-0.50	0.00	-0.25	0.00
CT†	E	0.00	0.00	0.00	0.00	-0.08	0.14
AW†	E	-0.42	0.14	-0.33	0.29	-0.25	0.00
FE	H	0.00	0.00	0.83	0.29	0.08	0.14
KD	H	0.83	0.14	1.00	0.14	1.08	0.14
DC	H	2.50	0.25	-1.50	0.00	-0.33	0.14
MD	H	2.08	0.14	1.58	0.14	1.50	0.00
KD†	H	0.42	0.14	1.00	0.00	0.58	0.14
AMc†	H	0.50	0.25	0.50	0.00	0.33	0.14
AS†	H	3.12	0.14	1.83	0.29	3.02	0.14
LE†	H	1.67	0.14	1.75	0.00	2.00	0.00

#### SENIOR CITIZEN GROUP

MrM	M	0.67	0.29	-2.00	0.50	-1.33	0.14
MrN	M	-1.00	0.25	-1.25	0.43	-1.17	0.14
MrMk	M	0.33	0.38	-2.42	0.14	-1.00	0.00
MrH	H	2.50	0.00	4.08	0.14	2.58	0.14
MrS	H	1.00	0.00	0.92	0.14	1.33	0.14
MrHd	H	2.50	0.00	2.50	0.00	3.25	0.00
MrB	H	2.00	0.00	1.75	0.00	1.92	0.14
MrSs	H	4.08	0.14	4.42	0.14	4.25	0.00
MrMs	H	3.33	0.14	2.75	0.00	3.17	0.14
MrMy	H	1.08	0.14	0.67	0.29	0.83	0.14
MrsC†	M	-2.08	0.14	-3.33	0.29	-2.33	0.14
MrsMk†	M	0.50	0.00	-0.58	0.14	-0.17	0.14
MrsS†	M	-2.33	0.14	-2.00	0.00	-2.00	0.00
MrsN†	H	1.83	0.14	2.75	0.25	2.42	0.14
MrsM†	H	4.92	0.14	3.83	0.14	3.25	0.25
MrsL†	H	5.58	0.14	4.50	0.00	4.58	0.14
MrsMl†	H	2.00	0.00	1.42	0.14	1.58	0.14
MrsH†	H	1.92	0.14	1.83	0.14	2.33	0.14
MrsHd†	H	1.25	0.00	0.75	0.25	1.42	0.14
MissH†	H	1.92	0.14	1.75	0.00	2.08	0.14

# APPENDIX 5.3: REFRACTIVE SPHERO-CYLINDRICAL COMPONENTS

\*† denotes female subject

\* Refractive groups : M = myope; H = hyperope; E = emmetrope

\* Sphero-cylinders derived using the equations of Fowler (1989)

\* Power in dioptres (D)

SUBJ	Refractive Group	SPH (D)	CYL (D)	AXIS (°)
DL	M	-5.29	0.83	112.5
NS	M	-3.42	1.01	175.3
AW	M	-1.04	0.24	112.5
CS	M	-1.92	1.25	136.9
CSd	M	-1.17	0.43	140.6
PG	M	-4.61	1.05	80.8
CC	M	-4.87	0.49	60.5
SS	M	-2.34	0.26	35.6
GL	M	-4.00	0.43	95.6
SP	M	-5.17	2.75	179.2
DW	M	-3.70	0.82	157.5
PP	M	-6.20	1.32	80.8
BW	M	-3.77	0.79	99.2
JR	M	-3.51	2.03	85.3
SP†	M	-2.84	0.69	97
LMcP†	M	-3.43	0.69	96.9
JB†	M	-5.50	0.83	116.6
MDH†	M	-6.68	0.69	82.9
CN†	M	-3.35	0.37	58.3
CP†	M	-1.45	0.49	74.5
SD†	M	-5.13	0.35	67.5
AJ†	M	-0.10	1.07	25.7
DT†	M	-4.72	3.03	15.8
EH†	M	-6.03	1.90	127.4
RP†	M	-2.50	0.01	91.1
NB†	M	-11.89	1.12	121.7
GH†	M	-2.50	0.67	135
KR†	M	-16.84	1.34	131.4
SJ	E	-0.26	0.26	9.3
RS	E	-0.01	0.26	144.3
CN	E	-0.35	0.53	35.8
IM	E	-0.54	0.75	121.7
RSt	E	-0.75	0.34	135
SMc	E	-0.43	0.53	125.8
FE	E	-0.51	0.26	125.7
DD	E	-0.17	0.12	112.5
KM	E	-0.60	0.12	22.5
TE	E	-0.34	0.26	80.9
PI	E	-0.25	0.50	44.9
RD	E	-0.06	0.35	22.5
MB†	E	-0.05	0.86	75.5
FK†	E	-0.33	0.17	44.9
SL†	E	-0.30	0.49	109.6
DC†	E	0.25	0.43	160.6
KM†	E	-0.24	0.47	22.5
SP†	E	-0.27	0.12	67.5
HJ†	E	-0.35	0.95	153.9

HO†	E	-0.60	0.71	112.5
LK†	E	-0.08	0.17	135
GB†	E	-0.50	0.50	180
CT†	E	-0.08	0.17	44.9
AW†	E	-0.51	0.26	125.7
FE	H	-0.12	1.07	70.7
KD	H	0.73	0.37	121.7
DC	H	-1.67	4.33	11.3
MD	H	1.42	0.83	26.6
KD†	H	0.39	0.63	78.4
AMc†	H	0.33	0.33	44.9
AS†	H	1.64	1.68	159.9
LE†	H	1.41	0.59	130.9

#### SENIOR CITIZEN GROUP

MrM	M	-2.16	2.98	13.3
MrN	M	-1.25	0.26	9.3
MrMk	M	-2.42	2.75	179.2
MrH	H	2.23	2.12	69.1
MrS	H	0.58	0.76	138.2
MrHd	H	1.75	1.50	135
MrB	H	1.74	0.26	170.7
MrSs	H	4.08	0.33	91
MrMs	H	2.72	0.63	168.4
MrMy	H	0.66	0.42	5.7
MrsC†	M	-3.44	1.46	164.5
MrsMk†	M	-0.60	1.11	6.5
MrsS†	M	-2.40	0.47	112.5
MrsN†	H	1.82	0.95	97.6
MrsM†	H	3.13	2.50	32.1
MrsL†	H	4.33	1.42	20.1
MrsMI†	H	1.39	0.63	11.6
MrsH†	H	1.42	0.92	137.6
MrsHd†	H	0.51	0.97	150.5
MissH†	H	1.57	0.53	144.2



# APPENDIX 6.1: PACHOMETRIC MEASUREMENTS

\* † denotes female subject

\* Refractive Groups : M = myope; E = near-emmetropes; H = hyperopes.

\* Mean and standard deviation (SD) values were calculated from three readings for each parameter

\* Dimensions in mm

SUBJ	Refractive Group	Corneal Thickness	
		Mean	SD
DL	M	0.47	0.01
NS	M	0.507	0.06
AW	M	0.503	0.06
CS	M	0.463	0.012
CSd	M	0.50	0.05
PG	M	0.475	0.012
CC	M	0.50	0.00
SS	M	0.50	0.01
GL	M	0.517	0.006
SP	M	0.523	0.006
DW	M	0.51	0.01
PP	M	0.51	0.01
BW	M	0.493	0.00
JR	M	0.51	0.00
SP†	M	0.467	0.02
LMcP†	M	0.48	0.01
JB†	M	0.502	0.006
MDH†	M	0.48	0.01
CN†	M	0.465	0.005
CP†	M	0.513	0.006
SD†	M	0.473	0.012
AJ†	M	0.433	0.02
DT†	M	0.483	0.006
EH†	M	0.503	0.003
RP†	M	0.497	0.006
NB†	M	0.497	0.006
GH†	M	0.493	0.012
KR†	M	0.495	0.005
SJ	E	0.503	0.006
RS	E	0.493	0.06
CN	E	0.493	0.012
IM	E	0.51	0.01
RSt	E	0.503	0.006
SMc	E	0.56	0.00
FE	E	0.457	0.015
DD	E	0.473	0.012
KM	E	0.437	0.006
TE	E	0.615	0.009
PI	E	0.51	0.01
RD	E	0.533	0.012
MB†	E	0.493	0.012
PK†	E	0.502	0.003
DL†	E	0.437	0.015
DC†	E	0.467	0.006
KM†	E	0.512	0.012
SP†	E	0.477	0.006
HJ†	E	0.49	0.01

HO†	E	0.477	0.006
LK†	E	0.497	0.006
GB†	E	0.503	0.003
CT†	E	0.517	0.006
AW†	E	0.533	0.006
FE	H	0.48	0.00
KD	H	0.49	0.01
DC	H	0.503	0.015
MD	H	0.50	0.00
KD†	H	0.493	0.003
AMc†	H	0.55	0.01
AS†	H	0.523	0.012
LE†	H	0.505	0.005

# SENIOR CITIZEN GROUP

MrM	M	0.46	0.00
MrN	M	0.462	0.003
MrMk	M	0.483	0.006
MrH	H	0.52	0.00
MrS	H	0.50	0.00
MrHd	H	0.463	0.006
MrB	H	0.55	0.00
MrSs	H	0.503	0.006
MrMs	H	0.45	0.01
MrMy	H	0.497	0.006
MrsC†	M	0.483	0.015
MrsMk†	M	0.467	0.005
MrsS†	M	0.49	0.00
MrsN†	H	0.483	0.005
MrsM†	H	0.503	0.005
MrsL†	H	0.487	0.006
MrsMl†	H	0.49	0.01
MrsH†	H	0.507	0.006
MrsHd†	H	0.457	0.015
MissH†	H	0.437	0.015

# APPENDIX 7.1: PURKINJE IMAGE HEIGHT RATIOS IN THREE MERIDIANS.

\* † denotes female subject

\* Refractive Groups: M = myope; E = near-emmetrope; H = hyperope.

\* Mean and standard deviation (SD) are calculated from ten measurements of the heights of each of the images I and II.

\* Image heights are expressed in mm

SUBJ	REF.GRP M	IMAGE	90°			180°			45°		
			HEIGHT	SD	RATIO	HEIGHT	SD	RATIO	HEIGHT	SD	RATIO
DL		I	35.76	0.042							
		0.052				35.08	0.042		34.88		
		II			0.789			0.833			0.823
		0.000	28.22	0.052		29.22	0.052		28.70		
NS		I	37.04	0.042		35.36	0.052	35.02	0.032		
					0.864			0.860			0.874
		II	32	0.00		30.4	0.00		30.62	0.032	
		I	37.44	0.042		36.38	0.042	36.02	0.031		
					0.830			0.863			0.836
		II	31.08	0.052		31.4	0.00		30.84	0.052	
CS		I	37.08	0.052		39.60	0.00		35.22	0.032	
					0.820			0.880			0.854
		II	30.40	0.00		34.84	0.052	30.10	0.000		
		I	35.86	0.042		36.88	0.042	36.48	0.052		
					0.819			0.850			0.837
		II	29.38	0.052		31.36	0.042	30.52	0.048		
PG		I	38.96	0.042		38.24	0.052	37.82	0.032		
					0.826			0.838			0.805
		II	32.20	0.00		32.04	0.052	30.44	0.042		
		I	34.02	0.048		35.33	0.048	35.64	0.042		
					0.758			0.824			0.791
		II	25.80	0.00		29.1	0.00		28.20	0.00	
SS		I	35.52	0.052		34.93	0.048	36.14	0.048		
					0.811			0.833			0.867
		II	28.80	0.00		29.10	0.00		31.34	0.048	
		I	35.42	0.032		35.52	0.042	34.86	0.048		
					0.835			0.863			0.843
		II	29.56	0.042		30.66	0.052	29.38	0.047		
SP		I	37.66	0.048		34.32	0.042	34.56	0.048		
					0.779			0.810			0.768
		II	29.36	0.00		27.80	0.000	26.54	0.00		
		I	36.68	0.052		35.72	0.042	35.50	0.053		
					0.815			0.862			0.860
		II	29.88	0.052		30.82	0.042	30.52	0.052		
PP		I	36.04	0.048		37.02	0.042	36.60	0.00		
					0.828			0.837			0.812
		II	29.84	0.048		30.98	0.042	29.72	0.042		
		I	36.60	0.00		37.63	0.048	36.52	0.052		
					0.805			0.860			0.841
		II	29.46	0.048		32.35	0.053	30.72	0.032		
JR		I	34.04	0.042		35.63	0.048	34.08	0.052		
					0.847			0.854			0.870
		II	28.82	0.057		30.44	0.053	29.66	0.048		

REF GRP		E						
SJ	I	37.1	0.053	35.02	0.042	34.96	0.042	
			0.788			0.828		0.816
RS	II	29.22	0.032	28.99	0.032	28.50	0.00	
	I	37.26	0.048	36.18	0.042	36.46	0.048	
CN			0.801			0.850		0.818
	II	29.84	0.042	30.74	0.052	29.80	0.048	
IM	I	35.78	0.032	35	0.00		34.20	0.00
			0.836			0.861		0.858
RSt	II	29.92	0.032	30.12	0.042	29.34	0.042	
	I	37.10	0.053	38.25	0.053	37.10	0.053	
SMc			0.846			0.843		0.860
	II	31.40	0.00	32.25	0.053	31.90	0.053	
FE	I	35.90	0.053	36.03	0.048	34.70	0.053	
		0.812		0.848			0.832	
DD	II	29.16	0.042	30.55	0.053	28.88	0.042	
	I	36.22	0.032	36.64	0.052	35.10	0.053	
KM		0.857		0.857			0.872	
	II	31.04	0.042	31.40	0.00		30.60	0.053
TE	I	36.04	0.032	35.84	0.048	36.12	0.052	
			0.847			0.872		0.863
PI	II	30.51	0.032	31.27	0.048	31.16	0.042	
	I	35.74	0.048	34.49	0.031	36.08	0.052	
FD		0.814		0.850			0.829	
	II	29.10	0.053	29.32	0.042	29.92	0.053	
RE	I	36.96	0.042	37.29	0.032	36.20	0.00	
			0.777			0.843		0.806
PI	II	28.72	0.052	31.45	0.053	29.16	0.042	
	I	37.62	0.032	37.2	0.00		37.10	0.052
KD			0.787			0.828		0.830
	II	29.60	0.00	30.8	0.00		30.80	0.00
DC	I	37.62	0.032	36.57	0.048	36.50	0.053	
			0.801			0.850		0.812
MD	II	30.14	0.048	31.08	0.042	29.66	0.048	
	I	36.70	0.053	36.13	0.048	35.88	0.052	
MD			0.787			0.847		0.793
	II	28.88	0.052	30.59	0.032	28.46	0.052	
REF GRP		H						
FE	I	37.42	0.032	37.90	0.00		37.04	0.048
			0.809			0.842		0.825
KD	II	30.26	0.048	31.91	0.032	30.56	0.042	
	I	34.84	0.042	35.64	0.052	34.76	0.042	
DC			0.852			0.880		0.870
	II	29.70	0.053	31.37	0.048	30.24	0.042	
MD	I	38.12	0.052	36.65	0.053	37.48	0.052	
		0.802		0.849			0.802	
MD	II	30.58	0.032	31.1	0.00		30.04	0.048
	I	36.76	0.042	37.23	0.048	37.26	0.048	
MD			0.797			0.856		0.818
	II	29.30	0.052	31.84	0.042	30.48	0.052	

REF GRP		M						
SP†	I	36.84	0.048	37.96	0.052	36.98	0.032	
		0.853		0.870			0.879	
LMcP†	II	31.44	0.048	33.02	0.048	32.5	0.00	
	I	36.22	0.032	37.62	0.052	36.46	0.048	
			0.817			0.863		0.834
JB†	II	29.60	0.00	32.17	0.048	30.42	0.032	
	I	35.22	0.032	36.73	0.048	34.90	0.053	
			0.794			0.830		0.778
MDH†	II	27.96	0.042	30.50	0.00		27.14	0.042
	I	37.16	0.042	38.27	0.048	36.78	0.032	
			0.823			0.831		0.842
CN†	II	30.58	0.032	31.8	0.00		30.96	0.048
	I	34.32	0.052	35.40	0.00		34.10	0.00
			0.824			0.860		0.838
CP†	II	28.30	0.053	30.45	0.053	28.60	0.048	
	I	36.18	0.032	37.51	0.032	36.46	0.048	
			0.841			0.843		0.835
SD†	II	30.44	0.042	31.63	0.048	30.44	0.042	
	I	35.60	0.00	35.25	0.053	34.66	0.048	
			0.774			0.814		0.785
AJ†	II	27.56	0.042	28.70	0.00		27.20	0.00
	I	37.14	0.048	36.96	0.052	36.34	0.048	
			0.782			0.835		0.791
DT†	II	29.06	0.048	30.88	0.042	28.76	0.048	
	I	37.74	0.048	35.18	0.042	35.72	0.048	
			0.837			0.860		0.857
BH†	II	31.60	0.00	30.27	0.048	30.60	0.00	
	I	34.08	0.052	33.85	0.053	33.08	0.052	
			0.804			0.845		0.844
RP†	II	27.40	0.00	28.60	0.00		27.92	0.042
	I	35.76	0.048	34.87	0.048	36.26	0.048	
			0.788			0.840		0.802
NB†	II	28.18	0.032	29.30	0.00		29.06	0.042
	I	37.04	0.048	37.20	0.00		36.70	0.053
			0.777			0.852		0.824
GH†	II	28.78	0.032	31.69	0.032	30.26	0.048	
	I	35.56	0.042	35.55	0.053	35.14	0.048	
			0.864			0.866		0.864
KR†	II	30.72	0.052	30.80	0.00		30.36	0.042
	I	39.66	0.048	39.4	0.00		38.06	0.048
			0.831			0.838		0.836
	II	32.96	0.042	33.01	0.032	31.80	0.00	

REF GRP		E						
MB†	I	34.39	0.032	36.47	0.048	35.60	0.052	
			0.828			0.791		0.803
RK†	II	28.47	0.032	28.85	0.052	28.59	0.042	
	I	35.36	0.048	36.17	0.048	35.28	0.052	
			0.816			0.848		0.838
DL†	II	28.86	0.00	30.70	0.052	29.56	0.048	
	I	37.96	0.042	36.94	0.048	36.90	0.00	
			0.819			0.850		0.827
DC†	II	31.10	0.00	31.40	0.052	30.50	0.053	
	I	35.28	0.052	36.28	0.042	36.52	0.052	
			0.832			0.844		0.866

	II	29.34	0.048	30.64	0.042	31.61	0.048	
KM†	I	35.60	0.00	36.03	0.048	35.30	0.053	
			0.814			0.834		0.835
SPT	II	28.98	0.042	30.04	0.032	29.48	0.052	
	I	33.42	0.032	34.49	0.032	33.02	0.032	
			0.760			0.783		0.758
HD†	II	25.42	0.048	27.02	0.00		25.02	0.048
	I	35.04	0.042	35.60	0.00		34.94	0.048
			0.826			0.858		0.824
HJ†	II	28.94	0.042	30.54	0.042	28.78	0.052	
	I	34.94	0.048	36.13	0.048	35.16	0.042	
			0.834			0.856		0.854
LK†	II	29.16	0.048	30.94	0.042	30.04	0.053	
	I	37.32	0.052	37.26	0.052	36.78	0.032	
			0.816			0.809		0.783
GB†	II	30.47	0.032	30.16	0.042	28.80	0.048	
	I	35.36	0.042	35.61	0.032	34.88	0.052	
			0.807			0.840		0.830
CT†	II	28.53	0.048	29.91	0.00		28.95	0.048
	I	36.98	0.032	38.07	0.048	36.56	0.048	
		0.780		0.841			0.818	
AW†	II	28.83	0.042	32.02	0.048	29.88	0.052	
	I	35.63	0.042	35.57	0.048	34.58	0.032	
			0.817			0.832		0.822
	II	29.10	0.053	29.61	0.042	28.41	0.00	

REF GRP  
H

KD†	I	38.00	0.00	36.9	0.00		36.74	0.048
			0.824			0.850		0.831
AMc†	II	31.32	0.053	31.33	0.053	30.52	0.032	
	I	37.04	0.042	38.15	0.053	36.56	0.042	
			0.810			0.839		0.819
AS†	II	30.02	0.032	32.02	0.00		29.95	0.032
	I	36.94	0.048	38.33	0.048	37.06	0.048	
			0.792			0.819		0.787
LE†	II	29.28	0.053	31.37	0.042	29.18	0.042	
	I	34.06	0.00	34.58	0.042	33.54	0.048	
			0.810			0.820		0.803
	II	27.60	0.048	28.34	0.00		26.92	0.053

SENIOR CITIZEN GROUP

REF GRP  
M

MrM	I	38.58	0.032	35.22	0.042	37.04	0.042	
			0.737			0.834		0.766
MrN	II	28.42	0.042	29.39	0.057	28.36	0.048	
	I	36.86	0.048	35.04	0.052	36.52	0.052	
			0.802			0.835		0.833
MrMk	II	29.58	0.048	29.27	0.048	30.40	0.042	
	I	36.74	0.048	33.35	0.052	35.06	0.048	
			0.846			0.870		0.858
	II	31.10	0.048	29.02	0.042	30.10	0.053	

REF GRP  
H

MrH	I	36.56	0.042	33.96	0.052	35.40	0.047	
			0.769			0.862		0.815
MrS	II	28.10	0.053	29.28	0.052	28.84	0.042	
	I	38.14	0.048	34.35	0.053	36.06	0.048	
			0.772			0.855		0.813
MrHd	II	29.44	0.042	29.36	0.042	29.32	0.048	
	I	34.98	0.032	32.30	0.00		33.38	0.032
			0.761			0.849		0.791
MrB	II	26.64	0.032	27.41	0.032	26.42	0.052	
	I	39.00	0.00	37.18	0.042	39.24	0.042	
			0.752			0.823		0.810
MrSs	II	29.30	0.053	30.6	0.047	31.77	0.042	
	I	38.14	0.048	35.45	0.053	38.26	0.048	
			0.786			0.847		0.808
MrMs	II	29.96	0.042	30.02	0.042	30.92	0.053	
	I	32.20	0.00	31.26	0.052	31.96	0.042	
			0.809			0.846		0.812
MrMy	II	26.04	0.042	26.41	0.052	25.64	0.042	
	I	39.98	0.057	37.30	0.00		38.78	0.057
			0.864			0.868		0.888
	II	34.56	0.048	32.40	0.042	34.44	0.042	

REF GRP  
M

MrsC†	I	35.54	0.048	33.37	0.048	34.08	0.870	
			0.860			0.860		0.850
MrsMk†	II	30.56	0.042	28.70	0.053	28.96	0.042	
	I	36.66	0.048	34.03	0.048	35.64	0.042	
			0.798			0.816		0.796
MrsS†	II	29.26	0.042	27.78	0.032	28.35	0.052	
	I	36.76	0.042	33.75	0.053	35.84	0.042	
			0.814			0.838		0.843
	II	29.94	0.052	28.28	0.048	30.20	0.048	

REF GRP  
H

MrsN†	I	35.18	0.032	33.47	0.048	34.34	0.048	
			0.821			0.875		0.854
MrsM†	II	28.90	0.052	29.30	0.048	29.34	0.042	
	I	37.18	0.032	34.05	0.052	36.40	0.00	
			0.808			0.842		0.828
MrsL†	II	30.08	0.042	28.68	0.048	30.14	0.042	
	I	36.94	0.048	35.33	0.048	36.64	0.042	
			0.784			0.863		0.822
MrsMI†	II	28.96	0.048	30.48	0.052	30.12	0.048	
	I	36.74	0.048	35.25	0.053	35.88	0.052	
			0.797			0.844		0.811
MrsH†	II	29.30	0.052	29.74	0.052	29.10	0.047	
	I	35.56	0.042	33.16	0.052	34.50	0.052	
			0.805			0.860		0.827
MrsHd†	II	28.62	0.042	28.51	0.032	28.52	0.052	
	I	33.14	0.048	30.99	0.032	31.52	0.052	
			0.770			0.814		0.776
	II	25.54	0.052	25.24	0.042	24.46	0.048	

# APPENDIX 7.2. PURKINJE IMAGE RATIOS FOR THE ONE SOURCE AND TWO SOURCE METHODS

\* † denotes female subject.

\* Refractive groups : M = myopes; E = near-emmetropes; H = Hyperopes.

\* Purkinje image ratios are calculated from ten measurements of each of the images I and II in the 90° meridian only.

		RATIO	
SUBJ	REF GRP	ONE SOURCE	TWO SOURCE
YOUNG SUBJECT GROUP			
DL	M	0.789	0.791
NS	M	0.864	0.873
AW	M	0.830	0.837
CS	M	0.820	0.820
CSd	M	0.819	0.816
PG	M	0.826	0.834
OC	M	0.758	0.762
SS	M	0.811	0.816
GL	M	0.835	0.843
SP	M	0.779	0.776
DW	M	0.815	0.822
PP	M	0.828	0.825
BW	M	0.805	0.806
JR	M	0.847	0.841
SP†	M	0.853	0.844
LMcP†	M	0.817	0.813
JB†	M	0.794	0.802
MDH†	M	0.823	0.817
CN†	M	0.824	0.816
CP†	M	0.841	0.831
SD†	M	0.774	0.774
AJ†	M	0.782	0.784
DT†	M	0.837	0.835
EH†	M	0.804	0.812
RP†	M	0.788	0.782
NB†	M	0.777	0.783
GH†	M	0.864	0.856
KR†	M	0.831	0.836
SJ	E	0.788	0.792
RS	E	0.801	0.805
CN	E	0.836	0.833
IM	E	0.846	0.842
RSt	E	0.812	0.805
SMc	E	0.857	0.862
FE	E	0.847	0.844
DD	E	0.814	0.819
KM	E	0.777	0.784
TE	E	0.787	0.792
PI	E	0.801	0.806
FD	E	0.787	0.785
MB†	E	0.828	0.822
RK†	E	0.816	0.818
DL†	E	0.819	0.821
DC†	E	0.832	0.828
KM†	E	0.814	0.809



SP†	E	0.760	0.753
HO†	E	0.826	0.828
HJ†	E	0.834	0.835
LK†	E	0.816	0.808
GB†	E	0.807	0.811
CT†	E	0.780	0.782
AW†	E	0.816	0.810
FE	H	0.809	0.809
KD	H	0.852	0.854
DC	H	0.802	0.804
MD	H	0.797	0.796
KD†	H	0.824	0.828
AMc†	H	0.810	0.804
AS†	H	0.792	0.796
LE†	H	0.810	0.813

#### SENIOR CITIZEN GROUP

MrM	M	0.737	0.742
MrN	M	0.802	0.805
MrMk	M	0.846	0.842
MrH	H	0.769	0.773
MrS	H	0.772	0.771
MrHd	H	0.761	0.767
MrB	H	0.752	0.750
MrSs	H	0.786	0.789
MrMs	H	0.809	0.810
MrMy	H	0.864	0.866
MrsC†	M	0.860	0.864
MrsMk†	M	0.798	0.802
MrsS†	M	0.814	0.808
MrsN†	H	0.821	0.830
MrsM†	H	0.808	0.805
MrsL†	H	0.784	0.780
MrsMl†	H	0.797	0.803
MrsH†	H	0.805	0.802
MrsHd†	H	0.770	0.770
MissH†	H	0.819	0.815

# APPENDIX 7.3: POSTERIOR CORNEAL RADIUS IN THREE MERIDIANS.

\* † denotes female subject

\* Refractive groups: M = myope; E = near-emmetrope; H = hyperope.

\* Results shown are based on ten measurements for each Purkinje image height in each of the three meridians

\* Dimensions in mm

SUBJ	Refractive Group	MERIDIAN (°)		
		90	180	45
DL	M	6.21	6.62	6.55
NS	M	6.87	6.78	6.89
AW	M	6.68	6.98	6.74
CS	M	6.67	7.21	6.96
CSd	M	6.63	6.95	6.84
PG	M	6.88	7.23	6.93
OC	M	5.83	6.37	6.09
SS	M	6.44	6.64	6.84
GL	M	6.42	6.65	6.51
SP	M	6.37	6.21	6.09
DW	M	6.42	6.80	6.72
PP	M	6.08	6.84	6.47
BW	M	6.61	7.11	6.89
JR	M	6.34	6.67	6.65
SP†	M	6.98	7.28	7.25
LMcP†	M	6.51	6.98	6.71
JB†	M	6.12	6.56	6.35
MDH†	M	6.66	6.92	6.90
CN†	M	6.35	6.66	6.51
CP†	M	6.79	6.89	6.87
SD†	M	5.99	6.31	6.08
AJ†	M	6.31	6.74	6.38
DT†	M	6.75	6.92	6.88
EH†	M	5.94	6.30	6.25
RP†	M	6.11	6.56	6.28
NB†	M	6.36	6.55	6.32
GH†	M	6.67	6.65	6.66
KR†	M	7.22	7.18	7.31
SJ	E	6.23	6.53	6.45
RS	E	6.60	7.02	6.75
CN	E	6.36	6.65	6.50
IM	E	7.01	7.14	7.16
RSt	E	6.59	6.67	6.55
SMc	E	6.86	6.89	6.98
FE	E	6.94	7.18	7.10
DD	E	6.27	6.55	6.39
KM	E	6.32	6.90	6.56
TE	E	6.42	6.81	6.78
TE	E	6.49	6.93	6.64
FD	E	6.40	6.65	6.36
MB†	E	6.31	6.32	6.25
RK†	E	6.30	6.64	6.48
DL†	E	6.87	7.11	6.90
DC†	E	6.50	6.71	6.80

KMt	E	6.48	6.66	6.59
SPt	E	5.82	5.98	5.81
HJt	E	6.43	6.79	6.66
HOt	E	6.41	6.75	6.45
LKt	E	6.81	6.85	6.62
GBt	E	6.32	6.50	6.45
CTt	E	6.58	7.01	6.86
AWt	E	6.29	6.53	6.37
FE	H	6.69	7.08	6.87
KD	H	6.62	6.87	6.79
DC	H	6.88	6.80	6.51
MD	H	6.62	7.08	6.74
KDt	H	6.61	6.93	6.79
AMct	H	6.69	7.03	6.84
ASt	H	6.51	7.01	6.67
LEt	H	6.06	6.37	6.20

#### SENIOR CITIZEN GROUP

MrM	M	6.14	6.67	6.29
MrN	M	6.44	6.63	6.56
MrMk	M	6.57	6.49	6.51
MrH	H	6.18	6.59	6.36
MrS	H	6.06	6.65	6.41
MrHd	H	6.18	6.94	6.67
MrB	H	6.43	6.88	6.77
MrSs	H	6.47	6.76	6.55
MrMs	H	6.21	6.53	6.31
MrMy	H	7.15	7.13	7.24
MrsCt	M	6.52	6.41	6.38
MrsMkt	M	5.97	6.10	5.92
MrsSt	M	6.27	6.45	6.46
MrsNt	H	6.13	6.57	6.37
MrsMt	H	6.52	6.48	6.30
MrsLt	H	6.32	6.74	6.47
MrsMlt	H	6.32	6.74	6.47
MrsHt	H	6.12	6.48	6.29
MrsHdt	H	5.73	5.99	5.85
MissHt	H	6.16	6.60	6.29

# APPENDIX 7.4: POSTERIOR CORNEAL SPHERO-CYLINDRICAL COMPONENTS

\* † denotes female subject

\* Refractive Groups : M = myope; E = near-emmetrope; H = hyperope

\* Values derived using the equations of Fowler(1989)

SUBJ	Refractive Group	SPHERE (mm)	CYLINDER (mm)	AXIS (°)
DL	M	6.16	0.50	107.6
NS	M	6.74	0.17	152.8
AW	M	6.66	0.35	74.5
CS	M	6.67	0.54	92.1
CSd	M	6.62	0.34	98.7
PG	M	6.84	0.43	72.2
CC	M	5.83	0.54	88.9
SS	M	6.21	0.65	126.1
GL	M	6.42	0.24	83.9
SP	M	6.08	0.42	34.5
DW	M	6.39	0.44	105
PP	M	6.09	0.75	90.4
BW	M	6.61	0.50	92.9
JR	M	6.29	0.43	110.6
SP†	M	6.94	0.38	109.3
LMcP†	M	6.51	0.48	85.8
JB†	M	6.11	0.44	92.6
MDH†	M	6.61	0.35	111.4
CN†	M	6.35	0.31	90.9
CP†	M	6.79	0.11	100.9
SD†	M	5.98	0.35	88.2
AJ†	M	6.27	0.52	73
DT†	M	6.74	0.19	103.9
EH†	M	5.90	0.44	107.9
RP†	M	6.10	0.46	83.1
NB†	M	6.29	0.33	62.6
GH†	M	6.65	0.02	180
KR†	M	7.09	0.22	140.2
SJ	E	6.21	0.34	102.9
RS	E	6.59	0.44	82
CN	E	6.36	0.29	89
IM	E	6.98	0.20	114.5
RSt	E	6.54	0.18	58.3
SMc	E	6.77	0.21	130.9
FE	E	6.94	0.25	97
DD	E	6.26	0.30	80.2
KM	E	6.32	0.59	85.1
TE	E	6.36	0.51	110.1
PI	E	6.48	0.46	81.2
FD	E	6.32	0.41	63.4
MB†	E	6.25	0.13	47.2
FK†	E	6.30	0.34	91.1
DL†	E	6.84	0.30	71.6
DC†	E	6.37	0.46	121.4
KM†	E	6.48	0.18	96.3
SP†	E	5.78	0.24	65.8
HJ†	E	6.43	0.37	96.3

HO†	E	6.37	0.43	71.3
LK†	E	6.62	0.42	67.7
GB†	E	6.31	0.20	101.9
CT†	E	6.57	0.45	98.4
AW†	E	6.28	0.25	80.8
FE	H	6.69	0.39	87.8
KD	H	6.61	0.27	99.9
DC	H	6.51	0.66	41.5
MD	H	6.60	0.51	57.2
KD†	H	6.61	0.32	93.6
AMc†	H	6.69	0.34	86.6
AS†	H	6.49	0.54	79.8
LE†	H	6.06	0.31	87.2

#### SENIOR CITIZEN GROUP

MrM	M	6.12	0.58	78.3
MrN	M	6.43	0.20	100.1
MrMk	M	6.49	0.09	13.3
MrH	H	6.18	0.41	86.5
MrS	H	6.05	0.60	96.2
MrHd	H	6.16	0.80	98.3
MrB	H	6.41	0.50	102.5
MrSs	H	6.46	0.32	77.9
MrMs	H	6.20	0.34	79.7
MrMy	H	7.04	0.20	42.1
MrsC†	M	6.36	0.20	28.5
MrsMk†	M	5.91	0.25	60.9
MrsS†	M	6.22	0.28	113.9
MrsN†	H	6.13	0.44	92.6
MrsM†	H	6.30	0.40	42.1
MrsL†	H	6.31	0.44	82
MrsMl†	H	6.31	0.44	82
MrsH†	H	6.12	0.36	88.4
MrsHd†	H	5.73	0.26	87.8
MissH†	H	6.13	0.49	79.3

APPENDIX 7.5 : POSTERIOR CORNEAL RADIUS IN THREE MERIDIANS, REPEAT READINGS.

\* † denotes female subject

\* Refractive Groups: M = myope; E = near-emmetrope; H = hyperope

\* Results shown are based on ten measurements for each Purkinje image height in each of the three meridians

\* Dimensions in mm

\* n = 23

SUBJ	Refractive Group	MERIDIAN		
		90°	180°	45°
CS	M	6.66	7.20	6.94
CC	M	5.80	6.36	6.12
DW	M	6.43	6.76	6.74
PP	M	6.05	6.84	6.50
BW	M	6.64	7.12	6.87
JR	M	6.34	6.62	6.70
SP†	M	7.02	7.28	7.22
MDH†	M	6.64	6.93	6.92
CN†	M	6.36	6.68	6.53
AJ†	M	6.30	6.77	6.42
NB†	M	6.39	6.52	6.35
KR†	M	7.23	7.19	7.35
RS†	E	6.56	6.67	6.60
DD	E	6.26	6.60	6.38
RD	E	6.40	6.67	6.39
SP†	E	5.81	5.96	5.79
HO†	E	6.44	6.75	6.42
GB†	E	6.33	6.50	6.47
CT†	E	6.60	7.01	6.80
FE	H	6.70	7.06	6.82
MD	H	6.62	7.09	6.77
KD†	H	6.61	6.90	6.75
LE†	H	6.04	6.38	6.24

APPENDIX 7.6 : POSTERIOR CORNEAL SPHERO-CYLINDRICAL COMPONENTS, REPEAT READINGS.

\* † denotes female subject

\* Refractive Groups : M = myope; E = near-emmetrope; H = hyperope

\* Values derived using the equations of Fowler (1989)

\* N = 23

SUBJ	Refractive Group	SPHERE (mm)	CYLINDER (mm)	AXIS (°)
CS	M	6.66	0.54	91.1
CC	M	5.80	0.57	94.1
DW	M	6.38	0.44	110.7
PP	M	6.05	0.80	94
BW	M	6.64	0.48	88.8
JR	M	6.22	0.52	118.8
SP†	M	7.00	0.30	104.1
MDH†	M	6.59	0.40	111.5
CN†	M	6.36	0.32	91.8
AJ†	M	6.27	0.52	76.9
NB†	M	6.33	0.25	60.9
KR†	M	7.07	0.28	139
RS†	E	6.56	0.11	82.4
DD	E	6.25	0.35	81.8
RD	E	6.34	0.40	66.5
SP†	E	5.76	0.24	64.1
HO†	E	6.36	0.47	65.8
GB†	E	6.31	0.20	106.5
CT†	E	6.60	0.41	89.3
FE	H	6.69	0.38	80.8
MD	H	6.61	0.50	80.1
KD†	H	6.61	0.29	89
LE†	H	6.04	0.35	95

# APPENDIX 7.7: ASSESSMENT OF MAGNIFICATION AND DISTORTION OF CORNEAL P.I. PHOTOGRAPHS

\* Figures shown in the table refer to the distances measured between grid lines from photographs taken directly from the video monitor screen.

\* Real distance between the individual grid lines was 1mm. Distance between the furthest grid lines in the horizontal and vertical meridians was measured as 8.02mm ( $\pm 0.045$ ) and 8.00mm ( $\pm 0.00$ ) respectively.

\* Distances were measured with calipers to the nearest 0.10 mm. Five measurements were made of each of the grid squares.

FILM ROLL		GRID SIZE FROM PHOTOGRAPH		MAGNIFICATION	
		HORIZONTAL	VERTICAL	HORIZONTAL	VERTICAL
A	Mean	48.88	48.96	6.095	6.12
	SD	0.11	0.089		
B		48.96	49.02	6.105	6.127
		0.055	0.045		
C		49.44	49.18	6.165	6.147
		0.055	0.045		
D		49.68	49.04	6.195	6.13
		0.045	0.054		
E		49.38	49.00	6.157	6.125
		0.045	0.00		
F		49.22	49.18	6.137	6.148
		0.11	0.045		
G		49.02	49.18	6.112	6.147
		0.045	0.045		
H		48.88	48.96	6.095	6.12
		0.084	0.055		
I		49.02	48.98	6.112	6.123
		0.045	0.045		
J		49.00	48.98	6.11	6.123
		0.00	0.045		
AVE		49.148	49.048	6.128	6.131
		$\pm 0.271$	$\pm 0.094$		$\pm 0.012$



# APPENDIX 9.1. SPHERO-CYLINDRICAL COMPONENTS OF ONE-SURFACE CORNEA

\* † denotes female subject

\* Refractive groups : M = myopes; H = hyperopes; E = near-emmetropes

\* Power in dioptres (D)

Anterior Corneal Power				
Subj	Ref Group	SPH	CYL	AXIS
DL	M	43.03	1.28	20.7
NS	M	42.06	0.55	108.3
AW	M	41.96	0.70	163.8
CS	M	41.33	1.07	174.6
CSd	M	41.70	0.87	14.9
PG	M	39.76	1.66	11.7
OC	M	44.39	1.10	177.1
SS	M	42.92	0.56	18.4
GL	M	43.98	0.49	7.1
SP	M	42.52	2.37	95.4
DW	M	43.07	0.65	172.5
PP	M	41.91	2.61	179
BW	M	41.23	0.96	174
JR	M	43.55	2.07	7.1
SP†	M	40.69	1.09	4.4
LMcP†	M	42.17	1.09	3.2
MDH†	M	41.28	1.28	5.1
CN†	M	43.91	0.75	9.3
CP†	M	41.58	0.92	29.4
SD†	M	44.50	0.62	174.5
AJ†	M	42.50	0.87	160.1
DT†	M	42.41	2.13	101.1
EH†	M	45.63	1.13	8.4
RP†	M	43.73	1.05	8.4
NB†	M	42.58	0.52	9.3
GH†	M	43.91	0.27	103.2
KR†	M	39.23	1.16	55.7
SJ	E	43.39	0.51	13.3
RS	E	41.33	0.70	173.7
CN	E	43.86	1.26	161.3
IM	E	40.40	0.87	175.2
RSt	E	43.25	0.29	140.6
SMc	E	42.19	0.23	22.5
FE	E	41.27	0.83	17.4
DD	E	44.27	0.49	173.1
KM	E	41.89	1.13	171.9
TE	E	41.43	0.86	7.2
PI	E	41.84	0.89	7.2
RD	E	42.53	0.79	106.7
MB†	E	43.40	1.62	173.1
FK†	E	43.57	1.02	172
DL†	E	40.86	0.53	149.4
DC†	E	43.04	0.94	12.6
KM†	E	42.70	0.73	151.1
SP†	E	45.52	0.20	170.8
HJ†	E	42.98	1.49	0.4
HO†	E	43.29	1.01	172
LK†	E	40.89	0.55	169.2

GB†	E	44.04	0.12	89.9
CT†	E	41.00	0.30	22.5
AW†	E	43.57	1.02	172
FE	H	40.74	1.08	176.2
KD	H	43.33	0.59	14.6
DC	H	39.83	3.25	112.4
MD	H	41.04	0.87	155
KD†	H	41.75	1.24	17.3
AMc†	H	40.79	0.88	5.2
AS†	H	40.19	2.01	5.7
LE†	H	44.12	2.02	12.8

Senior Citizen group

MrM	M	42.38	0.59	87.2
MrN	M	42.86	0.72	132.8
MrMk	M	43.97	1.50	95.2
MrH	H	43.34	1.07	98.9
MrS	H	43.58	0.97	24.8
MrHd	H	41.54	1.97	156.3
MrB	H	40.79	0.41	128
MrSs	H	42.20	0.57	100.7
MrMs	H	44.26	0.85	16.9
MrMy	H	41.05	0.43	117.2
MrsC†	M	44.82	0.81	103.1
MrsMk†	M	45.82	0.72	142.5
MrsS†	M	44.45	0.30	5.7
MrsN†	H	45.09	0.93	174.6
MrsM†	H	41.96	3.28	120.6
MrsL†	H	42.92	0.82	120.9
MrsMl†	H	42.81	0.88	0.2
MrsH†	H	44.98	0.42	22.5
MrsHd†	H	46.21	1.35	43.6
MissH†	H	44.69	1.19	168.2

## APPENDIX B. Supporting Publications

1) Royston, J.M., Dunne, M.C.M. & Barnes, D.A (1989)

An analysis of three meridional keratometric measurement of the anterior corneal surface.

*Ophthal. Physiol. Opt.* 9: 322-323.

2) Royston, J.M., Dunne, M.C.M. & Barnes, D.A (1989)

A new method for determining the radius and toricity of the posterior corneal surface.

Presented at the Annual Meeting of the American Academy of Optometry, New Orleans, Louisiana, USA.

Abstract in *Optom. Vis. Sci.* 10 (Suppl): 141.

3) Royston, J.M., Dunne, M.C.M. & Barnes, D.A (1990, in press)

Measurement of posterior corneal surface toricity.

*Optom. Vis. Sci.*

4) Royston, J.M., Dunne, M.C.M. & Barnes, D.A (1990, in press)

Measurement of posterior corneal radius using slit-lamp and Purkinje image techniques.

*Ophthal. Physiol. Opt.*

5) Dunne, M.C.M, Royston, J.M. & Barnes, D.A. (1990)

The influence of the posterior corneal surface upon total corneal astigmatism.

Accepted for presentation at the Annual Meeting of the American Academy of Optometry, December, 1990. Abstract to be published in

*Optom. Vis. Sci.*

## REFERENCES

- Alsbirk, P.H. (1974) Optical pachymetry of the anterior chamber. A methodological study of errors of measurement using Haag Streit 900 Instruments. *Acta Ophthalmologica* , **52**, 747-758.
- Anstice, J. (1971) Astigmatism- its components and their changes with age. *American Journal of Optometry & A.A.A.O.* , **48**, 1001-1006.
- Atkinson, J., Braddick, O. and French, J. (1980) Infant astigmatism - its disappearance with age .*Vision Research* , **20**, 891-893.
- Aubert, H. (1885) Nahert sich die hornhautkrümmung am meisten der ellipse? *Pflüger's Archiv die Gesamte Physiologie*, **35**, 597-621. Cited by Ludlam and Wittenberg (1966b).
- Bailey, N.T.J. (1983) Statistical methods in biology. 2nd. edn. Hodder & Stoughton, London.
- Baldwin, W.R. (1964) The relationship between the axial length of the eye and certain other anthropometric measurements in myopes. *American Journal of Optometry & A.A.A.O.* , **41**, 513-522.
- Baldwin, W.R. and Mills, D. (1981) A Longitudinal Study of Corneal Astigmatism and Total Astigmatism. *American Journal of Optometry and Physiological Optics* , **58**, 206-211.
- Bannon, R.E. and Walsh, R. (1945) On Astigmatism. Part 4 - Incidence of Astigmatism. *American Journal of Optometry & A.A.A.O.* , **22**, 263-277.
- Benedek, G.B. (1971) Theory of the transparency of the eye. *Applied Optics*, **10**, 459-473.
- Bennett, A.G. (1960) Refraction by Automation? *Optician*, London, **139**, 5-9.
- Bennett, A.G. (1965) Lens usage in the Supplementary Ophthalmic Service. *Optician*, **149**, 131-137.
- Bennett, A.G. (1984) Astigmatic effect of a tilted crystalline lens. *Ophthalmic Optician* , **24**, 793-794.
- Bennett, A.G. and Rabbetts, R.B. (1984) *Clinical Visual Optics* . Butterworth, London.
- Bennett, A.G. (1989) Pers. comm.

- Berg, F. (1929) Vergleichende messungen der form der vorderen hornhautflache mit ophthalmometer und mit photographischer method. *Acta Ophthalmology*, **7**, 386-423. Cited by Clark (1973).
- Bier, N. (1956) A study of the cornea in relation to contact lens practice. *British Journal of Physiological Optics*, **13**, 79-92.
- Binder, P.S., Kohler, J.A. and Rorabaugh, D.A. (1977) Evaluation of an electric corneal pachometer. *Investigative Ophthalmology and Visual Science*, **161**, 855-858.
- Blix, M. (1880) Oftalmometriska studier. *Acta. Soc. Med. Upsal.*, **15**, 349-421. Cited by Von Bahr (1948).
- Bonnet, R. and Cochet, P. (1962) New method of topographic ophthalmometry - its theoretical and clinical applications (trans. Eagle, E.) *American Journal of Optometry & A.A.A.O.*, **39**, 227-251.
- Borish, I.M. (1970) *Clinical Refraction*. Professional Press, Chicago.
- Brown, N. (1972) An advanced slit image camera. *British Journal of Ophthalmology*, **56**, 624-631.
- Brubaker, R.F., Reinecke, R.D. and Copeland, J.C. (1969) Meridional refractometry, 1. Derivation of equations. *Archives of Ophthalmology*, **81**, 849-853.
- Burek, H. (1990) Tri-meridional analysis using arbitrary meridians. *Ophthalmic and Physiological Optics*, **10**, 280-285.
- Carter, J.H. (1963) Residual Astigmatism of the Human Eye. *Optometry Weekly*, **54**, 1271-1272. (Cited by Borish, 1970).
- Charman, W.N. (1972) Diffraction and the precision of measurement of corneal and other small radii. *American Journal of Optometry & A.A.A.O.*, **49**, 672-679.
- Charman, W.N. and Jennings, J.A.M. (1976) Objective measurement of the longitudinal chromatic aberration of the human eye. *Vision Research*, **16**, 999-1005.
- Clark, B.A.J. (1973a) Keratometry: a review. *Australian Journal of Optometry*, **56**, 94-100.
- Clark, B.A.J. (1973b) Conventional keratoscopy - a critical review. *Australian Journal of Optometry*, **56**, 140-155.

- Clark, B.A.J. (1974a) Topography of some individual corneas. *Australian Journal of Optometry*, **57**, 65-69.
- Clark, B.A.J. (1974b) Mean topography of normal corneas. *Australian Journal of Optometry*, **57**, 107-114.
- Cocius, A. (1867) Über den Mechanismus der Akkommodation des menschlichen Auges. *Ophthalmometrie und Spannungsmessung am kranken Auge*. Leipzig, 1872. Cited by El Hage (1971)
- Cox, J.L., Farrell, R.A., Hart, R.W. and Langham, M.E. (1970) The transparency of the mammalian cornea. *Journal of Physiology* (London), **210**, 601-616.
- Czellitzer, A. (1927) Total Refraktion und Hornhautrefraktion mit besonderer Berücksichtigung des physiologischen Linsen-Astigmatismus. *Klin. Monatsbl. f. Augenh.*, **79**, 301-312. Cited by Duke-Elder & Abrams (1970).
- Davson, H. (1984) *Physiology of the Eye*, 5th Edition. Churchill Livingstone, Edinburgh.
- Donaldson, D.D. (1966) Measurement of the corneal thickness. *Archives of Ophthalmology*, **76**, 25-31.
- Donders, F.C. (1864) *On the Anomalies of Accommodation and Refraction of the Eye*. New Sydenham Society, London.
- Duke-Elder, S. and Abrams, D. (1970) Ophthalmic optics and refraction. *System of Ophthalmology*, Vol. V. Kimpton, London.
- Duke-Elder, S. and Wybar, K.C. (1961) The anatomy of the visual system. *System of Ophthalmology*, Vol. II. Kimpton, London.
- Edmund, C. and La Cour, M. (1986) Some components effecting the precision of corneal thickness measurement performed by optical pachometry. *Acta Ophthalmologica*, **64**, 499-503.
- Ehlers, N. (1965) The precorneal film. *Acta Ophthalmologica Supplement*, **81**, 1-136.
- El Hage, S.G. (1971) Suggested new methods for photokeratoscopy: A comparison of their validities. Part I. *American Journal of Optometry & A.A.A.O.*, **48**, 897-912.
- Emsley, H.H. (1974) *Visual Optics*, Vol.1, Hatton, London.

- Eriksen, (1893) *Hornheindemaalinger*. Aarhus, Denmark. Cited by Ludlam and Wittenberg (1966b).
- Exford, J. (1965) A Longitudinal Study of Refractive Trends After Age Forty. *American Journal of Optometry & A.A.A.O.* ,**42**, 685-692.
- Farrell, R.A., McCally, R.L. and Tatham, P.E.R. (1973) Wave-length dependencies of light scattering in normal and cold swollen rabbit corneae and their structural implications. *Journal of Physiology* (London), **233**, 589-612.
- Ferree, C.E., Rand, G. and Hardy, C. (1931) Refraction for the peripheral field of vision. *Archives of Ophthalmology* , **5**, 717-731.
- Feuk, T. (1970) On the transparency of the stroma of the mammalian cornea. *IEE Transactions on Bio-Medical Engineering*, **BME17**, 186-190.
- Fledelius, H.C. (1976) Prematurity of the eye . Ophthalmic 10 year follow up of children of low and normal birthweight. *Acta Ophthalmologica Supplement*, **128**, 1-233.
- Fledelius, H.C. and Stubgaard, M. (1986) Changes in the refraction and corneal curvature during growth and adult life. *Acta Ophthalmologica*, **64**, 487-491.
- Fowler, C.W. (1989) Assessment of toroidal surfaces by the measurement of curvature in three fixed meridians. *Ophthalmic and Physiological Optics*, **9**, 79-80.
- Fujii, T., Maruyama, S. and Ikeda, M. (1972) Determination of corneal configuration by measurement of its derivatives. *Optica Acta*, **19**, 425-430,
- Fulton, A.B., Dobson, V., Salem, D., Mar, C., Petersen, R. and Hansen, R. (1980) Cycloplegic refraction in infants and young children. *American Journal of Ophthalmology* , **90**, 239-247.
- Gardiner, P.A. (1962) Corneal power in myopic children. *British Journal of Ophthalmology*, **46**, 138-143.
- Girard, L.G. (1970) *Corneal Contact Lenses*, 2nd ed., Mosby, St.Louis.
- Gordon, R.A. and Donzis, P.B. (1985) Refractive Development of the Human Eye. *Archives of Ophthalmology* , **103**, 785-789.



- Grosvenor, T. (1961) Clinical use of the keratometer in evaluating corneal contour. *American Journal of Optometry & A.A.A.O.*, **38**, 237-245.
- Grosvenor, T. (1977) A longitudinal study of refractive changes between the ages of 20 and 40 . Part 4, changes in astigmatism. *Optometry Weekly*, **68**, 475-478.
- Guillon, M, Lydon, D.P.M. and Wilson, C. (1986) Corneal topography: a clinical model. *Ophthalmic and Physiological Optics*, **6**, 47-56.
- Gullstrand, A. (1890) Betrag zur Theorie des Astigmatismus. *Skand. Arch. fur Physiologie II*. Cited by Ludlam and Wittenberg (1966).
- Gullstrand, A. (1911) Einfuhrung in Methoden des Dioptrik des Auges. Leipzig. Cited by Duke-Elder and Abrams (1970).
- Gullstrand, A. (1924) Von Helmholtz's Treatise on Physiological Optics. (Ed Southall, J.P.C.) Optical Society of America, Rochester.
- Gwiazda, J., Scheiman, M., Mohindra, I. and Held, R. (1984) Astigmatism in Children : Changes in axis and amount from birth to six years. *Inv. Ophth. & Vis. Sci.* **25**, 1, 88-92.
- Haine, C.L., Long, W.F. and Reading R.W. (1973) Laser meridional refractometry : a preliminary report. *Optometry Weekly* , **64**, 1064-1067.
- Haine, C.L., Long, W.F. and Reading R.W. (1976) Laser meridional refractometry. *American Journal of Optometry and Physiological Optics*, **53**, 194-204.
- Hartinger, H. (1935) Revue d'Optique. In *Optique Physiologique*, ed. Le Grand, Y., ch.II, p.154. Cited by El Hage (1971).
- Helmholtz, H. (1924) *Physiological Optics* , Vol. 1, (trans. Southall, J.P.C.) *Optical Society of America* .
- Henson, D.B. (1983) *Optometric Instrumentation*. Butterworths, London.
- Hess, C. von,(1911) Greafe-Saemisch Handbuch der Gesamten Augenheilkunde, 3 neubearb, Aufl. Leipzig, W. Engelmann, 1911. Cited by Baldwin and Mills (1981).

- Hirji, N.K. and Larke, J.R. (1978) Thickness of the human cornea measured by topographic pachometry. *American Journal of Optometry and Physiological Optics*, **55**, 97-100.
- Hirsch, M.J. (1959) Change in astigmatism after age 40 years. *American Journal of Optometry & A.A.A.O.*, **36**, 395-405.
- Hirsch, M.J. (1963) Changes in the astigmatism during the first eight years of school, an interim report from Ojai longitudinal study. *American Journal of Optometry & A.A.A.O.*, **41**, 137-141.
- Hirsch, M.J. (1964) The longitudinal study of refraction. *American Journal of Optometry & A.A.A.O.*, **41**, 137-141.
- Hockwin, O., Weiglin, E., Laser, H. and Dragmirescu, V. (1983) Biometry of the anterior eye segment by Scheimpflug photography. *Ophthalmic Research*, **15**, 102-108.
- Holden, B.A. (1970) *The Development and Control of Myopia and the Effects of Contact Lenses on Corneal Topography*. Ph.D. Thesis, City University, London. Cited by Watkins (1972).
- Howland, H.C., Atkinson, J., Braddick, O. and French, J. (1978) Infant astigmatism measured by photorefracton. *Science*, Vol. 22, 331-333.
- Hruby, K. (1950) Die Beziehungen zwischen Hornhautastigmatismus und Gesamtastigmatismus des Auges. *Arch. f. Ophth.*, **150**, 91-119. Cited by Duke-Elder and Wybar (1970).
- Jackson, E. (1932) Changes in Astigmatism. *American Journal of Ophthalmology*, **16**, 967-974.
- Jaeger, G. (1952) Tiefenmessung der menschlichen vorderkammer mit plan-parallelen platten. *Albert von Graefes Archiv fur Klinische und Experimentelle Ophthalmologie*, **153**, 120-131.
- Javal et Schiotz (1881) Un ophthalmomètre pratique. Trans. International Medical Congress VIII. Session London, 1881, p.30, *Annales d'Oculistique*, **87**, 1881. Cited by El Hage (1971).
- Javal (1890) *Memories d'Ophthalmologie*. Paris, Masson. Cited by Ludlam and Wittenberg (1966a).
- Jenkins, T.C.A. (1963) Aberrations of the eye and their effects on vision. Part1. *British Journal of Physiological Optics*, **20**, 59-91.

- Juillerat, G. and Koby, F.E. (1928) Determination de l'epaisseur de la cornee sur la vivant aumoyen de la lampe a fente. *Rev. Gen. Ophthalm.* , **42**, 203-227. Cited by Von Bahr (1948).
- Kiely, P.M., Smith, G. and Carney, L.G. (1982) The mean shape of the human cornea, *Optica Acta*, **29**, 1027-1040.
- Kiely, P.M., Smith, G. and Carney, L.G. (1984) Meridional variations of corneal shape. *American Journal of Optometry and Physiological Optics*, **61**, 619-626.
- Knoll, H.A. (1961a) Corneal contours in the general population as revealed by the photokeratoscope. *American Journal of Optometry & A.A.A.O.*, **38**, 389-397.
- Knoll, H.A. (1961b) Photokeratoscopy and corneal contours. In *Encyclopedia of Contact Lens Practice*, 9th supplement, Vol.II, Ch.VII. International Optics Publishing Co., Indiana.
- Knoll, H.A. (1980) Position of the corneal apex in the normal eye. *American Journal of Optometry and Physiological Optics*, **57**, 124-125.
- Kooijman, A.C. (1983) Light distribution on the retina of a wide-angle theoretical eye. *Journal of the Optical Society of America*, **73**, 1544-1550.
- Kratz, D.J. and Walton, W.G. (1949) A modification of Javal's rule for the correction of astigmatism. *American Journal of Optometry & A.A.A.O.*, **26**, 295-306.
- Kronfeld, P.C. and Devney, C. (1931) Ein beitung zur kentis der refraktionskurve. *Albrecht von Graefes Archiv fur Klinische und Experimentelle Ophthalmologie* , **126**, 487-501.
- Kruse-Hansen, F. (1971) A clinical study of the normal human central corneal thickness. *Acta Ophthalmologica*, **49**, 82-88.
- Lancaster, W.B. (1943) Terminology in ocular motility and allied subjects. *American Journal of Ophthalmology*, **26**, 122-132.
- Laurence, L. (1920) *General and Practical Optics* , 3rd edn., pp. 153, 593-602. The School of Optics , London.
- Le Grand, Y. and El Hage S.G. (1980) *Physiological Optics* . Springer-Verlag, Berlin.

- Leibowicz, M. (1928) Hornhautkrumming und Astigmatismus. *Ztschr. f. Ophth. Optik.* **16**, 33-70. Cited by Tait (1956).
- Leighton, D.A. and Tomlinson, A. (1972) Changes in axial length and other dimensions of the eyeball with increasing age. *Acta Ophthalmologica*, **50**, 815-826.
- Lindsted, F. (1916) Über messungen der tiefe des vorderen augenkammer mittels eines neuen für klinischen bestimmten instruments. *Archiv für Augenheilkunde*, **80**, 104-167. Cited by Stenstrom (1953).
- Littman, H. (1951) Grundlegende betrachtungen zur ophthalmometrie. *Albrecht von Graefes Archiv für Klinische und Experimentelle Ophthalmologie*, **133**, 152-156. Cited by Clark (1973a).
- Llandolt, E. (1878) The Refraction and Accommodation of the Eye [trans. Culver, C.M.] Lippincott Co., Philadelphia. Cited by Lyle (1971).
- Lobeck, G. (1937) Über den durchmesser der netzhautgefasse am gesunden und kranken menschen. *Albrecht von Graefes Archiv für Klinische und Experimentelle Ophthalmologie*, **151**, 249-274. Cited by Goldmann (1968).
- Long, W.F. (1974) A mathematical analysis of multi-meridional refractometry. *American Journal of Optometry & Physiological Optics*, **51**, 260-263.
- Loper, L.R. (1959) The relationship between angle lambda and the residual astigmatism of the eye. *American Journal of Optometry & A.A.A.O.*, **36**, 365-377.
- Lowe, R.F. (1966) New instruments for measuring anterior chamber depth and corneal thickness. *American Journal of Ophthalmology*, **62**, 7-11.
- Lowe, R.F. (1969) Central corneal thickness. *British Journal of Ophthalmology*, **53**, 824-826.
- Lowe, R.F. and Clark, B.A.J. (1973) Posterior corneal curvature. Correlations in normal eyes and in eyes involved with primary angle closure glaucoma. *British Journal of Ophthalmology*, **57**, 464-470.
- Ludlam, W.M. and Wittenberg, S. (1966a) The effect of measuring corneal toroidicity with reference to the line of sight. *British Journal of Physiological Optics*, **23**, 178-185.

- Ludlam, W.M. and Wittenberg, S. (1966b) Measurements of the ocular dioptric elements utilising photographic methods. Part II. Cornea-theoretical considerations. *American Journal of Optometry & A.A.A.O.*, **43**, 249-267.
- Lyle, W.M. (1965) The Inheritance of Corneal Astigmatism, Ph.D. Dissertation, Indiana University. Cited by Baldwin and Mills (1981).
- Lyle, W.M. (1971) Changes in corneal astigmatism with age. *American Journal of Optometry & A.A.A.O.* , **48**, 467-478.
- McBrien, N.A and Millodot, M. (1985) Clinical evaluation of the Canon AutoRef R-1. *American Journal of Optometry and Physiological Optics* , **62**, 786-792.
- Malacara, D. (1974) Measurement of Visual Refractive Defects with a Gas Laser. *American Journal of Optometry and Physiological Optics*, **51**, 15-23.
- Mandell, R.B. (1960) Jesse Ramsden; an inventor of the ophthalmometer. *American Journal of Optometry & A.A.A.O.* , **37**, 633-638.
- Mandell, R.B (1962) Reflection point ophthalmometry: a method to measure corneal contour. *American Journal of Optometry & A.A.A.O.* , **39**, 513-537.
- Mandell, R.B (1964) Corneal areas utilised in ophthalmometry *American Journal of Optometry & A.A.A.O.* , **41**, 150-153.
- Mandell, R.B. (1965) Contact Lens Practice: Basic and Advanced. Thomas, Springfield, Illinois.
- Mandell, R.B. (1969) Reply to comments by Ludlam (1969) on Mandell and St. Helen (1969) *American Journal of Optometry & A.A.A.O.* , **46**, 768-772.
- Mandell, R.B. and Polse, K.A. (1969) Keratokonus: spatial variation of corneal thickness as a diagnostic test. *Archives of Ophthalmology*, **82**, 182-187.
- Mandell, R.B. and St. Helen, R. (1969) Position and curvature of the corneal apex. *American Journal of Optometry & A.A.A.O.* , **46**, 25-29.
- Mandell, R.B. and St.Helen, R. (1971) Mathematical model of corneal contour. *British Journal of Physiological Optics*, **26**, 183-197.

- Marin-Amat, M. (1956) Les variations physiologiques de la courbure de la corne pendant de vie. Leur importance et transcendence dans la refraction oculaire. *Bull. Soc. Belge. Ophthal.* , **113**, 251-293. Cited by Weale (1982).
- Martola, E.L. and Baum, J.L. (1968) Central and peripheral corneal thickness. A clinical study. *Archives of Ophthalmology*, **79**, 28-30.
- Mattheissen, L. (1902) Über aplanatische brechung und spiegelung in oberflächen zweiter ordnung und die hornhautrefraction. *Pfluger's Archiv fur die gesamte Physiology*, **91**, 295-309. Cited by Ludlam and Wittenberg (1966b)
- Matsumura, I., Maruyama, S., Ishikawa, Y., Hirano, R., Kobayashi, K. and Kohayakawa, Y. (1983) The Design of an Open View Autorefractometer. In *Advances in Diagnostic Visual Optics* . Breinin, G.M. and Seigel, I.M. (Eds). Springer series in Optical Sciences, 41, pp. 36-42. Springer, Berlin.
- Maurice, D.M. (1957) The structure and transparency of the cornea. *Journal of Physiology*, (London), **136**, 263-286.
- Maurice, D.M. and Giardini, A.A. (1951) Optical apparatus for measuring the corneal thickness and average thickness of the human cornea. *British Journal of Ophthalmology*, **35**, 169-177.
- Millodot, M. (1981) Effect of ametropia on peripheral refraction. *American Journal of Optometry and Physiological Optics* , **58**, 691-695.
- Millodot, M. (1984) Peripheral refraction in aphakic eyes. *American Journal of Optometry and Physiological Optics* , **61**, 586-589.
- Millodot, M. and O'Leary, D. (1978) The discrepancy between retinoscopic and subjective measurements: effect of age. *American Journal of Optometry and Physiological Optics* , **55**, 309-316.
- Mishima, S. (1968) Corneal thickness. *Survey of Ophthalmology*, **13**, 57-96. Cited by Watkins (1972) .
- Mishima, S. and Hedbys, B.O. (1968) Measurement of corneal thickness with the Haag-Streit Pachometer. *Archives of Ophthalmology*, **80**, 710-713.
- Mohindra, S. and Held, R. (1981) Refraction in humans from birth to five years. *Documenta Ophth. Proc. Series* **28**, 19-27.

- Mohindra, S., Held, R., Gwiazda, J. and Brill, S. (1978) Astigmatism in infants. *Science (New York)*, **202**, 329-331.
- Monod, M. (1927) Les modifications de l'astigmatisme corneen avec l'age. *Bull. Soc. Fr. Ophthalmol.* , **40**, 230-239. Cited by Baldwin and Mills (1981).
- Morgan, M.W., Mohny, J. and Ohmstead, J.M.D. (1943) Astigmatic Accommodation. *Archives of Ophthalmology*, **30**, 2. (Cited by Borish, 1970).
- Nicoletti, G. (1927) The Influence of the Posterior Corneal Surface on the Total Astigmatism. *Ann. di ottal. e clin. ocul.* , **55**, 987-994. Cited by Kronfeld and Devney (1930).
- Noto, F. (1961) Form of the anterior corneal surface. *Acta Societatis Ophthalmologicae Japonicae*, **65**, 447-468.
- O'Leary, D. and Millodot, M. (1978) The discrepancy between retinoscopic and subjective measurements: effects of light polarisation. *American Journal of Optometry and Physiological Optics* , **55**, 553-556.
- Obrig, T. (1957) Contact Lenses, 3rd ed., Chilton, Philadelphia.
- Olsen, T. and Ehlers, N. (1984) The thickness of the human cornea as determined by the specular method. *Acta Ophthalmologica*, **62**, 859-871.
- Payne, S.M. (1919) Hypermetropia responsible for heterophoria, astigmatism and myopia. *American Journal of Ophthalmology* , **2**, 30-39. (Cited by Baldwin and Mills, 1981).
- Phillips, R.A. (1952) Changes in corneal astigmatism. *American Journal of Optometry & A.A.A.O.* , **29**, 379-380.
- Phillips, D., Sterling, W. and Dwyer, W.O. (1975) Validity of the laser refraction technique for determining cylindrical error. *American Journal of Optometry and Physiological Optics*, **52**, 328-331.
- Reinecke, R.D., Carroll, J., Beyer, C.K. and Montross, R.T. (1972) An innovation in eye care. *Sight Saving Rev.* , **42**, 35-41.
- Rubin, M. (1975) *Contact Lens Practice, Visual, Therapeutic and Prosthetic*, 1st ed., Balliere Tindall, London.

- Sallman, L. (1934) Untersuchungen über den Linsenastigmatismus. *Arch. f. Ophth.*, **131**, 492-504. Cited by Duke-Elder and Wybar (1970).
- Saunders, H.J. (1981) Age dependence of human refractive error. *Ophthalmic and Physiological Optics*, **1**, 159-174.
- Scheimpflug, T. (1906) Der photoperspectograph and seine anwendung. *Photographische Korrespondenz*, **43**, 516. Cited by Brown (1972).
- Scheiner, C. (1619) *Oculus Sive Fundamentum Opticum* . Innsbruck. Cited by Ludlam (1967).
- Senff, R. (1846) in Handwörterbuch der physiol., III. Cited by El Hage (1971).
- Sheard, W. (1920) Ophthalmometry and its application to ocular refraction and eye examination. *American Journal Of Physiological Optics* , **4**, 357-397. Cited by Ludlam and Wittenberg (1967).
- Slataper, F.J. (1950) Age norms of refraction and vision. *Archives of Ophthalmology* , **43**, 466-481.
- Smith, J.W. (1969) The transparency of the corneal stroma. *Vision Research*, **9**, 393-396.
- Snell, R.S. and Lemp, M.A. (1989) *Clinical Anatomy of the Eye*, Blackwell Scientific Publications, London.
- Sørensen, S.K. (1944) L'astigmatisme du christallin determine comme la difference entre l'astigmatisme cornéen et l'astigmatisme total illustré par l'examen de ses variations d'après l'âge. *Acta Ophthalmologica (Kbh)* , **22**, 341-385.
- Sorsby, A., Benjamin, B., Davey, J.B., Sheridan, M. and Tanner, J.M. (1957) Emmetropia and its aberrations. Medical Research Council Special Report Series No. 293. HMSO, London.
- Sorsby, A., Benjamin, B. and Sheridan, M. (1961) Refraction and its components during growth of the eye from the age of three. Medical research Council Special Report Series No. 301. HMSO, London.
- Sorsby, A., Sheridan, M. and Leary, G.A. (1960) Vision, visual acuity and ocular refraction in young men. *British Medical Journal*, **1**, 1394-1398.



- Southall, J.P.C. (1924) English translation of "Helmholtz's Treatise on Physiological Optics", Vol. 1. The Optical Society of America. Cited by Lowe and Clark (1973).
- Southall, J.P.C. (1937) Introduction to Physiological Optics. Oxford University Press, London. Cited by Lyle (1971).
- Steiger, A. (1913) *Die entstehung der spharischen refraktionen des menschlichen auges*. Karger, Berlin. Cited by Sorsby et al., (1951).
- Steindorff, K. (1947) Deskriptive anatomie des auges der wirbeltiere und des menschen. *Tabul. Biol. Berl.* , **22**, 166-297. Cited by Charman (1983).
- Stenstrom, S. (1946) Investigation of the variation and correlation of the optical elements of human eyes [trans. (1948) Woolf, D.] *American Journal of Optometry*, Monograph 58.
- Stenstrom, S. (1953) An apparatus for the measurement of the depth of the anterior chamber based on the principle of Lindsted. *Acta Ophthalmologica*, **31**, 265-270.
- Stone, J. (1962) The validity of some existing methods of measuring corneal contour with suggested new methods. *British Journal of Physiological Optics*, **19**, 205-230.
- Sulzer, D. (1892) La forme de la cornee humaine et son influence sur la vision. *Archives d'Ophthalmologie (Paris)*, **12**, 32-50. Cited by Ludlam and Wittenberg (1966b).
- Sutcliffe, J.H. (1907) One-position ophthalmometry. *Optician and Photographic Trades Review*, **33**, Supplement, p.8. Cited by El Hage (1971)
- Tait, E.F. (1956) Intraocular Astigmatism. *American Journal of Ophthalmology* , **41**, 813-824.
- Tomlinson, A. (1972) A clinical study of the central and peripheral thickness and curvature of the human cornea. *Acta Ophthalmologica*, **49**, 73-82.
- Tomlinson, A. and Schwartz, C. (1979) The position of the corneal apex in the normal eye. *American Journal of Physiological Optics*, **56**, 236-240.
- Tornquist, R. (1953) Shallow anterior chamber in acute glaucoma. *Acta Ophthalmologica Supplement*, **39**, 1-74.

- Tron, E (1934) Ueber die optischen grundlagen der ametropie. *Albrecht von Graefes Archiv fur Klinische und Experimentelle Ophthalmologie*, **132**, 182-223. Cited by Borish (1970).
- Tscherning, M. (1890) Etude sur la position du cristallin de l'oeil human. In Javal, E. *Memoires d'Ophthalmométrie*, Masson, Paris. Cited by Duke-Elder (1970).
- Tscherning, M. (1904) Physiologic Optics [trans. Weiland, C.]. Keystone, Philadelphia.
- Tscherning, M. (1924) Physiologic Optics [trans. Weiland, C.]. Keystone, Philadelphia.
- Ulbrich, H. (1914) Messung der kammertiefe. *Klinische Monatsblatter fur Augenheilkunde*, **53**, 244. Cited by Goldmann (1968).
- Van Veen, H.G. and Goss, D.A. (1988) Simplified System of Purkinje Image Photography for Phakometry. *American Journal of Optometry and Physiological Optics*, **65**, 905-908.
- Von Bahr, G. (1948) Measurements of the thickness of the cornea. *Acta Ophthalmologica (Basel)*, **26**, 247-265.
- Walton, W.G. (1950) Refractive changes in the eye over a period of years. *Am. Optom. & A.A.A.O.*, **27**, 267-286.
- Whitefoot, H.D. and Charman, W.N. (1980) A comparison between laser and conventional subjective refraction. *Ophthalmic Optician*, **20**, 169-173.
- Williams, O.A. (1963) Latent Astigmatism in Practice. *Am. J. Optom. & A.A.A.O.*, **40**,
- Woodruff, M.E. (1971) Cross sectional studies of corneal and astigmatic characteristics of children between the twenty-fourth and seventy-second month of life. *Am. J. Optom. & A.A.A.O.*, **48**, 650-659.
- Worthey, J.A. (1977) Simplified analysis of meridional refraction data. *American Journal of Optometry and Physiological Optics*, **54**, 771-775.